THE USE OF TETRAZINE-NORBORNENE CLICK PRODUCTS IN SUPRAMOLECULAR HYDROGEL CROSSLINKING AND THE DESIGN OF DYNAMIC HYROGELS

A Dissertation

by

SAMANTHA ELIZABETH HOLT

Submitted to the Graduate and Professional School of
Texas A&M University
in partial fulfillment of the requirements for the degree of

DOCTOR OF PHILOSOPHY

Chair of Committee,	Daniel L. Alge
Committee Members,	Isaac Adjei
	Roland R. Kaunas
	Andreea Trache
Head of Department,	Michael McShane

May 2022

Major Subject: Biomedical Engineering

ABSTRACT

Herein, the discovery and application of a novel class of supramolecular secondary interactions between the cycloaddition products of the inverse electron-demand Diels Alder (IEDDA) tetrazine-norbornene click reaction is described. First, a direct comparison of the bulk properties of poly(ethylene glycol) (PEG) hydrogels crosslinked with either the radical-mediated thiol-norbornene reaction or the tetrazine-norbornene reaction revealed significant and unexpected differences in the two gels. These differences in the storage moduli, swelling, and susceptibility to hydrolytic degradation of the two gel formulations could not be attributed to differences in crosslink density or crosslinking reaction efficiency. However, molecular dynamics simulations suggested the existence of supramolecular interactions between the tetrazine-norbornene click products (TNCP) which could provide additional physical crosslinking of the network. This was confirmed by the gelation of multi-arm PEG macromers end-functionalized with TNCP in the absence of covalent crosslinking. Unlike other supramolecular crosslinking moieties, TNCP can be synthesized *in situ* in physiologic conditions with the bio-orthogonal IEDDA reaction without the need for exogenous initiators or adjustment in pH, temperature, or ion concentrations. *In situ* TNCP installation was then leveraged as a mechanism for bio-orthogonal, controlled gel stiffening in a pre-existing and enzymatically-degradable covalent PEG-peptide network. Pendant TNCP groups demonstrated a concentration-dependent effect on bulk gel modulus, and TNCP installation yielded an approximately 2 kPa increase in shear

storage modulus over the course of 4-6 hours. This approach had no effect on the viability of encapsulated cells and the increase in gel stiffness was long-lasting in culture conditions. Finally, TNCP-functionalized gelatin was used to create a shear-thinning, extrudable hydrogel. As in PEG-peptide hydrogels, the installation of pendant TNCP groups in covalently crosslinked gelatin networks increased the bulk shear storage modulus of the gel. Additionally, supramolecular gelatin gels were formed via installation of TNCP along norbornene-functionalized gelatin molecules. These supramolecular gel-TNCP hydrogels exhibited fitness for extrusion, demonstrating both shear thinning and rapid recovery of gel stiffness after shear. In short, this work presents the use of the bio-orthogonal IEDDA tetrazine reaction to synthesize supramolecular interacting domains *in situ* in hydrogel biomaterials. Future studies will serve to expand the remarkably broad potential applicability of this chemistry.

ACKNOWLEDGEMENTS

It may be cliché to say, “It takes a village,” but there is no doubt that this work would not have been possible without the efforts, care, and support of a great many people who all deserve my thanks.

Firstly, I would like to thank my advisor, Professor Daniel Alge, for his support at every stage in my dissertation work. Your insight, expertise, and support for my training and professional development have been absolutely invaluable in preparing me for my scientific career. I am grateful for both your patience for and guidance in refining my often unusual ideas.

I would also like to thank my collaborators in my dissertation research, Dr. Lisa M. Pérez, Prof. Akhilesh Garharwar, and Kaivalya Deo. I would also like to acknowledge the other collaborators I have had the pleasure of working with in my time at Texas A&M University: Prof. Andreea Trache, Prof. Gonzalo Rivera, Briana Bywaters, Dr. Navaneeth R.K. Pandian, Prof. Vladislav Yakovlev, Vsevolod Cheburkanov, James Gonzales, Prof. Alex Walsh, Anna Theodossiou, and Jim Tronolone. Thank you so much for your advice, hard work, and collegiality.

To Dr. Trache especially, thank you so much for being a professional and personal mentor. Your kindness and advice in times of trouble have been infinitely helpful. I appreciate your frank and honest perspective and your generosity of heart.

I would like to also acknowledge my wonderful undergraduate researchers, who I’ve had the great honor of mentoring, however briefly. Thank you to Amanda Rakoski, Julio Arroyo, Isabelle Agurcia, Austen Fricks, Emily Poux, Ananya Sridhar, Austin

Hughes, Emma Rader, and Devon Roeming for your hard work and your patience with me. I am wishing you all the best in the future!

I would also like to acknowledge my lab mates for their help and support. To Sarea and especially Tyrell—thanks for being my coffee buddies! Additionally, I would like to acknowledge all my colleagues who have lent a listening ear as well as their personal and professional advice over the past few years. Thank you to Abhay, Giriraj, and again Kaivalya; Michaela, Ping, Mike, Brian, Kristen, Connor, and Alec; Robert Rogers, Robert Reese, and Eli; and Travis and Matt.

To my friends: I can't thank you enough for your love and support. Stacy, Romi, Becca, Charlotte, Lindsay, Lucy—consider yourselves co-authors. This dissertation absolutely could not have happened without you. Your kindness and thoughtfulness have kept me going for years now, and I am so incredibly lucky to have you in my life.

To my family: I can't thank you enough for your love and care. To my parents, my very first mentors, thank you for your patience and unwavering faith and support. It can be difficult to yoke purpose to passion, and in teaching me to do so from a young age, I am ever grateful that your tenacity matched (and maybe exceeded!) mine. And to my sisters, Ashley and Hannah, I owe you both my gratitude for sitting with me in every joy, triumph, discomfort, and pain. Thank you for keeping me laughing! I love you all.

CONTRIBUTORS AND FUNDING SOURCES

Contributors

This work was supervised by a dissertation committee consisting of advisor Prof. Daniel L. Alge as well as Prof. Isaac Adjei and Prof. Roland R. Kaunas of the Department of Biomedical Engineering and Prof. Andreea Trache of the Department of Medical Physiology.

Molecular dynamics simulations in Chapter 2 were provided by Dr. Lisa M. Pérez, currently the Associate Director of the Texas A&M High Performance Research Computing. Undergraduate researchers Amanda Rakoski, Julio Arroyo, Isabelle Agurcia, Austen Fricks, Emily Poux, Marissa Heintschel, Devon Roeming, and Emma Rader assisted with hydrogel synthesis and characterization as detailed in Chapters II and III. Gelatin-norbornene synthesis and characterization detailed in Chapter IV was conducted by Thomas Tigner of the Department of Biomedical Engineering. Extrudability testing in Chapter IV was conducted in collaboration with Kaivalya Deo and Prof. Akhilesh Gaharwar of the Department of Biomedical Engineering.

All other work conducted for the dissertation was completed by the student independently.

Funding Sources

Graduate study was supported by a fellowship from Texas A&M University. This work was also made possible in part by the National Institute of Arthritis and Musculoskeletal and Skin Diseases under Grant Number R21 AR071625. Its contents

are solely the responsibility of the authors and do not necessarily represent the official views of the National Institute of Arthritis and Musculoskeletal and Skin Diseases.

NOMENCLATURE

DLS	Dynamic light scattering
ECM	Extracellular matrix
G’	Shear storage modulus
G”	Shear loss modulus
GelNB	Gelatin-norbornene
GelTNCP	Gelatin functionalized with tetrazine-norbornene click products
HA	Hyaluronic acid
HBTU	O-(benzotriazol-1-yl)-N,N,N',N'-tetramethyl-uronium hexafluorophosphate
IEDDA	Inverse electron-demand Diels Alder
KCGPQ-A	Peptide KCGPQGIAGQCK
KCGPQ-W	Peptide KCGPQGIWGQCK
LAP	Lithium acylphosphinate
mPEG-NH2	Methoxy-poly(ethylene glycol)-amine
mPEG-SH	Methoxy-poly(ethylene glycol)-thiol
mPEG-Tz	Methoxy-poly(ethylene glycol)-tetrazine
NMP	1-methyl-2-pyrrolidinone
NMR	Nuclear magnetic resonance
PAAm	Poly(acrylamide)
PBS	Phosphate buffered saline
PEG	Poly(ethylene glycol)
PEG-2-NB	Poly(ethylene glycol)-di-norbornene

PEG-2-SH	Poly(ethylene glycol)-di-thiol
PEG-4-NB	Poly(ethylene glycol)-tetra-norbornene
PEG-4-SH	Poly(ethylene glycol)-tetra-thiol
PEG-4-Tz	Poly(ethylene glycol)-tetra-tetrazine
PEG-8-NB	Poly(ethylene glycol)-octa-norbornene
PEGDA	Poly(ethylene glycol)-diacrylate
PHEMA	Poly(2-hydroxyethyl methacrylate)
Pluronic	Poly(ethylene glycol)-co-poly(propylene glycol)-co-poly(ethylene glycol)
PNIPAM	Poly(N-isopropylacrylamide)
pTNCP	Pendant tetrazine-norbornene click products
PVA	Poly(vinyl alcohol)
TNCP	Tetrazine-norbornene click products
Tz-COOH	Tetrazine-carboxylic acid
UV	Ultraviolet

TABLE OF CONTENTS

Page

LIST OF FIGURES

Page

LIST OF TABLES

Page

CHAPTER I

INTRODUCTION AND LITERATURE REVIEW

Hydrogels are networks of hydrophilic polymers which have a high affinity for water but do not dissolve in aqueous environments.[1] Because of their unique structure and properties among polymeric materials, they have become a popular choice for a variety of medical and biological applications, including drug delivery,[2] cell culture,[3] and regenerative medicine.[4, 5] These hydrogel biomaterials can be broadly classified according to their composition: either made from natural polymers, such as protein-derived gelatin or polysaccharide hyaluronic acid (HA), or synthetic polymers like poly(vinyl alcohol) (PVA) or poly(ethylene glycol) (PEG). Furthermore, a broad variety of strategies for chemical modification of these polymers have been developed to add desired structural and functional features and facilitate the assembly of hydrogel networks.

The assembly of this network via crosslinking of the polymer is fundamental to a hydrogel's properties. The junctions or 'tie points' at the sites of crosslinking connect polymer chains and prevent their dissolution, giving the hydrogel form.[6] The resultant structure has three main characteristics which determine the bulk properties of the gel: the mesh size, the polymer volume fraction, and the molecular weight between crosslinks.[1, 6] By changing these structural characteristics, one can tune the mechanical and diffusive properties of the gel. Most frequently, these changes are made by tuning the crosslinking density of the gel, the relative frequency of crosslinking junctions in a

given volume, by tuning the molecular weight, functionality, and concentration of the constituent polymers.

A plethora of methods for hydrogel crosslinking have been explored. Broadly, they are divisible into two categories: chemical crosslinking via covalent bonds, and physical crosslinking through non-covalent interactions such as ionic bonds, hydrogen bonds, electrostatic interactions, pi-pi interactions, van der Waals forces, or any combination of these. The choice of method for crosslinking can have a significant impact on the properties and potential applications of the resultant gel. In the following sections, crosslinking mechanisms for hydrogel biomaterials and their application will be reviewed.

I.1 Chemical Crosslinking

I.1.1 Chain Growth Reactions

Chain growth polymerization, also known as addition polymerization, begins with the generation of an active center by an initiator.[7] Next, the reaction propagates at the active site through the sequential addition of monomers to the growing polymer chain before the reaction is finally terminated via neutralization of the active site.[7] Chain growth crosslinking reactions were some of the earliest chemical crosslinking mechanisms applied in synthetic hydrogel biomaterials to achieve user control of the material's properties. For example, in an early example of hydrogel cell culture substrates, Hubbell and colleagues utilized free radical vinyl polymerization to crosslink hydrogel biomaterials made from PEG-diacrylate (PEGDA) and incorporate acryloyl-functionalized moieties to impart biological functions, including alpha-hydroxy acid to

enable biodegradability[8] and cell adhesive peptides to enable cellular adhesion to the surface of the gels.[9] Additionally, West and colleagues demonstrated the incorporation of two acryloyl-functionalized peptides, one for cell adhesion as well as one for cell-mediated enzymatic gel degradation. They successfully utilized this platform to culture dermal fibroblasts as well as smooth muscle cells.[10]

Radical-mediated vinyl polymerization is a popular choice because it can easily be controlled via the incorporation of photo- or thermal-initiators. It has been applied in hydrogels made from both synthetic polymers, including PEG, poly(2-hydroxyethyl methacrylate) (PHEMA),[11] PVA and poly(acrylamide) (PAAm).[12] Additionally, chain growth free radical vinyl polymerization has been utilized in natural polymers as well to control mechanical properties. Most notably, Alsberg and colleagues demonstrated the use of free radical vinyl polymerization to crosslink hydrogels made from methacryloyl-functionalized alginate,[13] and soon after Khademhosseini and colleagues demonstrated a similar approach using methacryloyl-functionalized gelatin.[14] Gelatin-methacryloyl has proven especially popular and has since been applied in 3D bioprinting,[15, 16] regenerative medicine,[17] and tissue-engineered models of disease.[18-20]

I.1.2 Step Growth Reactions

Step growth polymerizations, in contrast to chain growth polymerization reactions, occur between multifunctional monomers where each functional group can serve as a site of reactivity.[7] Essentially, while chain growth polymerization is centered around active centers, step growth polymerization reactions can occur in parallel at any available (i.e., unreacted) functional group in the system. This allows step growth

crosslinking reactions to achieve critical conversion and gelation much more quickly than chain growth crosslinking reactions with greater homogeneity of the network.[21, 22] While free radical vinyl polymerization is the most common chain-growth crosslinking reaction in hydrogel biomaterials, there are several popular step growth crosslinking reactions, many of which fit the 'click' chemistry paradigm.

In their seminal review, Sharpless et al. established the definitive criteria for click chemistry reactions. Click reactions are modular, highly selective, wide in scope, high-yielding, stereospecific, require mild reaction conditions (e.g. use no solvent or use a benign solvent such as water, insensitive to oxygen, proceed at mild temperatures and pH), and produce inoffensive, if any, by-products which can easily be removed from the product.[23] These features make click reactions highly amenable to use in biochemical and biological systems, which has led to their use in a wide variety of biomedical applications, including bioconjugation,[24] drug discovery,[25, 26] proteomics research,[27] and the assembly and modification of hydrogel biomaterials.[4, 28] The click chemistry toolkit for step-growth hydrogel crosslinking includes the thiol-alkene Michael addition[29, 30] and radical-mediated thiol-ene reactions,[31] copper-catalyzed azide-alkyne chemistry,[32, 33] strain-promoted azide-alkyne cycloadditions,[34] and the inverse electron-demand Diels Alder (IEDDA) reaction,[35] among others.

I.1.3 Dynamic Covalent Crosslinking

Generally, covalent crosslinking reactions are irreversible, though recently there has been increasing interest in and exploration of dynamic, reversible covalent crosslinking in hydrogel biomaterials.[36, 37] Specifically, step growth crosslinking via

dynamic covalent bonds has been leveraged to engineer hydrogels with unique properties, including pH-responsive gelation[38] as well as time-dependent viscoelastic behavior such as stress relaxation.[39] These reactions, which include oxime ligation,[40] hydrazone ligation,[39] and the Diels-Alder reaction between furans and maleimides,[41] can also be considered click reactions. Because of their dynamic reversibility which enables them to break and re-form, dynamic covalent crosslinks can provide the gel self-healing and shear-thinning characteristics[42] which are desirable for tissue engineering.

I.2 Physical Crosslinking

I.2.1 Ionic Crosslinking

Ionic crosslinking includes the complexation of charged polymers with either counter ions (ionotropic crosslinking) or other charged polymers (polyelectrolyte complexation). The crosslinking of the naturally-derived polysaccharide alginate via complexation with divalent calcium cations is a classic example of ionotropic crosslinking. Tuning the concentration of Ca^{2+} enables control of the mechanical properties and stability of the gel.[43] Another polymer which undergoes ionotropic crosslinking is κ-carrageenan, which gels in the presence of monovalent potassium cations in aqueous conditions.[44] The stability of ionotropically-crosslinked gels can be low as the counter ions can diffuse out of the material over time in a hypotonic environment. To address this concern, both alginate and κ-carrageenan have been functionalized with methacryloyl groups to enable secondary covalent stabilization of the networks via radical polymerization.[45, 46]

Polyelectrolyte complexation has also been used to address concerns of gel stability, as complexed ionic polymers diffuse more slowly than small counter ions. This approach can utilize charged natural or synthetic polymers. For instance, Chiellini et al. incorporated the cationic natural polysaccharide chitosan with the anionic natural polypeptide poly(γ-glutamic acid) to create a hydrogel they then used to fabricate a microstructured electrospun scaffold for 3D cell culture.[47] In contrast, Gong et al. utilized two synthetic polymers, anionic poly(sodium 4-styrenesulfonate) and cationic poly(diallyl dimethylammonium chloride), to form hydrogels which could be induced to phase separate via de-salting and form micropores in the bulk gel.[48] Han and colleagues even added a radical-polymerized PAAm network to a chitosan/alginate polyelectrolyte complex to form mechanically tough and microporous gels. The gels including both the polyelectrolyte complex and the PAAm network exhibited increased mineralization for bone tissue engineering, which was attributed to increased apatite deposition around the anionic residues of sodium alginate.[49]

I.2.2 Domain-Specific Supramolecular Interactions

I.2.2.1 Supramolecular stacking assembly and low molecular weight hydrogelators

Physical crosslinking can also occur via supramolecular crosslinking, non-covalent interactions between specific molecular motifs. These domain-specific intermolecular interactions are inherently modular and can often be broadly applicable in gels of varying polymer compositions. Some small molecules and oligomers which undergo supramolecular assembly are known as low molecular weight hydrogelators

(LMWH). LMWH gelation is dependent on multiscale self-assembly; individual molecules 'stack,' often through a combination of hydrogen bonding, pi-pi interactions, and electrostatic interactions, to create nanofibrils which become entangled and form gels via physical interactions. For instance, oligopeptides functionalized with fluorenylmethoxycarbonyl (Fmoc) were some of the earliest LMWH used for hydrogel assembly.[50] Fmoc-functionalized dipeptides,[50] tripeptides,[51] and small oligopeptides[52] have all demonstrated the capacity for gelation at their critical concentration. These Fmoc-peptide gels exhibit injectability as well as *in vitro* and *in vivo* biocompatibility in certain applications.[51, 52] Alternatively, to reduce concerns of potential Fmoc toxicity, tripeptides end-functionalized with a nucleobase have also demonstrated supramolecular assembly and gelation.[53] However, the stability of gels made from these modified peptide LMWH can be low in the presence of cells and tissues due to the molecules' susceptibility to proteolysis. Instead of these naturally-occurring amino acids, non-proteinogenic amino acids have demonstrated use in the design of LMWH, including 2,3-diaminopropionic acid[54] and the dehydropeptide dehydrophenylalanine.[55, 56] A few functionalized biomolecules have presented alternatives to peptide-based LMWH, including a polynucleotide guanosine quartet modified with sodium borate[57] and coumarin-tris amphiphiles.[58]

I.2.2.2 Multivalent hydrogen bonding via ureidopyrimidinone

While individual hydrogen bonds are relatively weak, in large numbers they can form relatively strong and stable physical interactions. Ureidopyrimidinone (UPy) is a chemical group which forms supramolecular dimer complexes via four hydrogen bonds,

yielding reasonably stable yet reversible bonds so long as it is shielded by nearby hydrophobic domains. UPy was used to create LMWHs via functionalization of low molecular weight oligocaprolactones as well as oligopeptides in 2005.[59] These LMWH self-assembled into hydrogels in a similar manner to supramolecular stacking assembly. Since then, several polymers have been modified with pendant UPy groups to facilitate supramolecular gelation via hydrogen bonds, including poly(L-glutamic acid),[60] polycaprolactone,[61] and PHEMA,[62, 63] as well as alginate and gelatin.[64] A PEG-UPy block-co-polymer was also synthesized which incorporated UPy groups into the polymer backbone and could be used to form hydrogels.[65] Notably, the UPy domain required an attached short alkane in the chain in order to have sufficient hydrophobic shielding to achieve hydrogen bonding.

I.2.2.3 Molecular recognition motifs

Supramolecular crosslinking can also be achieved by borrowing domain-specific interactions from biomolecules in nature. Proteins and nucleic acids often form complex secondary and tertiary structures via physical interactions, and motifs which participate in this self-assembly have been applied for crosslinking hydrogel biomaterials. One notable example is the mixing-induced two component hydrogel system designed by the Heilshorn group which exploits the interactions between conserved tryptophan-containing WW domains and proline-rich regions to form engineered protein hydrogels.[66] These hydrogels exhibit tunable viscoelastic properties.[67] However, the protein engineering techniques which their synthesis requires are uncommon to most biomaterials labs.

Alternatively, the self-assembly of complementary nucleic acids such as DNA can be used to crosslink hydrogels. For instance, Kopeçek and colleagues grafted peptide-nucleic acids (PNA) to PHEMA polymer chains and induced gelation by adding DNA with a complementary sequence to complex with the PNA.[68] The DNA/PNA sequences could be modified to obtain either double- or triple-helical crosslinking assemblies, with the triple-helical crosslinked hydrogels exhibiting greater mechanical stiffness and stability.[68]

I.2.2.4 Host-guest interactions and polymer inclusion complexation

Host-guest interactions, also referred to as polymer inclusion complexation, rely on the assembly of two specific chemical domains: the "host", which features a three-dimensional structure with a central cavity, and the "guest", which fits into the interior of the cavity of the "host".[69] Unique among supramolecular interactions, host-guest interactions not only depend on non-covalent bonds but also on the dimensions of both the host and the guest motifs. The modularity and potential for specificity of these supramolecular domains have made host-guest interactions attractive for use in hydrogel assembly as well as in drug delivery applications.

The two major host motifs which have been used in hydrogel crosslinking are cyclodextrins and cucurbit[8]uril. Cyclodextrins, a class of macrocyclic oligosaccharides, include both α- and β-cyclodextrin and interact mainly with aromatic residues as guests, although PEG is also known to form inclusion complexes with α-cyclodextrin. Host-guest interactions between PEG and α-cyclodextrin have been used to form hydrogels from high-molecular weight linear PEG molecules,[70] low-molecular

weight (10 kDa) multi-arm PEG macromers,[71] PEG-grafted chitosan,[72] PEG-grafted dextran,[73] and pluronics (triblock co-polymers of poly(ethylene glycol)-co-poly(propylene glycol)-co-poly(ethylene glycol)).[74] More recently, β-cyclodextrin polymers assembled via radical polymerization of acrylated monomers have been utilized to form hydrogels with gelatin,[75] acrylamide,[76] and adamantane-functionalized pluronic.[77] Alternatively, cucurbit[8]uril host-guest complexation, with napthyl and viologen serving as guests, has been utilized in gels made from PAAm[78] and cellulose with PVA.[79] The dynamic nature of these interactions has been utilized to create gels with tunable viscoelasticity and dynamic properties. For instance, Song et al. incorporated varying amounts of an adamantane-PEG-peptide conjugate into a β-cyclodextrin-functionalized poly(organophosphazene) gel to change the concentration of cell adhesion peptides and modulate the lineage specification of mesenchymal stem cells.[80] Zhang et al. also leveraged β-cyclodextrin host-guest interactions when creating gels for 3D cell culture with tunable storage and loss moduli using β-cyclodextrin-functionalized poly(methyl vinyl ether-*alt*-maleic acid) and poly(acrylamide-*co*-*N*-adamantyl acrylamide) combined in varying ratios.[81]

I.3 Biomaterial Applications of Hydrogels

I.3.1 Cell Culture Platforms

One of the most important applications of hydrogel biomaterials is as matrices for cell culture. The mechanically soft and highly hydrated environment of a hydrogel is inherently similar to the extracellular matrix (ECM), the noncellular component of tissue which consists of biopolymers such as proteins and glycosaminoglycans. Hydrogels can

be further engineered to recapitulate the ECM through the selective incorporation of bioactive peptides into the polymer network. Click reactions such as Michael-type addition,[29] radical-mediated thiol-ene,[82] strain-promoted azide-alkyne cycloaddition,[34] and tetrazine-norbornene IEDDA[35] chemistry have enabled cell-adhesive and enzymatically-degradable peptide motifs at user-specified concentrations in PEG hydrogels. Modular physical crosslinking, such as supramolecular UPy assembly[59] and β-cyclodextrin host-guest interactions,[80] can also be utilized for the selective incorporation of bioactive signaling molecules and cell-adhesive peptides. Tuning the polymer composition of the hydrogel and using naturally-derived biopolymers is another means of mimicking the ECM. This can be achieved by grafting click functional groups such as norbornene on natural polymers such as gelatin[83] or hyaluronic acid.[84] Furthermore, stimuli-controlled reactions, such as photomediated chain growth and click reactions, have been used to spatially pattern biochemical cues in 2D and 3D. This can introduce biomimetic heterogeneity in the cell culture microenvironment. For example, West et al. used two-photon laser scanning-controlled photomediated radical polymerization to achieve three-dimensional micropatterning of cell-adhesive peptides in PEG-based hydrogels.[85] Additionally, photocleavable o-nitrobenzyl ester groups incorporated into click-crosslinked networks can enable photomediated release of bioactive molecules[86] or ablation of the gel network.[87]

Another feature that makes hydrogels a useful tool for cell culture platforms is their mechanical tunability. Tuning the mechanical properties of chemically crosslinked hydrogels by modulating crosslinking density has been leveraged to uncover the

profound effects cell culture substrate stiffness can have on cell morphology and phenotype.[88-90] Furthermore, dynamic covalent and physical crosslinking methods have been exploited to tune gel viscoelastic properties, including stress relaxation and creep. Notably, human mesenchymal stem cells encapsulated in gels with fast stress relaxation times have been found to exhibit higher spreading and increased osteogenic differentiation than those in gels with slow relaxation times.[91] Human umbilical vascular endothelial cells have also been observed to exhibit higher spreading, branching, and integrin clustering in dynamic covalent-crosslinked gels with faster relaxing times as opposed to irreversibly covalently crosslinked gels.[92]

In addition, temporal control of gel crosslinking can be used to create mechanically dynamic cell culture platforms. Sequential or secondary covalent crosslinking has been used for dynamic stiffening of hydrogels by controllably increasing the crosslinking density of the network. Methods based on sequential polymerization using Michael addition,[93, 94] radical-mediated acrylate chemistry,[95, 96] and radical-mediated thiol-ene click chemistry[97, 98] as well as secondary crosslinking using inverse electron-demand Diels Alder (IEDDA) tetrazine click chemsitry[99] and tyrosine ligation using mushroom tyrosinase[100-102] or flavin mononucleotide[103] have been reported. However, an increase in covalent crosslinking density can limit cell motility and spreading, and such methods can have the added effect of locking cells in their starting shape[97] which may influence their phenotype.[104-107] As an alternative, dynamic reversible crosslinking using physical crosslinking methods such as ionotropic alginate crosslinking[108] and supramolecular methods such as oligonucleotide complexation[109] and

beta-cyclodextrin host-guest interactions[110] have also been used to cyclically stiffen and soften hydrogel networks. The controllable modulation of substrate stiffness has the potential to create *in vitro* models of pathologies and healthy physiological processes which exhibit increases in tissue stiffness, including fibrotic diseases,[111-114] cancer,[115] embryonic development,[116-118] and the regulation of cell division.[119]

I.3.2 Tissue Repair and Bioprinting

Extrudable and injectable hydrogels are of high interest as carriers for cell-based therapeutics, as well as more conventional chemotherapeutic drugs. Importantly, the clinical use of injectable cell therapies has been limited by low cell viability and retention post-delivery. However, injectable hydrogels can serve to protect cells from shear-induced damage during extrusion.[120] Extrudable hydrogels also can serve as bio-inks for extrusion-based 3D bioprinting of complex constructs for tissue engineering and regenerative medicine.[121, 122] In either application, the requirements for an extrudable or injectable hydrogel are the same: the material must flow under shear and then exhibit robust and stable mechanical properties after deposition or installation. These requirements are typically achieved via one of two approaches: *in situ* crosslinking or the use of shear-thinning materials.

In situ hydrogel crosslinking allows injection of the low viscosity sol before the formation of the elastic gel at the site of deposition. Many *in situ* crosslinking methods use stimuli-controlled covalent crosslinking, such as UV-photocontrolled reactions like radical-mediated thiol-ene chemistry[123] or free radical vinyl polymerization of gelatin-methacrylate.[124] However, stimulus-controlled physical crosslinking can also be used for

in situ gelation. Block-co-polymer systems can be tuned to create gels which exhibit a pH-[125] or temperature-[126-128] responsive phase transitions. While *in situ* crosslinking methods have the potential to rapidly achieve the desired robust mechanical properties at the delivery site, a slow-reacting gel may be deformed or the sol washed away before the polymerization reaction is complete. Furthermore, stimulus-controlled polymerization can be limited by the site of injection. For photomediated polymerization methods, opaque tissues can limit application. Temperature- and pH-mediated methods can exhibit variability from site-to-site, as these factors can vary between environments and organisms.

In contrast, shear-thinning hydrogels leverage dynamic bonds which can break and re-form to initiate flow under shear stress and recover their initial mechanical properties after the shear is removed (i.e., self-heal). The earliest injectable hydrogels relied on physical interactions between block co-polymers, such as pluronic,[129, 130] though these materials exhibited poor long-term stability and easily dissolved at the site of installation. Supramolecular crosslinking mechanisms such as host-guest interactions, multivalent hydrogen bonding domains, and molecular recognition motifs have been leveraged to create more stable shear-thinning injectable hydrogels. Additionally, shear-thinning hydrogels can be stabilized at the site of installation via secondary covalent Michael addition reaction[131, 132] or pH-responsive dynamic covalent crosslinking via Schiff base linkages,[133] boronic ester bonds,[134] oxaborole-diol bonds,[135] or hydrazone bonds.[136]

I.4 Significance and Approach

The overarching objective of this work was to improve the understanding of how the choice of crosslinking chemistry influences hydrogel properties and how these influences can be leveraged to engineer novel materials. Specifically, we addressed the hypothesis that supramolecular secondary interactions between the products of the tetrazine-norbornene IEDDA click reaction facilitated physical crosslinking and were responsible for differences in bulk hydrogel properties. Previously, step growth click crosslinking reactions with high efficiency, such as tetrazine-norbornene and radical-mediated thiol-ene click chemistry, were assumed to be interchangeable; hydrogels made from the same polymer with identical molecular weights, functionalities, and concentrations were expected to have nearly identical properties. However, a review of the published literature challenges this assumption. Fairbanks et al. synthesized hydrogels from 20 kDa, 4-arm end-functionalized PEG-norbornene crosslinked with a bis-cysteine enzymatically labile peptide and reported shear storage moduli ranging from 300 ± 20 to 1700 ± 360 Pa for 3–10 wt.% PEG macromer gels.[31] In contrast, Alge et al. synthesized gels from 20 kDa 4-arm end-functionalized PEG-tetrazine with a di-norbornene-functionalized enzymatically labile peptide crosslinker of a similar size and composition and achieved a 38% higher storage modulus (2345 ± 312 Pa) in gels made with 10 wt.% PEG, despite the relatively low (75%) degree of functionalization of the 4-arm PEG-tetrazine.[35] It was unlikely that these differences were attributable to differences in crosslinking efficiency given the exceptionally high efficiency of the

radical-mediated thiol-ene reaction,[31] particularly when compared with prior methods such as Michael addition crosslinking.[137]

The first aim of this work was to challenge the assumption that gels made from polymer chains with identical compositions and molecular weights, identical functionalities and identical concentrations will exhibit nearly identical properties, regardless of the crosslinking chemistry. This aim was achieved through a head-to-head comparison of PEG hydrogels chemically crosslinked via tetrazine-norbornene IEDDA and radical-mediated thiol-ene click chemistry, and the results showed radically different hydrogel properties (**Chapter II**). Subsequently, we aimed to address the gap in knowledge as to why there were such significant and unexpected differences in the properties of PEG-based gels synthesized with tetrazine-norbornene click chemistry.

It was hypothesized that secondary interactions between the tetrazine-norbornene click products (TNCP) may be responsible for these differences in gel properties. An investigation comparing tetrazine click-crosslinked and thiol-ene click-crosslinked PEG hydrogels confirmed the discovery of secondary, supramolecular interactions between TNCP which were alone sufficient to facilitate gelation in a multi-arm PEG system (**Chapter II**).

Following the discovery of supramolecular interactions between TNCP, Subsequently, applications of these supramolecular interactions were explored in a 3D cell culture platform (**Chapter III**) as well as in extrudable shear-thinning hydrogels (**Chapter IV**). First, monofunctional PEG-tetrazine was diffused into pre-existing, partially covalently crosslinked multi-arm PEG networks with free norbornene groups to

install pendant TNCP. As the tetrazine click reaction proceeded, pendant TNCP formed supramolecular crosslinks within the network, stiffening the bulk gel. This approach yielded an approximately 2 kPa increase in shear storage modulus in enzymatically-degradable PEG-peptide scaffolds over the course of 4-6 hours. Additionally, this approach demonstrated long-term retention of the elevated gel stiffness in culture conditions and no effect on the viability of encapsulated cells.

Finally, gelatin functionalized with pendant TNCP was utilized to create a shear-thinning and self-healing extrudable hydrogel. An increase in gel modulus due to TNCP supramolecular interactions in gelatin-based gels was first verified, confirming that TNCP supramolecular interactions had similar effects in gelatin hydrogels as seen in PEG hydrogels. Gelatin-norbornene was then functionalized with pendant TNCP, which induced gelation. These gelTNCP gels exhibited shear-thinning as well as recovery of their initial high viscosity after shear. Additionally, thiol-functionalized 4-arm PEG and a photoinitiator could be added to the supramolecular gel to facilitate photomediated secondary covalent crosslinking after extrusion. In short, TNCP supramolecular crosslinking is an exciting new addition to the toolkit of bio-orthogonal hydrogel crosslinking methods with broad potential applicability in both synthetic and natural polymers.

CHAPTER II

HYDROGEL SYNTHESIS AND STABILIZATION VIA TETRAZINE CLICK-INDUCED SECONDARY INTERACTIONS[1]

II.1 Introduction

Chemical reactions fitting the click chemistry paradigm have become an indispensable tool for the synthesis and functionalization of hydrogel biomaterials. Specifically, IEDDA click reactions between s-tetrazines and electron rich dienophiles like norbornene and trans-cyclooctene are attractive because of their bio-orthogonality. Importantly, tetrazine click reactions proceed readily under physiologic temperatures and pH in aqueous solvent without the need for an initiator or catalyst, do not react with surrounding biological molecules, and produce only gaseous nitrogen as a by-product. Since the demonstration of IEDDA tetrazine click reactions' utility for bioconjugation,[138] they have been applied in myriad applications including polymer functionalization,[139, 140] micelle functionalization,[141] synthesis of radiolabeled probes for PET imaging,[142, 143] fluorogenic labeling *in vitro* and *in vivo,*[144, 145] polymeric nanoparticle synthesis,[146] and polymer-nucleic acid conjugation.[147]

Due to its bio-orthogonality, tetrazine click chemistry has attracted significant interest in recent years for the synthesis of hydrogels for 3D cell culture and tissue

[1] Data in this chapter is reprinted with permission from "Hydrogel Synthesis and Stabilization via Tetrazine Click-Induced Secondary Interactions" by Samantha E. Holt, Amanda Rakoski, Faraz Jivan, Lisa M. Pérez, and Daniel L. Alge, 2020. *Macromolecular Rapid Communications*, 41(14), 2000287.

engineering. To date, studies have reported cell encapsulation in PEG,[35] alginate,[148, 149] and gelatin hydrogels[150] using the tetrazine-norbornene click reaction. Additionally, the bio-orthogonality of tetrazine click reactions makes them valuable tools for the delivery of sensitive protein drugs. Tetrazine-norbornene click-crosslinked gelatin containing laponite nanoparticles has been used as an injectable controlled release protein delivery platform,[151] and tetrazine-norbornene click chemistry has also been used to conjugate proteins to PEG microgels without compromising bioactivity.[152] Recent work has introduced stimuli-responsiveness to trans-cyclooctene-tetrazine IEDDA reactions to enable spatial and temporal control and create hydrogel microchannels and microfibers.[153-157] Additionally, tetrazine-norbornene IEDDA and nucleophilic thiol-yne click chemistry have been used together to form double network PEG hydrogels.[158]

In addition to the aforementioned work on IEDDA tetrazine click reactions, the literature on hydrogel biomaterials contains a plethora of research using Michael-addition thiol-ene reactions,[159, 160] radical-mediated thiol-ene reactions,[31] strain-promoted azide-alkyne cycloadditions,[161] and oxime click chemistry[40] to crosslink hydrogels for 3D cell culture and tissue engineering. To date, the field has largely operated under the assumption that so long as click reactions proceed with comparable efficiency, they can be used interchangeably to produce hydrogels with comparable bulk properties. The few direct comparisons between click crosslinking reactions that have been performed to date support this assumption, as they have shown that differences in bulk hydrogel properties can be attributed to differences in reaction efficiency and, thus, network homogeneity.[160, 162]

However, no previous direct comparisons of tetrazine click chemistry to other covalent click crosslinking strategies and their impact on hydrogel bulk properties exist in the literature. Because the tetrazine click reaction does not require the presence of free radicals, it may be more fitting for sensitive biological applications where radical-mediated reactions, such as radical-mediated thiol-ene click chemistry, could contribute to damage of surrounding proteins and other biomolecules. Potential differences in the bio-orthogonality of tetrazine click crosslinking and radical-mediated thiol-ene click crosslinking specifically motivated a direct comparison between the bulk properties of their resultant hydrogels.

Unexpectedly, the differences in mechanical properties and degradation between hydrogels made with tetrazine click crosslinking and radical-mediated thiol-ene crosslinking were found to be robust and significant. Herein, we report the discovery of strong secondary interactions between the cycloaddition products of the tetrazine-norbornene IEDDA click reaction in polymer hydrogels. This discovery was achieved by exploiting the ability of norbornene to react with s-tetrazines via IEDDA mechanism and with thiols via radical mediated thiol-norbornene (*i.e.*, thiol-ene) click chemistry[31] and performing a head-to-head comparison of these reactions for PEG hydrogel synthesis. Additionally, these supramolecular interactions were found to increase the stiffness and resistance to hydrolytic degradation of covalently crosslinked hydrogels compared to those crosslinked using radical-mediated thiol-ene click chemistry. Molecular dynamics simulations supported the presence of supramolecular interactions between the tetrazine-norbornene click products (TNCP) formed in the network. The presence of

supramolecular TNCP interactions was further confirmed by the non-covalent assembly of 4-arm PEG end-functionalized with TNCP in the absence of covalent crosslinking. The presence of TNCP supramolecular crosslinking has profound implications for the future application of tetrazine click chemistry in engineered hydrogel materials.

II.2 Materials and Methods

II.2.1 General Procedures and Methods

Unless otherwise specified, all chemicals and reagents were used as received from commercial sources. Lithium acylphosphinate (LAP) was synthesized according to established protocols.[163] 4-arm, 20 kDa PEG-tetra-thiol (PEG-4-SH) was purchased from Laysan Bio, Inc. and used without further modification.

II.2.2 PEG-Norbornene Macromer Functionalization

4-arm 20 kDa PEG-hydroxyl (JenKem Technologies USA) and 2 kDa linear PEG-hydroxyl (Laysan Bio, Inc.) were functionalized with norbornene acid as previously described[152] with slight modification to yield PEG-tetra-norbornene (PEG-4-NB) and PEG-di-norbornene (PEG-2-NB).

II.2.2.1 PEG-tetra-norbornene synthesis

Briefly, 10 g 4-arm 20kDa PEG-hydroxyl (0.5 mmol), 0.122 g 4-(dimethylamino)pyridine (0.5X to PEG-OH, 1 mmol, Sigma-Aldrich), 0.81 mL pyridine (5X to PEG-OH, 10 mmol Sigma-Aldrich), and 60 mL anhydrous dichloromethane (Acros Organics) were dissolved in round-bottom flask under argon. Separately, 1.22 mL 5-Norbornene-2-carboxylic acid (10 COOH:1 PEG-OH, 10 mmol, Alfa Aesar), 0.77 mL diisopropylcarbodiimde (5 mmol, Alfa Aesar), and 30 mL anhydrous

dichloromethane were mixed for 45 min at room temperature in a reaction vessel under argon to generate a dinorbornene anhydride, which was filtered to remove precipitated urea salts and then added to the round-bottom flask containing PEG. The solution was allowed to react overnight at room temperature, after which it was precipitated on ice in 10-fold excess of diethyl ether (Fisher Chemical) chilled to 4°C and vacuum filtered to yield a white precipitate of functionalized PEG. The product was then filtered twice and dried under vacuum for 24 h, dialyzed against deionized water for 48 h (MWCO = 10 kDa), and lyophilized to obtain purified PEG-norbornene. Norbornene functionalization was verified via proton NMR and analysis indicated 96% functionalization, **Figure II.1**. ^{1}H NMR (400 MHz, CDCl3) δ 6.22 – 6.07 (m, 1H), 5.94 (dd, J = 5.7, 2.8 Hz, 1H), 4.28 – 4.11 (m, 2H), 3.64 (s, ~454H per arm).

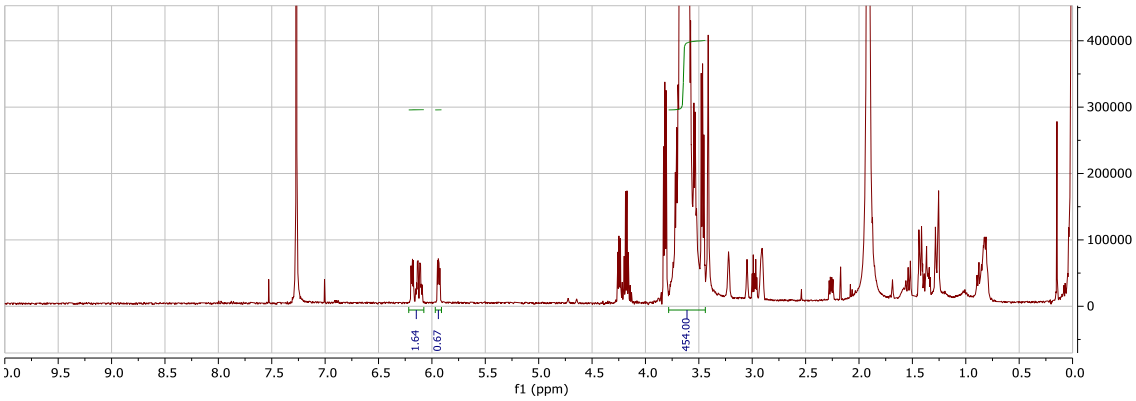

Figure II.1 ^{1}H NMR spectra of 20 kDa PEG-tetra-norbornene in CDCl3. Analysis indicated 96% end group functionalization. 1H NMR (400 MHz, CDCl3) δ 6.22 – 6.07 (m, 1H), 5.94 (dd, J = 5.7, 2.8 Hz, 1H), 4.28 – 4.11 (m, 2H), 3.64 (s, ~454H per arm). Reprinted from Holt et al.[164]

II.2.2.2 PEG-di-norbornene synthesis

2 kDa PEG-hydroxyl (Alfa Aesar) was functionalized with norbornene acid to yield PEG-di-norbornene as described above with the following modifications. 5.0 g 2kDa PEG-hydroxyl (2.5 mmol, 5.0 mmol -OH) was used, along with 0.30 g 4-(dimethylamino)pyridine (0.5X to -OH, 2.5 mmol, Sigma-Aldrich), 2.0 mL pyridine (5X to -OH, 25 mmol Sigma-Aldrich), and 20 mL anhydrous dichloromethane (Acros Organics). Additionally, 6.1 mL 5-Norbornene-2-carboxylic acid (10 COOH:1 PEG-OH, 50 mmol, Alfa Aesar), 3.9 mL diisopropylcarbodiimde (25 mmol, Alfa Aesar), and 15 mL anhydrous dichloromethane were used in the dinorbornene anhydride reaction. After being precipitated, filtered, and dried, the product was dialyzed against deionized water for 48 h (MWCO=1kDa) and lyophilized to obtain purified PEG-norbornene. Norbornene functionalization was verified via proton NMR and analysis indicated 90% functionalization, **Figure II.2**. ^{1}H NMR (400 MHz, CDCl3) δ 6.21 – 6.08 (m, 3H), 5.94 (dd, J = 5.7, 2.8 Hz, 1H), 4.30 – 4.09 (m, 4H), 3.64 (s, ~182H).

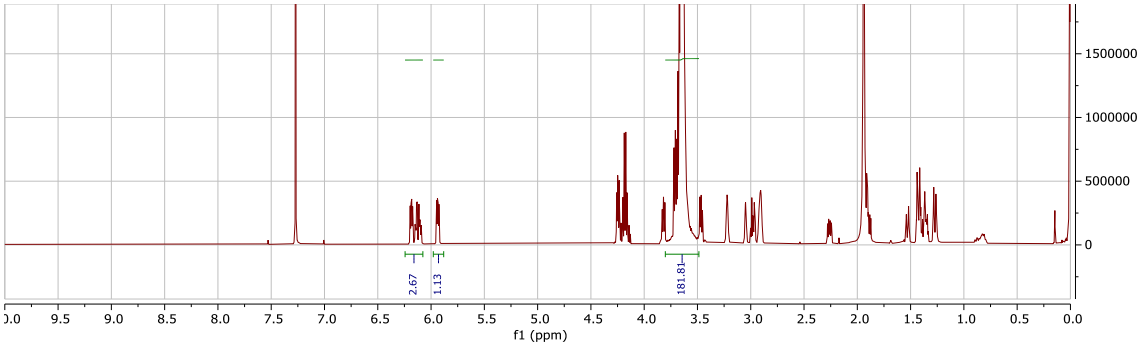

Figure II.2 ^{1}H NMR spectra of 2 kDa PEG-di-norbornene in CDCl3. Analysis indicated 90% end group functionalization. 1H NMR (400 MHz, CDCl3) δ 6.21 – 6.08 (m, 3H), 5.94 (dd, J = 5.7, 2.8 Hz, 1H), 4.30 – 4.09 (m, 4H), 3.64 (s, ~182H). Reprinted from Holt et al.[164]

II.2.3 PEG-Tetrazine Macromer Functionalization

II.2.3.1 PEG-tetra-tetrazine synthesis

4-arm, 20 kDa PEG-amine (JenKem USA) was functionalized with tetrazine carboxylic acid (Tz-COOH) to yield 4-arm PEG-tetrazine (PEG-4-Tz) as previously described with slight modification.[35] First, 5-(4-(1,2,4,5-Tetrazin-3-yl)benzylamino)-5-oxopentanoic acid (Tz-COOH) was synthesized by reacting 5-(4-(cyano)benzylamino)-5-oxopentanoic acid with hydrazine, formamidine acetate, and zinc triflate catalyst, as previously described.[165] 1.0 g 4 arm, 20 kDa PEG-NH_2 (0.05 mmol, 0.20 mmol -NH_2) was added to a dry, argon purged vessel, dissolved in 10 mL of 1-Methyl-2-Pyrrolidinone (NMP, Chem Impex) with 0.06 mL triethylamine (2X to -NH_2, 0.40 mmol, Alfa Aesar), and allowed to mix for approximately 15 min. In a separate dry, argon purged vessel 0.30 g of Tz-COOH (5X to -NH_2, 1.0 mmol) was dissolved in 5 mL NMP and activated with 0.38 g O-(Benzotriazol-1-yl)-N,N,N',N'-tetramethyl-uronium

hexafluorophosphate (5X to -NH_2, 1.0 mmol, HBTU, Chem Impex) for 5 min. The activated Tz-COOH was mixed with the PEG amine and allowed to react at room temperature for 15 h. The reaction mixture was then precipitated in 40 mL cold diethyl ether (4°C) and centrifuged to remove the salt byproducts, then dried under vacuum and dialyzed against ultrapure water for 48 h and lyophilized. Tetrazine functionalization was verified via proton NMR and indicated 80% functionalization, **Figure II.3**. ^{1}H NMR (500 MHz, DMSO-d6) δ 10.57 (s, 1H), 8.48 – 8.40 (m, 3H), 7.84 (t, *J* = 5.7 Hz, 1H), 7.53 (d, *J* = 8.1 Hz, 2H), 4.39 (d, *J* = 6.0 Hz, 3H), 3.50 (s, ~454H), 2.17 (t, *J* = 7.5 Hz, 2H), 2.09 (t, *J* = 7.5 Hz, 2H), 1.75 (p, *J* = 7.5 Hz, 2H).

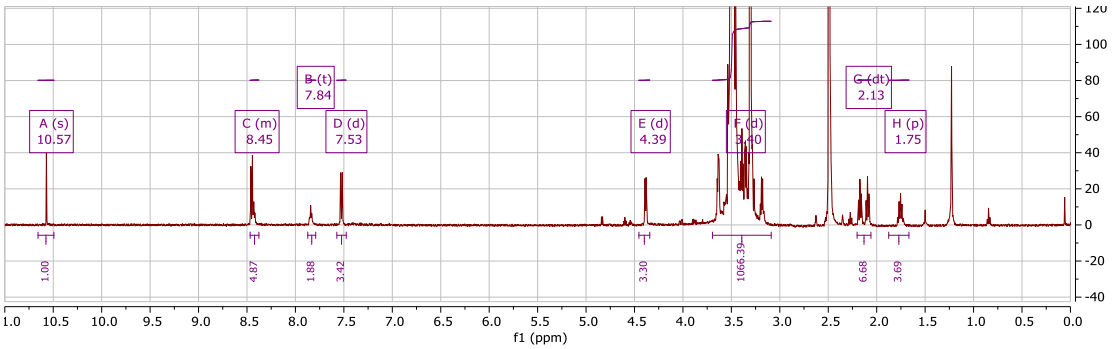

Figure II.3 ^{1}H NMR spectra of 20 kDa PEG-tetra-tetrazine in DMSO-d6. Analysis indicated 80% end group functionalization. ^{1}H NMR (500 MHz, DMSO-d6) δ 10.57 (s, 1H), 8.48 – 8.40 (m, 3H), 7.84 (t, *J* = 5.7 Hz, 1H), 7.53 (d, *J* = 8.1 Hz, 2H), 4.39 (d, *J* = 6.0 Hz, 3H), 3.50 (s, ~454H), 2.17 (t, *J* = 7.5 Hz, 2H), 2.09 (t, *J* = 7.5 Hz, 2H), 1.75 (p, *J* = 7.5 Hz, 2H). Reprinted from Holt et al.[164]

II.2.3.2 Methoxy-PEG-tetrazine synthesis

Linear 5 kDa methoxy-PEG-amine (mPEG-NH_2, Laysan Bio) was functionalized with Tz-COOH to yield methoxy-PEG-tetrazine (mPEG-Tz) as described above with the following modifications. 1.03 g of 5 kDa mPEG-NH_2 (0.20 mmol, 0.82 mmol -NH_2) was added to a dry, argon purged vessel and dissolved in 3 mL NMP with 0.23 mL triethylamine (2X to -NH_2,1.63 mmol). 0.37 g Tz-COOH (1.5X to -NH_2, 1.23 mmol) was dissolved in NMP and activated with 0.47 g HBTU (1.5X to -NH_2, 1.23 mmol) for 5 min. Tetrazine functionalization was verified via proton NMR and indicated 90% functionalization, **Figure II.4**. ^{1}H NMR (400 MHz, DMSO) δ 10.58 (s, 1H), 8.50 – 8.40 (m, 3H), 7.86 (t, J = 5.6 Hz, 1H), 7.57 – 7.50 (m, 2H), 4.39 (d, J = 6.0 Hz, 2H), 3.51 (s, ~454H), 2.14 (dt, J = 31.1, 7.5 Hz, 4H), 1.82 – 1.70 (m, 2H).

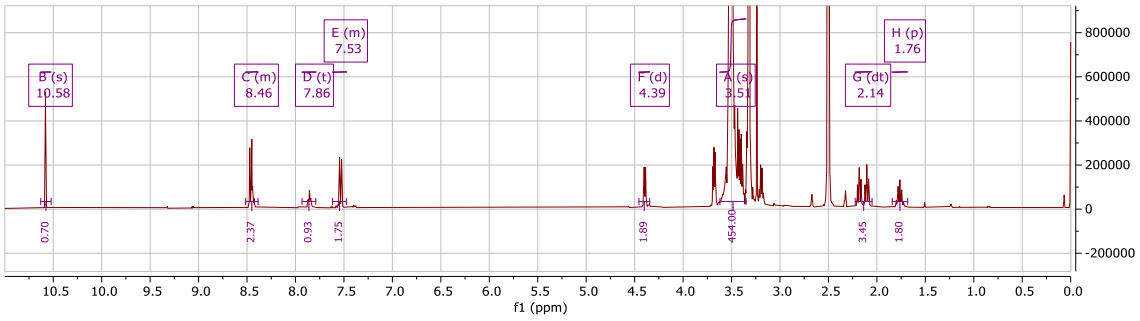

Figure II.4 ^{1}H NMR spectra of 5 kDa methoxy-PEG-tetrazine in DMSO-d6. Analysis indicated 90% end group functionalization. ^{1}H NMR (400 MHz, DMSO) δ 10.58 (s, 1H), 8.50 – 8.40 (m, 3H), 7.86 (t, J = 5.6 Hz, 1H), 7.57 – 7.50 (m, 2H), 4.39 (d, J = 6.0 Hz, 2H), 3.51 (s, ~454H), 2.14 (dt, J = 31.1, 7.5 Hz, 4H), 1.82 – 1.70 (m, 2H). Reprinted with permission from Holt et al.[164]

II.2.4 Synthesis and In Situ Gelation of Non-Covalently Crosslinked Hydrogels

A solution of PEG-4-NB at 10% w/w in deionized water was combined with mPEG-Tz at a 1:1 ratio of norbornene to tetrazine. Gels were allowed to polymerize at room temperature for 30 min, and then immediately dried under vacuum for 48 h. The dry mass of the combined sol and gel fractions was recorded. Dried gels were then swelled in double deionized water for 24 h on the orbital shaker at room temperature to wash out the uncrosslinked sol fraction. The swelled gels were dried again for 24 h under vacuum, and the dry mass of the remaining gel fraction was recorded. Sol fraction was calculated as the ratio of the sol fraction dry mass to the combined dry mass of the sol and gel fractions. Swelling ratio was also calculated. Gel samples were swelled to equilibrium for 64 hours in deionized water and the swollen mass was recorded. Gels were dried overnight at 60°C and dry mass was recorded. Swelling ratio, Q, was calculated using **Equation 1**, where W_s is the mass of the sample at equilibrium swelling and W_d is the dry mass of the sample.

Equation 1

$$Q = \frac{W_s - W_d}{W_d}$$

Gelation was monitored using time-sweep rheology for non-covalently crosslinked gels. A solution of 10% w/w PEG-4-NB in deionized water with mPEG-Tz added at a 1:1 tetrazine-ene ratio was pipetted between the lower Peltier plate and the 8 mm parallel plate of an Anton Parr Physica MCR 301 rheometer. G' and G" were then monitored as a function of time at a constant frequency of 1 rad s^{-1} and constant strain of 1% over the course of 2 h at 21°C (room temperature).

II.2.5 Characterization of Tetrazine-Norbornene Reaction Kinetics

The kinetics of the tetrazine-norbornene IEDDA reaction were tracked by monitoring the characteristic absorbance of unreacted tetrazine at 520 nm.[166] A solution of 5kDa mPEG-Tz at a concentration of 12 mM in phosphate buffered saline (PBS) was combined in a 96-well plate with either 6 mM of PEG-2-NB (2 kDa), 6 mM of PEG-2-NB that had been reacted with L-cysteine at a 1:1 thiol-ene ratio (not reported), or no additional norbornene-containing macromer. Using an Infinite M 200 Pro plate reader (Tecan), absorbance at 520 nm was measured over the course of 1 h with one reading per minute. Absorbance over time was averaged over three samples.

II.2.6 Dynamic Light Scattering

Dynamic Light Scattering (DLS) was performed using a Malvern Zetasizer Nano ZS. Samples were prepared at a concentration of 1 mg/mL in 0.2 μm syringe-filtered PBS. Those samples were then filtered through a 0.2 μm syringe filter with a PVDF membrane. Samples were added into 70 μL cuvettes which had been rinsed twice with 0.2 μm syringe-filtered PBS. Measurements were performed in triplicate in sets of 11 acquisitions.

II.2.7 Covalently Crosslinked Hydrogel Preparation

Two types of gel samples were prepared for characterization: IEDDA tetrazine-norbornene polymerized gels, referred to as tetrazine gels, and radical-mediated thiol-norbornene polymerized gels, referred to as thiol-ene gels.

Tetrazine gels were prepared by combining 7.5% w/w (3.54 mM) 20 kDa PEG-4-Tz with 1 mM norbornene-functionalized peptide GRGDS (synthesized as previously

described[35]) and 7.08 mM PEG-2-NB in PBS. The total ratio of tetrazine to norbornene in the pre-gel solution was 1:1. Pre-gel solution was added to 8 mm diameter and 1 mm thick silicone gaskets on top of glass slides treated with Sigmacote (Sigma Aldrich). Tetrazine gels were allowed to polymerize at room temperature for 30 min.

Thiol-ene gels were prepared by combining 7.5% w/w (3.73 mM) 20 kDa PEG-4-SH with 2 mM photoinitiator LAP, 1 mM norbornene-functionalized peptide GRGDS, and 7.45 mM PEG-2-NB in PBS. To prevent disulfide bond formation, PEG-4-SH was kept at -20°C in small aliquots used within two freeze-thaw cycles, kept at room temperature for less than 1 hr., and mixed thoroughly via vortex before use. The total ratio of thiol to norbornene in the pre-gel solution was 1:1. Pre-gel solution was added to 8 mm diameter and 1 mm thick silicone gaskets on top of glass slides treated with Sigmacote (Sigma Aldrich). Thiol-ene gels were then crosslinked via 365 nm UV light for 5 min at 10 mW/cm^2. For a 1 mm thick gel sample with a LAP concentration of 2 mM and light exposure for 5 min, light attenuation through the sample is expected to be less than 10%. Post-polymerization, both tetrazine and thiol-ene gels were swelled in excess PBS.

II.2.8 Gel Hydrolysis for NMR

Thiol-ene crosslinked gel samples were prepared as described above with the slight modification of the use of an 8 mm diameter, 2 mm height round silicone mold to create a sample with a pre-swollen volume of 105 μL. Gel samples were individually incubated in 1 mL 0.1 N NaOH at 37°C for 1 h, then frozen at -80°C for 4 h. Frozen samples were lyophilized overnight. The mass of lyophilized samples was measured and

samples were dissolved in 800 μL $CDCl_3$ for 48 h to ensure complete solvation. After 48 h, 400 μL of $CDCl_3$ was added to bring the sample volume back to 800 μL, and samples were centrifuged at 21,380 RCF for 5 min to separate residual salts. ^1H NMR was analyzed using a Bruker Avance Neo 400 Hz console.

II.2.9 Characterization of Swelling Ratio and Gel Fraction

Swelling ratio was characterized for thiol-ene and tetrazine click-crosslinked gels. Post- polymerization, gel samples were swelled to equilibrium overnight in PBS, and the swollen mass was recorded. Gels were dried overnight at 60°C and dry mass was recorded. Swelling ratio, Q, was calculated using Equation 1 as previously described.

Gel fraction was also characterized. Immediately post photopolymerization, thiol-ene and tetrazine click gels were dried under vacuum for 24 h and the dry mass of the combined sol and gel fractions was recorded. Dried gels were then swelled in double deionized water for 24 h on the orbital shaker at room temperature to wash out the uncrosslinked sol fraction. The swelled gels were dried again for 24 h under vacuum, and the dry mass of the remaining gel fraction was recorded. Sol fraction was calculated as the ratio of the sol fraction dry mass to the combined dry mass of the sol and gel fractions.

II.2.10 Rheological Characterization

Gel samples were swelled overnight (~18 hours) to equilibrium. Storage modulus (G') was assessed by taking the average over the linear viscoelastic region of a strain sweep from 0.01% to 20% strain at a frequency of 1 rad/s. Tests were performed on a TA Discovery HR-2 rheometer with parallel-plate geometry (8 mm diameter).

In-situ gelation experiments were performed using an Anton Paar Physica MCR 301 rheometer. For thiol-ene crosslinked gels, 40 μL of pre-gel solution prepared as described previously was added to the stage and a time sweep was performed at 1% strain and 1 rad/s at 37°C using an 8 mm diameter parallel-plate geometry. After 1 min the sample was exposed to 365 nm UV light at an intensity of 10 mW/cm^2 for 5 min, at which point the time sweep was terminated. Tetrazine click-crosslinked samples were prepared by adding 20 kDa PEG-4-Tz to the remaining components of the pre-gel solution immediately before adding a 40 μL sample to the stage. Time sweeps were performed at 1% strain and 1 rad/s at 37°C using an 8 mm diameter parallel-plate geometry over the course of 30 min.

II.2.11 Degradation Studies

Degradability via base-catalyzed hydrolysis was assessed. Gel samples were synthesized and swelled to equilibrium overnight. The starting mass of each sample was then recorded, and then gels were submerged in 0.1 N sodium hydroxide and kept at 37°C. The remaining wet mass was recorded every 15 minutes for the first 2 h, then every 2 h up to 8 h total, and then again at 24 h. After 24 h, remaining gel samples were rinsed in PBS and subjected to rheological analysis.

II.2.12 Computational Details

Model systems for thiol-norbornene and tetrazine-norbornene were subjected to solvent-explicit, all-atom molecular dynamics simulations using the GPU-accelerated DESMOND[167] software and the OPLS3 force field.[168, 169] A periodic TIP4P water orthorhombic box with a 20Å buffer was used for the solvation box. The NPT ensemble

class with a temperature of 300 K and a pressure of 1.01325 bar was used. Each molecular dynamic production run was carried out for 60.0 ns which included the multisim relaxation procedure. The recording interval was set to 20.0 ps for the trajectory and energy.

II.3 Results and Discussion

II.3.1 Comparison of Covalently Crosslinked Hydrogels

The dual reactivity of the cyclic alkene norbornene with either thiol groups via radical-mediated thiol-ene click chemistry or s-tetrazines via IEDDA click chemistry enabled the direct comparison of otherwise identical hydrogels made with either click crosslinking reaction. The requirements for the two reactions vary; while the IEDDA tetrazine reaction proceeds spontaneously under physiologic conditions (aqueous solution, pH 7.4, 37°C), the thiol-ene reaction requires the generation of free radicals most often supplied via a photo- or thermal initiator.

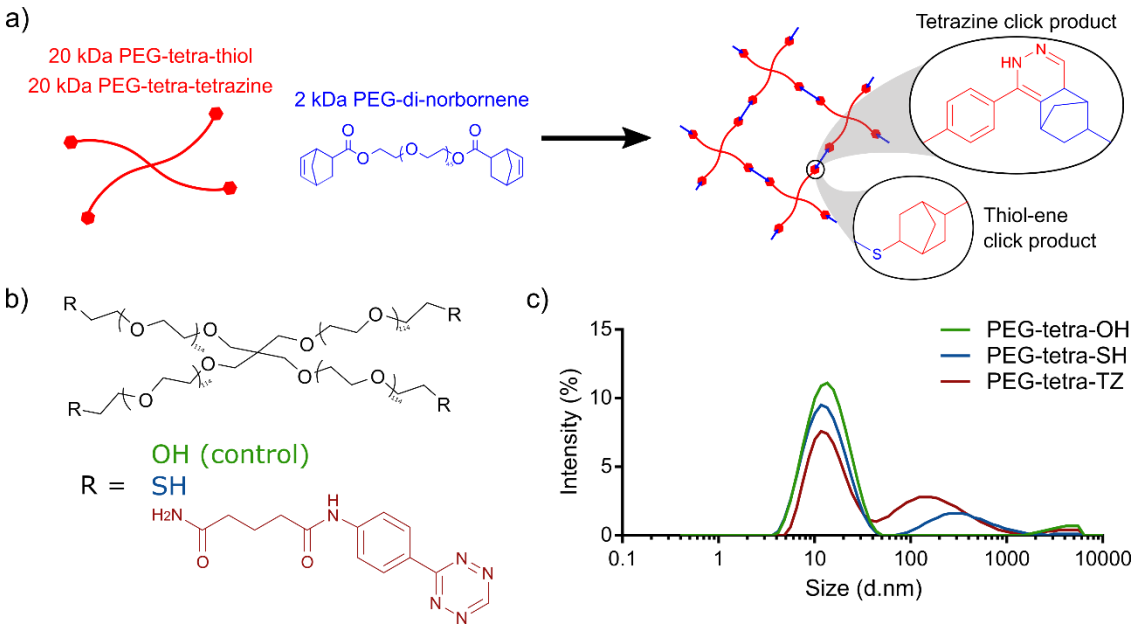

Figure II.5 (a) Dual reactivity of norbornene with either s-tetrazines or thiols to form a PEG hydrogel network. (b) Structure diagrams of tetrafunctional PEG macromers characterized via DLS. (c) DLS characterization indicates similar size and aggregation of PEG macromers functionalized with thiol or tetrazine.

To compare the impact, if any, of the choice of crosslinking chemistry on the properties of the resultant hydrogels, PEG hydrogels were synthesized by reacting PEG-2-NB (2 kDa) with either PEG-4-SH (20 kDa) for thiol-ene crosslinking or PEG-4-Tz (20 kDa) for tetrazine-norbornene crosslinking, **Figure II.5a**. The molecular weights and functionalities of the polymer macromers used in both gel formulations were chosen to be identical, with the only difference being the end functional groups, **Figure II.5b**. Characterization of both tetrafunctional macromers via DLS showed that they exhibited similar size and degree of aggregation, **Figure II.5c**. Additionally, both gel formulations

used identical concentrations of all components, with the exception of the photoinitiator used in the thiol-ene crosslinked gels.

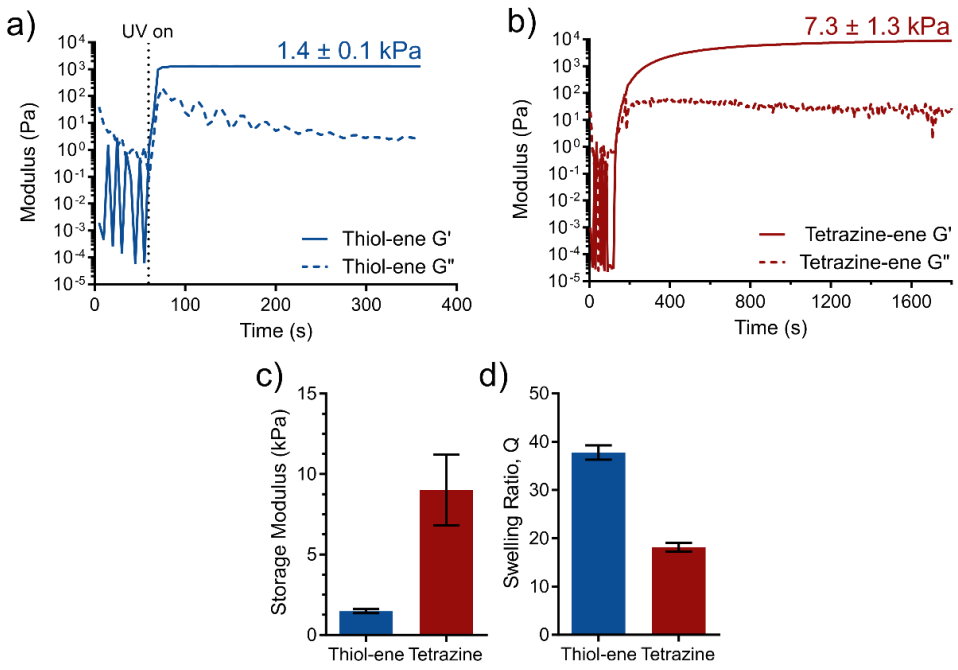

Figure II.6 (a) Modulus evolution via *in situ* rheology of thiol-ene crosslinked gels indicates rapid gelation following UV exposure. (b) Modulus evolution of tetrazine crosslinked hydrogels. (c) Tetrazine crosslinked hydrogels demonstrate a six-fold higher shear storage modulus compared to thiol-ene crosslinked hydrogels at equilibrium swelling. (d) Thiol-ene crosslinked hydrogels demonstrate a swelling ratio roughly double that of tetrazine crosslinked gels.

Unexpectedly, the two gel formulations demonstrated marked differences in bulk mechanical properties. First, as shown in **Figure II.6a** and **Figure II.6b**, rheological characterization of modulus evolution during *in situ* polymerization showed a five-fold

greater shear storage modulus of tetrazine-crosslinked gels compared to thiol-ene crosslinked gels (7.3 ± 1.3 kPa vs. 1.4 ± 0.1 kPa). Second, after swelling the gels to equilibrium in PBS, the difference persisted, with a more than six-fold greater shear storage modulus observed in the tetrazine-crosslinked gels compared to the thiol-ene crosslinked gels (9.0±1.8 kPa vs. 1.4±0.1 kPa, $p < 0.0001$), **Figure II.6c**. Finally, the swelling ratio of the tetrazine click crosslinked gels was about half that of the thiol-ene crosslinked gels (18±0.7 vs. 38±1.2, $p < 0.005$), **Figure II.6d**. Both the higher storage modulus and the lower swelling ratio would be expected in the case of a gel with a higher crosslinking density than the thiol-ene crosslinked gels. However, theoretically, the crosslinking density in the tetrazine crosslinked and thiol-ene crosslinked gels should have been the same.

Furthermore, tetrazine-crosslinked gels exhibited increased resistance to hydrolytic degradation compared to thiol-ene crosslinked hydrogels. The PEG-2-NB crosslinker used in both gel formulations contained a hydrolytically labile ester linkage connecting the end norbornene functional groups and the length of PEG at the center. To test accelerated hydrolytic degradation of both gel formulations, tetrazine and thiol-ene click crosslinked gels were incubated in a 0.1 N sodium hydroxide solution (pH=13) at 37°C and the wet mass of the gels was recorded over 24 hours. While the thiol-ene crosslinked gels dissolved completely within 15 min, the tetrazine-crosslinked gels exhibited no significant mass loss over a period of 24 h, **Figure II.7a**. Subsequent shear storage modulus measurements shown in **Figure II.7b** revealed a decrease from 9.0 ± 1.8 kPa to 2.0 ± 0.5 kPa in tetrazine crosslinked gels post-sodium hydroxide treatment.

Remarkably, the storage modulus of these gels after hydrolysis was higher than the initial storage modulus of the thiol-ene crosslinked gels (1.4±0.1 kPa).

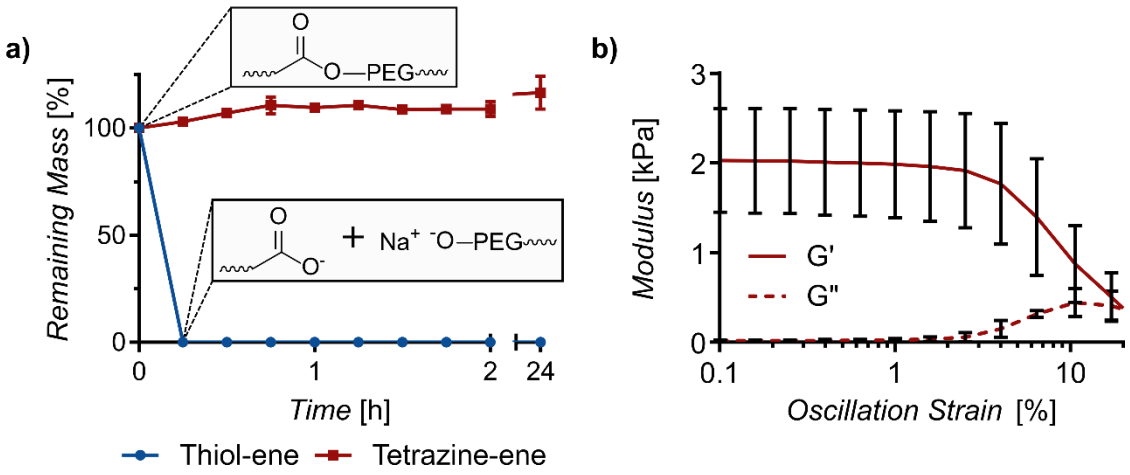

Figure II.7 (a) Thiol-ene crosslinked and tetrazine-crosslinked hydrogels gels were treated with 0.1 N NaOH for up to 24 h and mass loss over time was monitored. (b) Storage (G') and loss (G") modulus of tetrazine-crosslinked gels after base catalyzed hydrolysis via oscillatory rheology. Reprinted with permission from Holt et al.[164]

The relatively higher shear storage modulus, lower swelling, and higher resistance to degradation would suggest a substantially higher crosslinking density in the tetrazine crosslinked hydrogels compared to the thiol-ene crosslinked hydrogels. However, this is not supported by characterization and comparison of the crosslinking efficiency of the two reactions. First, quantification of the gel fraction of both gel formulations found no statistically significant difference between the thiol-ene crosslinked and tetrazine crosslinked gels (95±2.8% and 96±0.5 %, respectively, p =

0.43). Additionally, ^{1}H NMR of hydrolytically degraded thiol-ene crosslinked gels showed complete conversion of the norbornene alkene, **Figure II.8**. Norbornene conversion in tetrazine crosslinked gels was not quantified via proton NMR because a sample could not be obtained in solution, since they are not degradable via hydrolysis. However, given the complete conversion of norbornene indicated in three independent samples, the thiol-ene reaction efficiency must be close to 100%, consistent with the gel fraction data. These results are also consistent with previous reports on the efficiency of thiol-ene crosslinking.[31, 162, 170] Because the features of the tetrazine-crosslinked gels appear to be consistent with an even higher crosslink density (i.e., over 100%), these data suggest that these apparent differences in gel properties cannot be attributed to a deficiency in the thiol-ene crosslinking reaction. Instead, the observed differences in gel properties required an alternative explanation which then motivated investigation into tetrazine-norbornene click-induced secondary interactions.

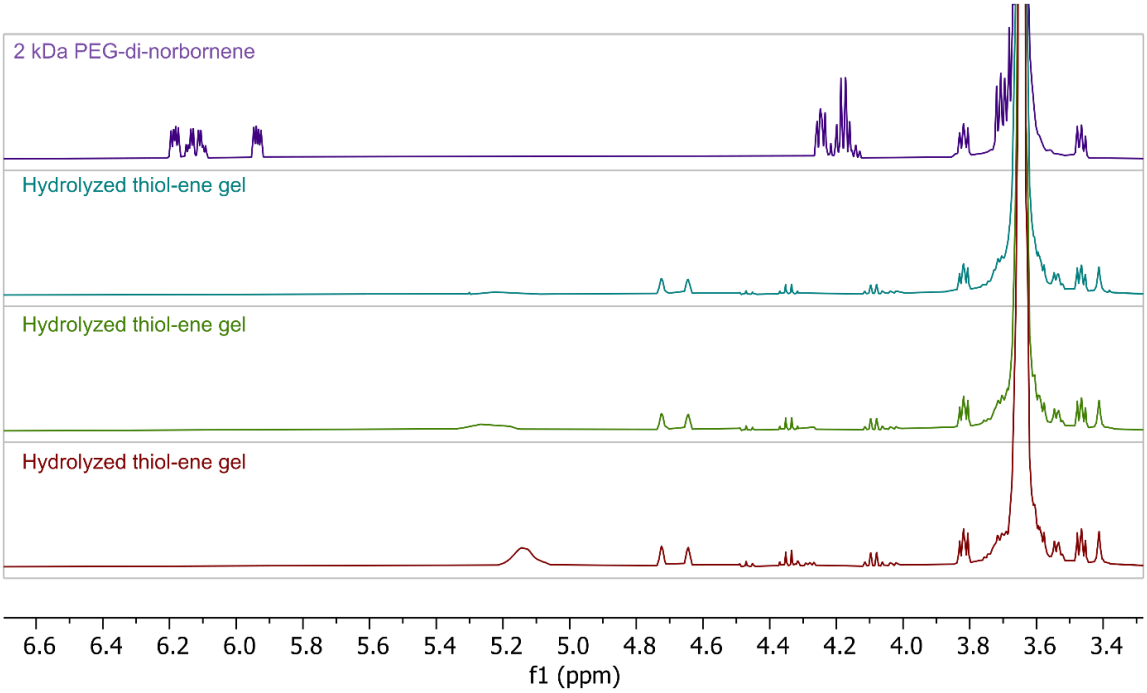

Figure II.8 ^{1}H NMR demonstration of thiol-ene crosslinking efficiency. Peaks indicating the presence of unreacted norbornene from δ5.93-5.95 and 6.09-6.20 are not seen in hydrolyzed thiol-ene crosslinked hydrogels. Reprinted with permission from Holt et al.[164]

II.3.2 Molecular Dynamics Simulations Support Click Product Interactions

To investigate whether tetrazine-norbornene click-induced secondary interactions were responsible for the differences in bulk hydrogel properties observed, molecular dynamics simulations were performed. The results indicated a marked propensity for secondary interactions between the tetrazine-norbornene cycloaddition products. Simulations compared either two thiol-ene products or two tetrazine-norbornene products tethered by a segment of PEG and capped with short segments of PEG, **Figure II.9a-c**. While both click products started the same distance apart in the simulations, the

distance between the apical hydrogens of the bridged cyclohexanes became and stayed small in the tetrazine-norbornene products, but varied greatly over time for the thiol-ene products, **Figure II.9a**. Thus, the thiol-ene products drifted together and then apart over time randomly, as they only showed some association via hydrophobic interactions and lacked the capacity for hydrogen bonding.

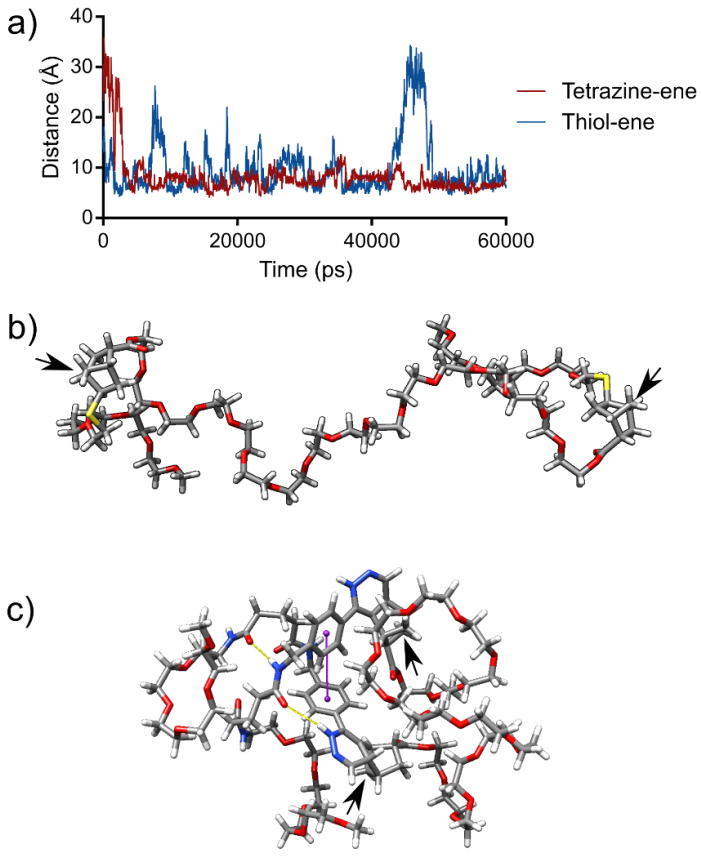

Figure II.9 (a) Distance in Ångstroms over time between apical carbons (indicated with arrows) of the (b) thiol-norbornene products and (c) tetrazine-norbornene products. Yellow lines indicate hydrogen bonds and purple lines indicate pi-pi stacking. Reprinted with permission from Holt et al.[164]

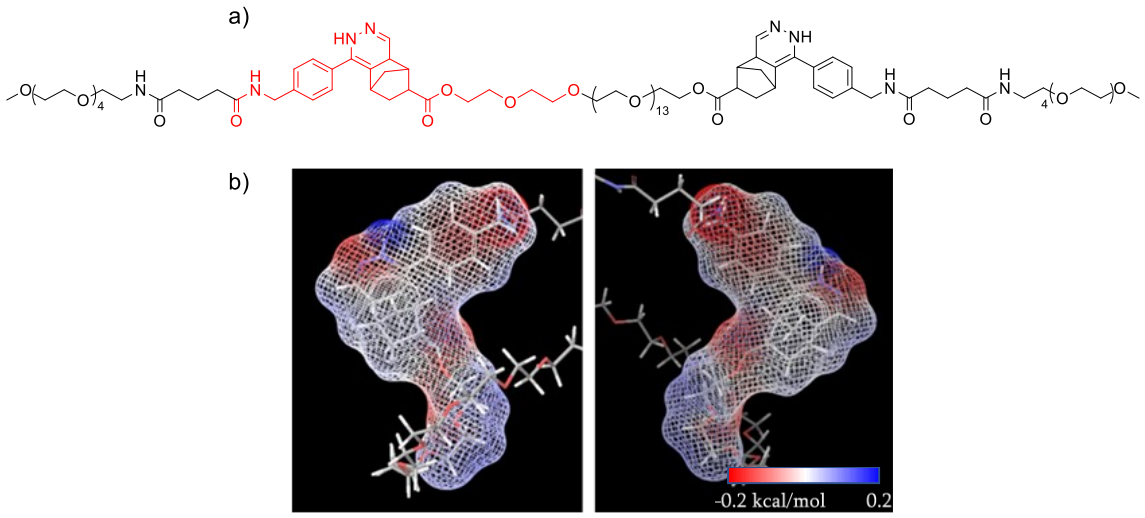

Figure II.10 Electrostatic potential map of tetrazine-norbornene click product. A surface map of the electrostatic potential of the tetrazine-norbornene cycloaddition product and its amide linkages to the PEG backbone show a relatively large, electrostatically neutral region around the bridged cyclohexane. (a) The structure of the model tetrazine-norbornene product, with the region reflected in the electrostatic potential maps highlighted in red. (b) 3D surface map of the front and back of the region of interest**.** Reprinted with permission from Holt et al.[164]

In contrast, the tetrazine-norbornene products showed interactions via hydrogen bonding, parallel displaced and T-shaped pi-pi stacking, and hydrophobic interactions between the relatively electrostatically neutral region around the bridged cyclohexane, **Figure II.10a-b**. Analysis of the interaction energy per atom of the click products showed stronger interactions between the tetrazine-norbornene products than between the thiol-ene products, with the van der Waals interactions dominant for the tetrazine-norbornene products, **Figure II.11**.

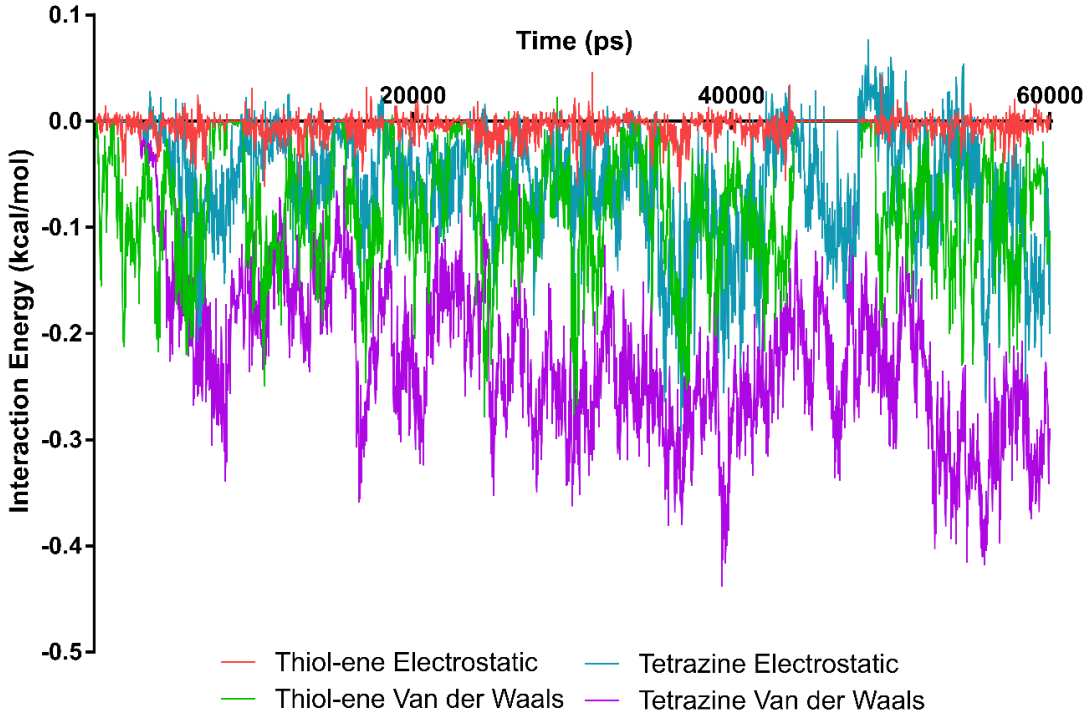

Figure II.11 Simulated averaged electrostatic and van der Waals interaction energies per atom between tetrazine-norbornene click product and thiol-ene click product regions of interest over time. A more negative value indicates a stronger interaction. Reprinted with permission from Holt et al.[164]

II.3.3 Demonstration of Supramolecular Gelation

Finally, based on our experimental and computational data, we hypothesized that hydrogels could be formed solely via tetrazine click-induced secondary interactions. To test this hypothesis, we reacted 20 kDa PEG-4-NB at a concentration of 10 wt.% with 5 kDa mPEG-Tz at a 1:1 ratio of tetrazine to norbornene, **Figure II.12a**. According to Flory-Stockmayer gelation theory,[171, 172] which is routinely used to predict functional group conversion required for step-growth crosslinking of polymer networks,[29, 31, 173, 174] a

tetrafunctional component reacted with a monofunctional component would have an infinite critical conversion. Thus, gelation due to covalent bonds between the tetrazine and norbornene is not possible. Nevertheless, in situ oscillatory rheology showed the crossover of the storage modulus (G') and the loss modulus (G") at approximately 425 seconds, indicating gelation, **Figure II.12b**. Moreover, the kinetics of G' evolution over time followed those of the tetrazine-norbornene reaction, indicating that formation of the cycloaddition product was driving gelation. Computational simulations supported this interpretation of the experimental data, as model tetrazine-norbornene products again exhibited strong non-covalent interactions while in close proximity to each other, **Figure II.12c**. Additionally, these gels exhibited a high gel fraction of 82±2% as well as a storage modulus of around 8 kPa (n=3) as detailed in **Table II.1**. This modulus is much higher than that of other non-covalently crosslinked, multi-arm PEG hydrogels. For example, hydrogels assembled with "Dock-and-Lock" peptide-peptide interactions exhibited a storage modulus on the order of hundreds of Pascals at their stiffest.[175] Similarly, Mixing-Induced Two-Component Hydrogels (MITCH) exhibited moduli on the order of tens of Pascals, even with the use of 8-arm PEG instead of 4-arm PEG.[176]

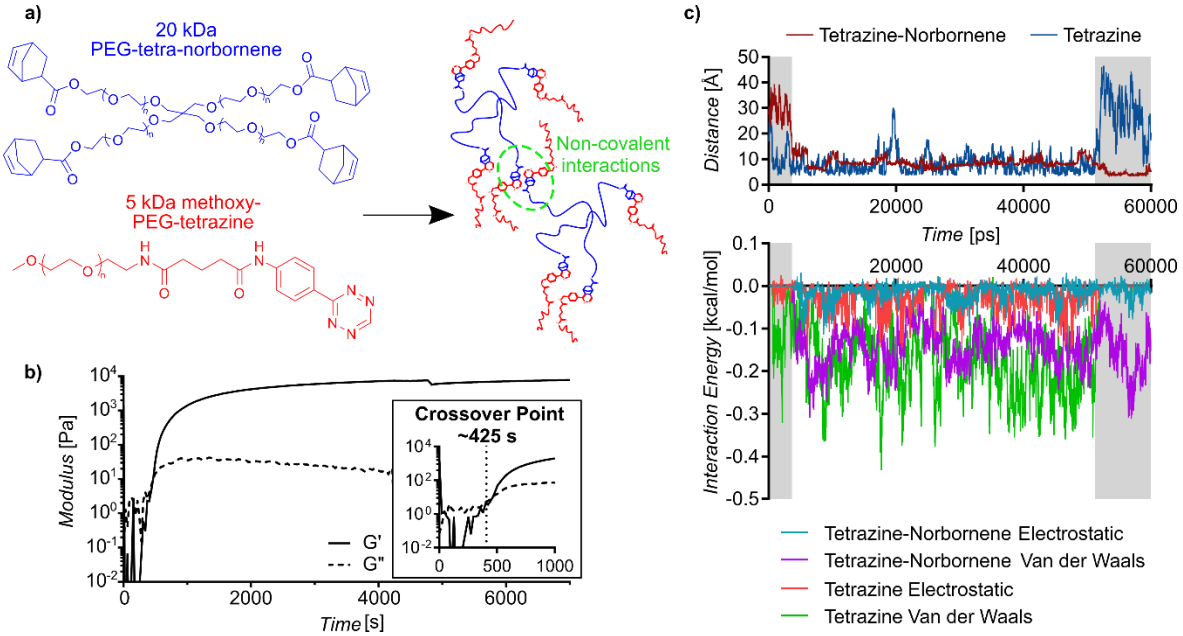

Figure II.12 (a) A 10% solution of 20 kDa 4-arm norbornene-functionalized PEG with 5 kDa monofunctional PEG-tetrazine added in a 1:1 ratio of tetrazine to norbornene (b) exhibits crossover of the storage (G') and loss (G") moduli via in situ oscillatory rheology, indicating gelation, at 425 s at 21°C. (c) Molecular dynamics simulations comparing interactions between unreacted tetrazine and tetrazine-norbornene cycloaddition products. A more negative value of interaction energy indicates a stronger interaction. Initially, the tetrazine-norbornene products are farther from each other than the tetrazines, and show little to no interaction (left region in gray). Then, the tetrazine-norbornene products drift together and remain so for the duration of the simulation. In contrast, the tetrazines drift apart later in the simulation (right region in gray) and lose all secondary interactions, as indicated in the interaction energy. Reprinted with permission from Holt et al.[164]

Table II.1 Characterization of non-covalently crosslinked hydrogels. Storage modulus G‘ is the final modulus post-crosslinking measured via in situ oscillatory rheology. (n=3)

Storage Modulus, G‘ [kPa] Pre-Swelling	Swelling Ratio, Q	Gel Fraction [%]
8.3 ± 0.5	163 ± 25	82 ± 2.1

II.4 Conclusions

In summary, we found that PEG hydrogels crosslinked via tetrazine-norbornene IEDDA chemistry exhibit more robust mechanical properties and remarkable resistance to base-catalyzed hydrolysis compared to thiol-ene click crosslinked gels due to stabilizing secondary interactions that emerge from the tetrazine-norbornene cycloaddition product. In addition, these secondary interactions alone are sufficient to assemble gels with storage moduli on the order of several kPa. This serendipitous discovery, as well as the multiple weak, non-covalent interactions between the tetrazine-norbornene products that drive their enhancement of gel stability, is reminiscent of small molecule hydrogelators, which self-assemble in water to form three-dimensional supramolecular networks.[177] Though click chemistry has been used previously to synthesize small molecule hydrogelators,[178-180] to our knowledge, this is the first demonstration of a bridging between conventional gellant systems, in which hydrogels are formed via covalent crosslinking of the polymer network, and the non-covalent, supramolecular assembly of small organic molecules which characterizes hydrogelators. Combining these two disparate mechanisms of gelation has great potential for designing and leveraging covalent and non-covalent assemblies to attain interesting new properties commonly seen in naturally-occurring biopolymers.

CHAPTER III

SUPRAMOLECULAR CLICK PRODUCT INTERACTIONS INDUCE DYNAMIC STIFFENING OF EXTRACELLULAR MATRIX-MIMETIC HYDROGELS[2]

III.1 Introduction

The dynamic nature of the extracellular matrix (ECM), the noncellular component of tissue, plays a significant role in tissue morphogenesis, renewal, and pathology progression. Tissue stiffening is a central feature of fibrotic diseases, including idiopathic pulmonary fibrosis,[111] hepatic fibrosis,[112] myocardial fibrosis,[113] and vascular disease.[114] Additionally, tissue stiffening has been implicated in malignant transformation in solid tumors and cancer aggression.[115] Furthermore, *in vitro* studies suggest that these differences in tissue stiffness contribute to differences in response to treatment and clinical outcomes. For example, *in vitro* 3D culture models of glioblastoma multiforme showed increased proliferation and EGFR-mediated signaling[181] and increasing resistance to the chemotherapy drug temozolomide in hydrogel substrates of increasing stiffness.[182] Despite the connections to pathology, tissue stiffening is also observed in embryonic development, particularly in neural crest cell migration[116, 117] and cardiac development,[118] and also plays a role in regulating cell division.[119] However, much of the role and mechanistic effects of ECM stiffening

---

[2] Data in this chapter is reprinted with permission from "Supramolecular click product interactions induce dynamic stiffening of extracellular matrix-mimetic hydrogels" by Samantha E. Holt, Julio Arroyo, Emily Poux, Austen Fricks, Isabelle Agurcia, Marissa Heintschel, Amanda Rakoski, and Daniel L. Alge, 2021. *Biomacromolecules*, 22(7), 3040-3048. Copyright 2021 American Chemical Society.

remain to be elucidated. Tissue engineering, which enables the replication of structural and functional features of tissue *in vitro*, offers the potential for a controlled environment in which to observe the effects of ECM stiffening on cell and tissue physiology.

Hydrogels are a popular class of polymeric biomaterials for cell culture and tissue engineering because of their tissue-like mechanical properties and high water content. Additionally, a plethora of strategies have been explored to grant hydrogels characteristics which mimic the structure and function of the ECM.[28, 183] Click chemistry in particular has proven useful in these endeavors as click reactions are high yielding, specific, can proceed under mild conditions in aqueous environments, and produce inoffensive, if any, by-products.[184] These features make click reactions especially attractive for use in biological systems. The wide variety of reactions in the click chemistry toolbox[185-187] have been used to create hydrogels with user-defined mechanical properties, to covalently crosslink natural polymers to enhance their mechanical properties, and to incorporate cell-adhesive peptide moieties into synthetic polymer networks, all while allowing for the incorporation of cells in the material. Furthermore, click chemistry-based strategies have been used to create hydrogels with user-controlled or cell-mediated degradation.

Several approaches employing click chemistry to enable the dynamic stiffening of hydrogels have been developed, which have recently been reviewed by LeValley and Kloxin[188] and Arkenberg et al.[189] However, these hydrogel platforms present limitations when deployed in tissue engineering applications. The most common approach is using

secondary or sequential crosslinking to increase the covalent crosslinking density over time. These methods include sequential polymerization using Michael addition,[93, 94] radical-mediated acrylate chemistry,[95, 96] and radical-mediated thiol-ene click chemistry[97, 98] as well as secondary crosslinking using inverse electron-demand Diels Alder (IEDDA) tetrazine click chemsitry[99] and tyrosine ligation using mushroom tyrosinase[100-102] or flavin mononucleotide.[103] However, an increase in covalent crosslinking density can limit cell motility and spreading, and such methods can have the added effect of locking cells in their starting shape[97] which may influence their phenotype.[104-107]

Other methods have controllably stiffened hydrogels by leveraging photo-[190] or redox-[191]responsive conformational changes of protein functional domains incorporated in the network to change the mesh size of the gel. However, these methods allow for limited increases in the gel modulus on the order of 10-100 Pa. Alternatively, reversible crosslinking using DNA binding,[109] beta-cyclodextrin host-guest interactions,[110] calcium-mediated alginate crosslinking,[108] and sortase transpeptidation[192] have also been used to cyclically stiffen and soften hydrogel networks. Each of these methods has limitations to application in biological systems. First, DNA-mediated crosslinking would have limited utility in tissues because of the prevalence of cell- and tissue-native nucleases. Second, the modulus of hydrogels made with reversible crosslinking methods is extremely sensitive to the concentration of the non-covalent crosslinking agents used. These non-covalent crosslinking agents--such as calcium cations or adamantane, which competitively associates with beta cyclodextrin--are not permanently bonded to the

network and could diffuse out over time. Additionally, these methods may have a limited achievable range of mechanical properties. For instance, Rosales et al. presented a reversible method of stiffening hydrogels by leveraging supramolecular interactions between cyclodextrins and azobenzene, which changes configuration and affinity for cyclodextrins when exposed to different wavelengths of light.[193, 194] However, this strategy reported a maximum increase in modulus of approximately 60%, while sequential crosslinking methods have yielded increases of up to 50-fold.[97] In a departure from other approaches, Abdeen et al. used carbonyl iron microparticles to modify polyacrylamide hydrogels to synthesize magnetoresponsive dynamic gels.[195] However, the range of moduli available with this platform is limited by the magnets used to tune the gel stiffness, and options that would allow for a highly tunable magnetic field are prohibitively expensive and unavailable to many labs.

Considering the limitations of previous methods, there exists a need for a method of dynamic hydrogel stiffening which is accessible, offers a wide range of achievable stiffnesses, and does not rely on increasing covalent crosslinking density. In addition, this method should ideally enable long-lasting stiffening of the matrix and allow for gel degradation when necessary. Finally, to enable implementation in cell culture environments, this method should be simple to use and easily adaptable to current cell culture protocols.

To address these needs, we have developed a novel system for creating dynamically stiffening hydrogels by leveraging previously discovered supramolecular interactions between inverse electron-demand Diels Alder (IEDDA) tetrazine-

norbornene click products (TNCP). First, by covalently crosslinking a PEG network via radical-mediated thiol-ene click chemistry, we create a hydrogel which can be customized with cell adhesive peptides as well as enzymatically degradable peptide crosslinkers and also contains unreacted pendant norbornene groups. Then, by swelling in a monofunctional PEG-tetrazine, we initiate the formation of pendant tetrazine-norbornene click products (pTNCP) which are covalently attached to the network but do not contribute to the covalent crosslinking of the network. As the IEDDA reaction proceeds and the pTNCP form, they associate with each other noncovalently, stiffening the network. This novel supramolecular-covalent hybrid network has broad potential utility in a wide range of tissue engineering applications, and its simplicity enables facile translation to existing hydrogel formulations and cell culture protocols.

III.2 Materials and Methods

III.2.1 General Materials

Materials obtained commercially were used without further modification unless otherwise noted. Peptides KCGPQGIWGQCK (KCGPQ-W), KCGPQGIAGQCK (KCGPQ-A), and CGRGDS were synthesized via standard Fmoc solid phase peptide synthesis. Lithium acylphosphinate (LAP) was synthesized as previously described.[163]

III.2.2 8-Arm PEG-Norbornene Functionalization

8-arm 40kDa PEG-hydroxyl (PEG-OH; JenKem) was end functionalized with norbornene carboxylic acid as previously described.[152] 10g PEG-OH (2 mM -OH groups, 1 eq.) was dissolved in anhydrous dichloromethane (DCM; Acros Organics) in a 250 mL round bottom flask and 0.81 mL pyridine (0.5 eq.; Sigma Aldrich) was added. In

a 100 mL reaction chamber, 1.55 mL N,N'-Diisopropylcarbodiimide (DIC, 5 eq.; Sigma Aldrich) and 2.46 mL 5-norbornene-2-carboxylic acid (10 eq.; Alfa Aesar) were combined in anhydrous DCM and reacted for 15 min to form norbornene anhydride. The anhydride product was filtered through the frit into the PEG solution and allowed to react overnight (~18 h). Norbornene-functionalized PEG (PEG-8-NB) was then precipitated in cold (4°C) diethyl ether (Fisher Chemical), dried, and dialyzed against ultrapure water. End functionalization of 86% was confirmed via 1H NMR, **Figure III.1**. ^{1}H NMR (400 MHz, D_2O) δ 6.22 – 6.06 (m, 2H), 5.89 (dd, *J* = 5.7, 2.8 Hz, 1H), 4.24 – 4.09 (m, 2H), 3.63 (s, 454H), 3.17 (s, 1H), 3.07 – 2.98 (m, 1H), 2.88 (s, 1H), 2.28 – 2.21 (m, 0H), 1.88 (ddd, *J* = 12.3, 9.2, 3.7 Hz, 1H), 1.78 (dt, *J* = 11.8, 4.1 Hz, 0H), 1.41 – 1.18 (m, 3H).

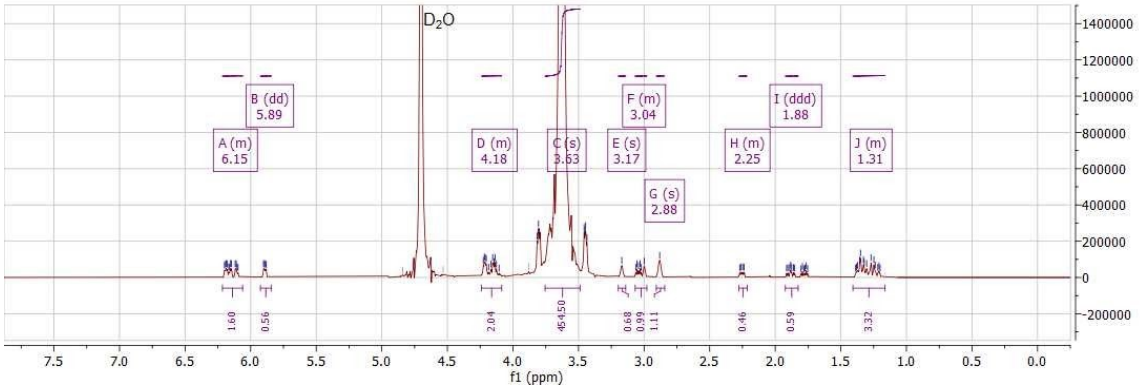

Figure III.1 ^{1}H NMR characterization of 40kDa PEG-8-NB functionalization in D_2O. End group functionalization confirmed at 86%. ^{1}H NMR (400 MHz, D2O) δ 6.22 – 6.06 (m, 2H), 5.89 (dd, J = 5.7, 2.8 Hz, 1H), 4.24 – 4.09 (m, 2H), 3.63 (s, 454H), 3.17 (s, 1H), 3.07 – 2.98 (m, 1H), 2.88 (s, 1H), 2.28 – 2.21 (m, 0H), 1.88 (ddd, J = 12.3, 9.2, 3.7 Hz, 1H), 1.78 (dt, J = 11.8, 4.1 Hz, 0H), 1.41 – 1.18 (m, 3H). Reprinted with permission from Holt et al.[196]

III.2.3 mPEG-Tetrazine Functionalization

Linear 5 kDa methoxy-PEG-amine (mPEG-NH2; Laysan Bio) was functionalized with tetrazine-carboxylic acid (Tz-COOH; BroadPharm) to yield methoxy-PEG-tetrazine (mPEG-Tz) as previously described.[164] Briefly, 1.03 g of 5 kDa mPEG-NH2 (0.82 mmol -NH2, 1 eq.) was dissolved in 3 mL 1-methyl-2-pyrrolidinone (NMP; Chem Impex) with 0.23 mL triethylamine (TEA, 2 eq., Alfa Aesar) and allowed to mix for approximately 15 min under argon blanket. In a separate argon-purged vessel, 0.37 g Tz-COOH (1.5 eq.) was dissolved in NMP and activated with 0.47 g HBTU (1.5 eq.; Chem Impex) for 5 min. The activated Tz-COOH was added to the mPEG-NH2 solution and allowed to react at room temperature for 15 h. The mPEG-Tz product was then precipitated in cold (4°C) diethyl ether, centrifuged to remove salt by-products, dialyzed against ultrapure water and lyophilized. Tetrazine functionalization of 90% was confirmed using 1H NMR, **Figure III.2**. ^{1}H NMR (400 MHz, DMSO) δ 10.58 (s, 1H), 8.50 – 8.40 (m, 3H), 7.86 (t, J = 5.6 Hz, 1H), 7.57 – 7.50 (m, 2H), 4.39 (d, J = 6.0 Hz, 2H), 3.51 (s, ~454H), 2.14 (dt, J = 31.1, 7.5 Hz, 4H), 1.82 – 1.70 (m, 2H).

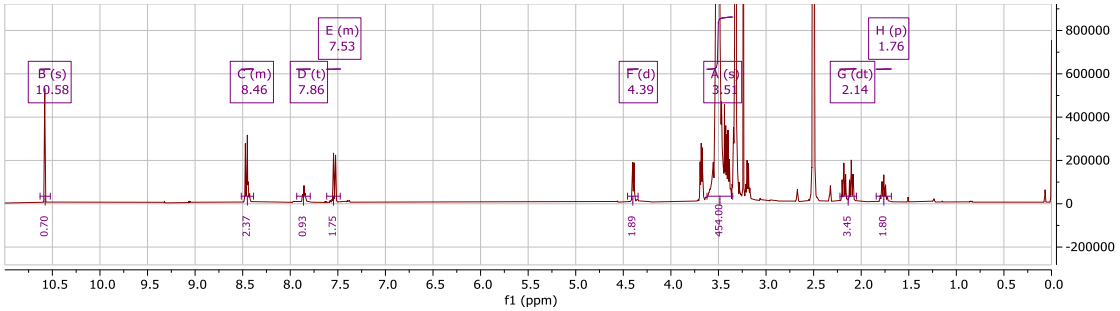

Figure III.2 5kDa methoxy-PEG-tetrazine. ^{1}H NMR indicated 90% end group functionalization with tetrazine. ^{1}H NMR (400 MHz, DMSO) δ 10.58 (s, 1H), 8.50 – 8.40 (m, 3H), 7.86 (t, J = 5.6 Hz, 1H), 7.57 – 7.50 (m, 2H), 4.39 (d, J = 6.0 Hz, 2H), 3.51 (s, ~454H), 2.14 (dt, J = 31.1, 7.5 Hz, 4H), 1.82 – 1.70 (m, 2H). Reprinted with permission from Holt et al.[196]

III.2.4 Hydrogel Synthesis

40 kDa PEG-8-NB at a concentration of 7.5 wt.% in phosphate buffered saline (PBS) was combined with a bis-cysteine MMP-degradable peptide crosslinker, either KCGPQ-W or KCGPQ-A, at a 1:2 thiol-ene ratio (6.32 mM thiol: 12.64 mM norbornene). To test the concentration-dependent effect of pTNCP on gel properties while controlling for total PEG content in the gels, varying concentrations of methoxy-PEG-thiol (mPEG-SH; Laysan Bio) were added to the pre-gel solutions as well, leaving varying concentrations of available norbornene to react with mPEG-Tz. The varying ratios of mPEG-Tz to mPEG-SH added to the gels are detailed in **Table III.1**. 60 µL pre-gel solution was added to 8 mm diameter, 1 mm thick round silicone molds and polymerized using 365 nm UV light at 20 mWcm^{-2} for 5 min, after which the gels were swelled overnight to equilibrium. Solutions of mPEG-Tz were prepared in PBS at concentrations corresponding to the concentrations of free norbornene groups available

in the gels (1, 3, and 5.32 mM). Each gel was incubated at room temperature on an orbital plate shaker in 400-500 μL of the corresponding mPEG-Tz solution overnight (15-18 h), with the exception of the gels with 0 mM free norbornene which were incubated under the same conditions in fresh PBS. The gel samples were stored in PBS at 4°C when not in use to prevent degradation.

Table III.1 Variable pTNCP fraction hydrogel formulations

[mPEG-Tz] (mM)	[mPEG-SH] (mM)	TNCP fraction (%)
0	5.32	0
1	4.32	19
3	2.32	56
5.32	0	100

III.2.5 Rheological Characterization

Shear oscillatory rheology was conducted using an Anton Paar Physica MCR 301 rheometer using an 8 mm parallel plate geometry. Gels were allowed to equilibrate to 37°C before testing. Shear storage and loss moduli were averaged over the course of a 60 s time sweep at 1% strain, 1 rad/s at 37°C (n=3). Frequency and amplitude sweeps verified that these parameters fell within the linear viscoelastic region.

III.2.6 Enzymatic Degradation

Hydrogel degradability was assessed via collagenase B degradation. Collagenase B (Roche) was dissolved in sterile-filtered PBS at a concentration of 0.2 mg/mL. Gels swollen to equilibrium were weighed and then each submerged in 1 mL collagenase solution. The gel samples were incubated in collagenase solution at 37°C. The gels were removed from solution, dried briefly to remove excess solution from the surface, and weighed at intervals of 5 min for the first 30 min, then intervals of 30 min until 90 min total, after which they were weighed every 60 min until the gels degraded completely.

III.2.7 Dynamic Hydrogel Stiffening

III.2.7.1 Gels made with PBS

A pre-gel solution in PBS was prepared using 7.5 wt.% 40 kDa PEG-8-NB, 2 mM LAP, 1 mM CGRGDS, and 3.16 mM either KCGPQ-W or KCGPQ-A (1:2 thiol-ene ratio). This solution was polymerized using 365 nm UV light at 20 $mWcm^{-2}$ for 5 min, leaving 5.32 mM free norbornene groups. The gel samples were swelled overnight (15-18 h) to equilibrium in PBS, after which their starting shear storage and loss moduli were measured. To initiate stiffening, the swollen gels were added to a solution of 5.32 mM mPEG-Tz in PBS on an orbital plate shaker. The storage and loss moduli of the gels were measured every hour over the course of 6 h. At each time point, the gels were rinsed for 5 min in sterile-filtered PBS, subject to rheological measurement, and then returned to the mPEG-Tz solution. After 6 h, the gels were allowed to soak in the solution for another 12 h on the orbital plate shaker for a total of 18 h of incubation in

mPEG-Tz. After that, the final storage and loss moduli were measured using the same rheological parameters.

III.2.7.2 Gels made with cell culture media

To test dynamic gel stiffening in cell culture conditions, the same pre-gel solution was prepared in sterile field with the KCGPQ-W peptide crosslinker in complete culture media (Dulbecco's Modification of Eagle's Medium (DMEM, 1X; Corning) infused with 10% fetal bovine serum (FBS; Atlanta Biologicals) and 1% penicillin-streptomycin (EMD Millipore)). 60 μL gel samples were polymerized in 8mm molds using 365 nm UV light at 10 mW cm^{-2} for 5 min, leaving 5.32 mM unreacted norbornene groups as before. These gels were swelled to equilibrium in 1 mL complete culture media at 37°C and 5% CO_2 to maintain a physiologic pH of the culture media and prevent accelerated hydrolysis. After initial swelling, the gels were removed from culture conditions and the storage and loss moduli were evaluated using the previously described rheological parameters. Then, the gels were each submerged in 500 μL sterile complete culture media supplemented with 5.32 mM mPEG-Tz. The gels were UV sterilized for 30 min to prevent the growth of contaminants, and then were incubated at 37°C and 5% CO_2 for a total of 4 h of swelling in mPEG-Tz. The gels were then removed from the mPEG-Tz solution and rinsed in 1 mL complete growth media on an orbital shaker for 10 min. Then, the storage and loss moduli were assessed again using the same rheological parameters. Afterwards, the gels were UV sterilized, submerged in 1 mL complete media each, and returned to culture conditions (37°C, 5% CO_2). The

storage and loss moduli were assessed via rheology again 1 day and 3 days after stiffening.

III.2.8 Characterization of Norbornene Consumption via NMR

Pre-gel solution was collected, along with gel samples post-thiol-ene polymerization (5.32 mM free norbornene) and after both thiol-ene and tetrazine-ene polymerization. The gel samples were rinsed overnight (15 h) in ultrapure water, and then hydrolyzed in 0.1 N NaOH for 1 h at 37°C. The degraded samples were homogenized by vigorous pipetting and then frozen, along with the collected pre-gel solution, at -80°C. All three were then lyophilized and resuspended in deuterium oxide. 1H NMR was performed on each sample using a Bruker Avance Neo 400 Hz console with an Ascend magnet and an automated tuning 5 mm broadband iProbe. For quantitative analysis, the peak integrals were normalized to the PEG peak at 3.7 ppm (454.5 H).

III.2.9 3T3 Cell Encapsulation and Viability

Cytocompatibility of 3D culture in dynamic hydrogels was tested using 3T3 murine fibroblasts (ATCC). 3T3s were maintained on tissue culture polystyrene flasks in complete growth media consisting of Dulbecco's Modification of Eagle's Medium (DMEM, 1X; Corning) infused with 10% fetal bovine serum (FBS; Atlanta Biologicals) and 1% penicillin-streptomycin (EMD Millipore). Cells were passaged every two days until collection for hydrogel encapsulation. Prior to encapsulation, cells were lifted and pelleted via centrifugation before resuspension in complete growth media. 3T3s were added to the pre-gel solution described for dynamic hydrogels at a density of 20,000

cells/gel. Then, 20 μL of gel precursor solution with cells was pipetted into sterile molds made by cutting the tips off 1 mL syringes. The gels were exposed to 365 nm UV light at 5 $mWcm^{-2}$ for 3 minutes and transported to sterile 24 well plates. An aliquot of complete media was supplemented with 5.32 mM mPEG-Tz and sterile filtered via 0.2 μm cellulose acetate syringe filter. Post-UV polymerization, the pTNCP gels were incubated in 450 μL of the sterile mPEG-Tz media solution. The gels were incubated at 37° and 5% CO_2 for 4 h, after which an additional 1 mL complete media was added to all gels. The media was changed to complete growth media after 24 h. Cell viability was assessed at 1 and 3 days after mPEG-Tz addition using a Live/Dead assay. The gels were then imaged at three separate locations each to provide accurate representation of live (green) and dead (red) cells throughout each gel. Quantitative analysis was performed using ImageJ.

III.2.10 Statistical Analysis

With the exception of time-series data analysis, statistical analysis was performed using GraphPad Prism 6. For these data, significance was determined via ANOVA with post-hoc two-tailed Student's t-test. P values less than 0.05 were considered significant. Means are reported with standard deviations. Time-series gel stiffening data was analysed in R. Because of the low sample size (n=3) and because the data consisted of repeated measures of the same samples, a linear mixed model was applied to the data to determine whether the increase in modulus over time was significant. P-values were calculated via Satterthwaite's degrees of freedom method. P-values less than 0.05 were considered significant.

Results and Discussion

III.2.11 Sequential Click Reactions for Click Product Installation

Previously, non-covalent interactions between TNCP were found to be sufficient to induce gelation in a multi-arm PEG system.[164] It was hypothesized that these same non-covalent interactions could be used to controllably stiffen a pre-existing covalent network through the *in situ* installation of pTNCP. First, covalent networks were formed via radical-mediated thiol-ene click chemistry. 7.5 wt.% 40 kDa PEG-8-NB was reacted with a bis-cysteine peptide crosslinker and 1 mM pendant cell-adhesive peptide CGRGDS at a 1:2 thiol-ene ratio, leaving 5.32 mM free norbornene groups. Next, the gels were swelled in a solution of monofunctional mPEG-Tz in PBS to install pTNCP via IEDDA click chemistry using the remaining norbornene groups, as represented in **Figure III.3a**. Initial attempts combined the two reactions in a 'one-pot' synthesis, but the solution failed to gel (not shown). This may be attributed to radical scavenging by the tetrazine groups inhibiting the thiol-ene reaction. However, dividing the gel synthesis into two steps was successful and enabled controlled stiffening of the gel upon addition of mPEG-Tz. This system was able to leverage sequential polymerization because of the ability of the cyclic alkene norbornene to react with either thiol groups or s-tetrazines, **Figure III.3b**. Proton NMR demonstrated approximately 65% norbornene conversion after the initial thiol-ene polymerization, slightly higher than the theoretical norbornene conversion of 57% calculated via Flory-Stockmayer gelation theory, **Figure III.3c**. [171, 172] The discrepancy in theoretical and observed conversion may have been due to an overestimation of PEG-8-NB functionalization or underestimation of the concentration

of the peptide stock solutions. However, all remaining norbornene groups were converted upon the addition of 5.32 mM mPEG-Tz, demonstrating successful installation of pTNCP.

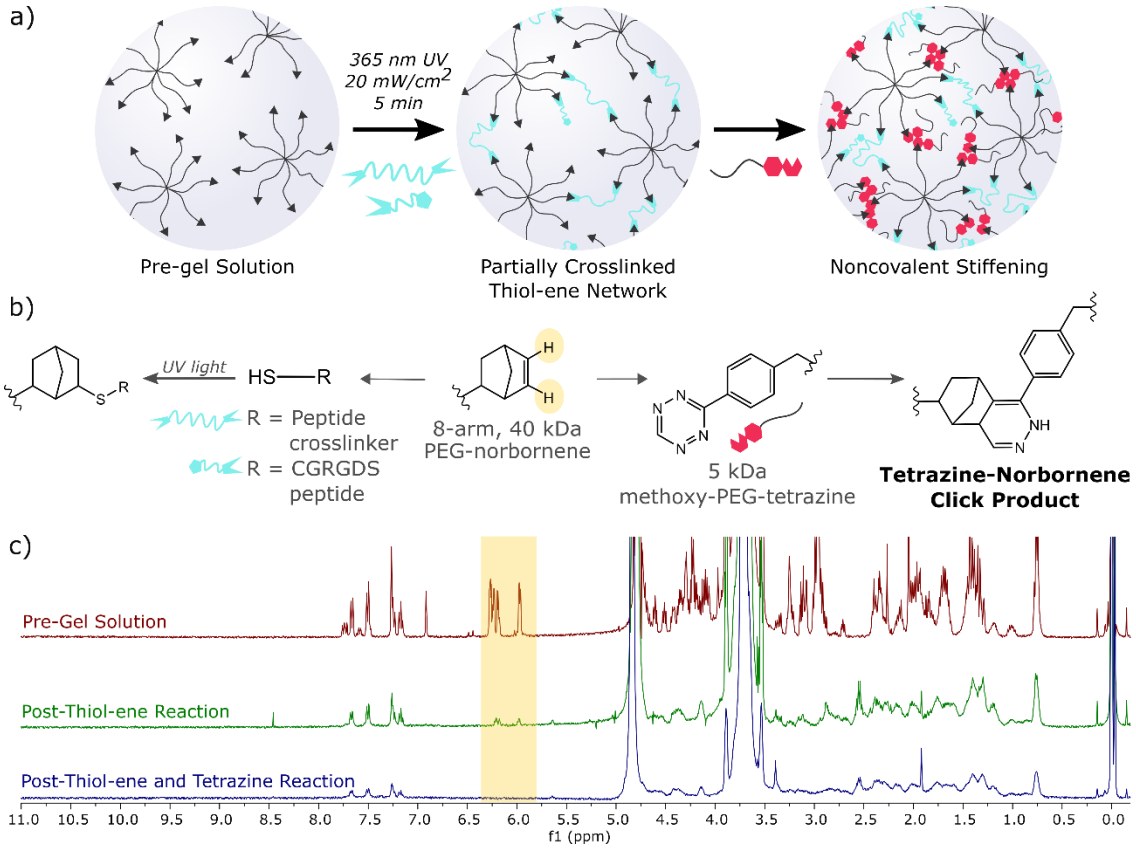

Figure III.3 (a) 7.5 wt.% PEG-8-NB was polymerized using radical-mediated thiol-ene click chemistry with 1 mM CGRGDS peptide and an enzymatically degradable peptide crosslinker at a 1:2 thiol-ene ratio to create a covalent network with 5.32 mM unreacted norbornene groups remaining, where pTNCP moieties are installed *in situ* via tetrazine-norbornene click chemistry. (b) Schematic of TNCP synthesis. (c) Protons on the alkene norbornene (highlighted) are represented by peaks from ~5.9-6.3 ppm in 1H and are consumed in the IEDDA reaction with tetrazine to form pTNCP. Reprinted with permission from Holt et al.[196]

III.2.12 Effect of TNCP Fraction and Crosslinker Selection on Gel Stiffness

Next, the relationship between the concentration of pTNCP and bulk hydrogel stiffness was investigated. To control for the total PEG content of the gels while varying the pTNCP concentration, monofunctional 5 kDa mPEG-SH was incorporated at varying concentrations in the gel via UV polymerization, **Figure III.4a**. The resulting pendant thiol-ene groups were the same size as the pTNCP, but did not display the same supramolecular associations. Additionally, two choices of enzymatically-degradable peptide crosslinker were compared which were identical but for the choice of either a tryptophan or an alanine residue. The aromatic indole of the tryptophan residue can participate in pi-pi stacking interactions,[197, 198] which were also implicated in TNCP supramolecular interactions.[164] We predicted that the tryptophan variant peptide would participate in interactions with the TNCP as well, which would result in stiffer gels than those made with the alanine variant peptide.

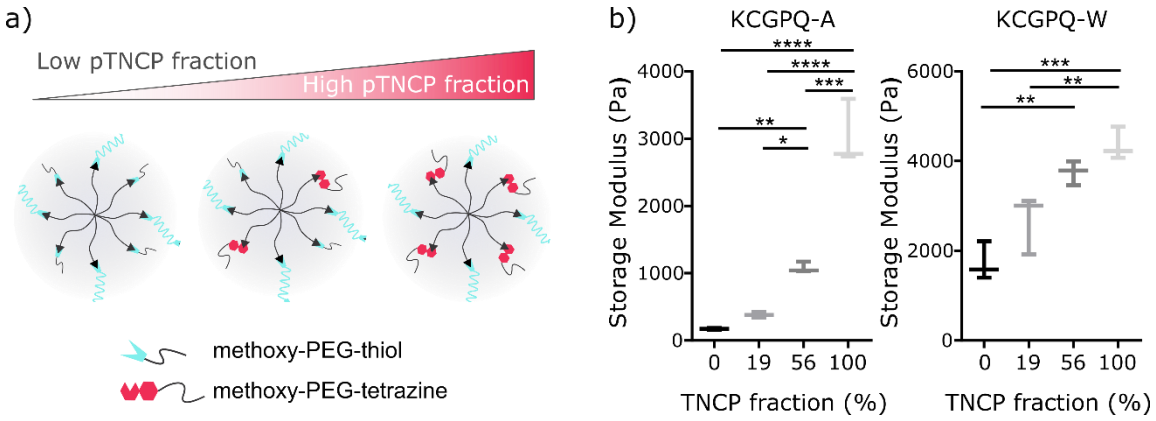

Figure III.4 (a) Differing ratios of 5 kDa methoxy-PEG-thiol to 5 kDa methoxy-PEG-tetrazine were used to adjust the TNCP fraction while keeping the PEG content of the gels consistent. (b) Increasing gel TNCP fraction increased the storage modulus in gels regardless of crosslinker selection, with 100% TNCP gels displaying 17- and 2.5-fold higher shear storage moduli in KCGPQ-A and KCGPQ-W crosslinked gels, respectively ($p<0.0001$, $p=0.0005$, $n=3$ for both). Reprinted with permission from Holt et al.[196]

Regardless of the choice of peptide crosslinker, increasing the TNCP fraction increased the shear storage modulus of the gels significantly, **Figure III.4b**. The increase was higher in the KCGPQ-A crosslinked gels, which were approximately 17-fold stiffer with a 100% TNCP fraction (5.32 mM pTNCP, 3034±481 Pa) than with a 0% TNCP fraction (172.4±15 Pa). Additionally, the modulus of the KCGPQ-W crosslinked gels was 2.5-fold higher in the 100% TNCP fraction gel formulation versus the 0% TNCP fraction controls (4353±365 Pa vs. 1730±427 Pa). Notably, at each TNCP fraction tested, the modulus of the KCGPQ-W crosslinked gels was much higher than that of the KCGPQ-A crosslinked gels. While the pTNCP supramolecular interactions have a clear impact on the storage modulus of the gels, these data suggest that the

presence of other aromatic residues can impact the storage modulus as well. However, the pTNCP-induced change in stiffness in the KCGPQ-A gels (2862 Pa) is significantly more than the tryptophan-attributed difference in stiffness between the KCGPQ-A and KCGPQ-W crosslinked 0% TNCP fraction gel formulations (1558 Pa).

III.2.13 Effect of pTNCP Installation on Gel Enzymatic Degradability

Next, the effect of the presence of pTNCP on enzymatic gel degradation was investigated. Previous studies indicated that the presence of TNCP supramolecular interactions in covalently crosslinked gels inhibited hydrolytic gel degradation.[164] However, gel degradation is important because it allows for cell spreading and migration in 3D culture. Again, two enzymatically-labile peptide crosslinker variants in the initial covalent network were compared (KCGPQ-W or KCGPQ-A), **Figure III.5a**. Gels were then modified with either 5.32 mM pendant thiol-ene groups (0% TNCP fraction) as a control or 5.32 mM pTNCP (100% TNCP fraction). All four groups were treated with 0.2 mg/mL collagenase B to simulate accelerated degradation in the presence of cell-secreted enzymes and the remaining mass was measured periodically.

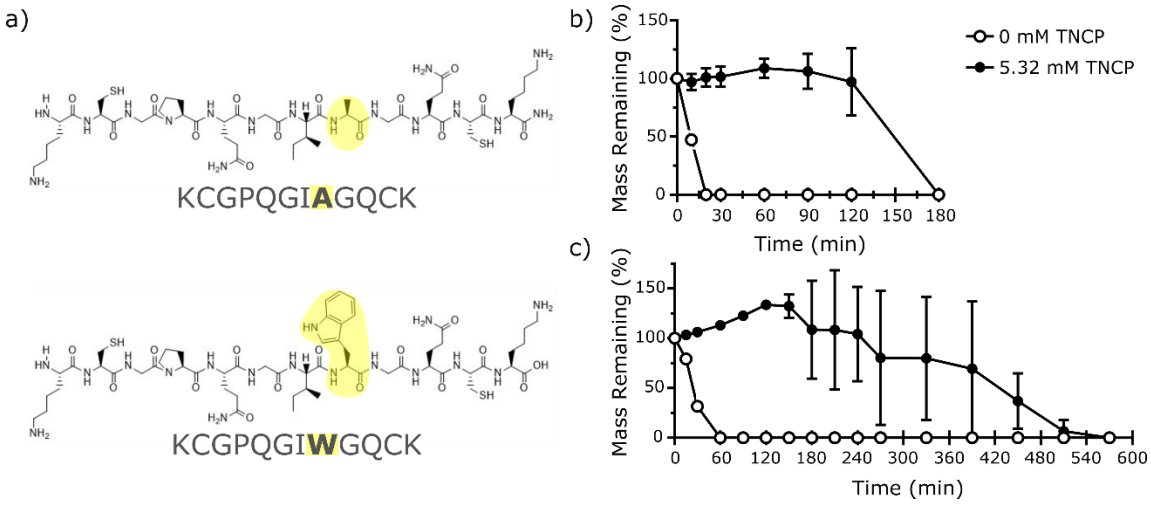

Figure III.5 (a) Degradable peptide crosslinkers with either an alanine residue (KCGPQ-A) or a tryptophan residue (KCGPQ-W) were compared in gels containing pendant tetrazine-norbornene click products (pTNCP) to determine impact on gel stiffness. (b) KCGPQ-A crosslinked gels with a 100% TNCP fraction (5.32 mM pTNCP) on average degraded completely after 180 min of treatment with 0.2 mg/mL collagenase B at 37°C, compared to 0% TNCP fraction gels which degraded completely within 15 min. (c) KCGPQ-W crosslinked gels with a 100% TNCP fraction on average degraded completely after 570 min under the same conditions, while KCGPQ-W crosslinked 0% TNCP fraction gels degraded within 60 min. Reprinted with permission from Holt et al.[196]

Regardless of choice of crosslinker, the pTNCP-containing gels displayed significantly slower degradation than control gels, with the pTNCP gels lasting almost 10-fold longer on average. The KCGPQ-A crosslinked control gels had degraded completely after 20 minutes, while those containing pTNCP displayed little mass loss up to 120 minutes and were found to be completely degraded after 180 minutes, **Figure III.5b**. The effect was even more dramatic in the KCGPQ-W crosslinked gels, which took nearly 10 hours (570 min) to degrade completely, **Figure III.5c**. However, the

degradation curve of the KCGPQ-W crosslinked pTNCP gels displayed two unique and interesting features: first, the gels swelled dramatically up to about 150 minutes, and second, there was a high degree of variability in the remaining mass after that point. Bulk-degrading hydrogels commonly swell and increase in mass as they degrade. This swelling is observed when the partial cleavage of the polymer network is enough to increase the average mesh size but insufficient for the network to dissolve. The high degree of swelling in the pTNCP-containing, KCGPQ-W crosslinked gels may indicate an extended preservation of the gel network even with the scission of the peptide crosslinkers of the covalent network.

Importantly, the presence of pTNCP clearly allows for gel degradation, unlike previously published tetrazine-norbornene covalently crosslinked hydrogels which displayed resistance to hydrolytic degradation.[164] This indicates pTNCP-mediated stiffening permits enzymatic degradation of the gel, which is necessary for cell spreading and motility in 3D culture. However, the presence of pTNCP does appear to significantly slow the rate of enzymatic degradation. Notably, reported stiffening methods using sequential or secondary covalent crosslinking in PEG-peptide hydrogels report delayed or inhibited enzymatic degradation. For instance, the method of Mabry and colleagues using sequential thiol-ene crosslinking in multi-arm PEG hydrogels produced non-degradable networks post-stiffening.[97] Arkenberg and colleagues report delayed enzymatic degradation of their gels stiffened using secondary covalent IEDDA crosslinking.[99] Future work will need to elucidate the effects of this delayed degradation

on cell migration and spreading and how these effects compare to sequential covalent crosslinking stiffening methods.

III.2.14 Controllable Dynamic Hydrogel Stiffening

Next, dynamic stiffening of gels upon addition of mPEG-Tz was characterized. To do so, the gels were swelled in 5.32 mM mPEG-Tz in PBS on an orbital plate shaker and their shear storage modulus was measured every hour for 6 hours. The gels were allowed to sit in the mPEG-Tz solution for an additional 12 hours before their final modulus was measured. Both the KCGPQ-W crosslinked and KCGPQ-A crosslinked gels displayed an approximately 2-fold increase in storage modulus over the course of 6 hours, **Figure III.6a-b**. The trends in modulus in the gels made with either crosslinker were found to be significant (KCGPQ-A: p=8.25e-9, KCGPQ-W: p=0.000158). The KCGPQ-A crosslinked gels demonstrated a consistent increase in modulus every hour until about 4 hours of mPEG-Tz addition when the modulus plateaus. In contrast, the modulus evolution of the KCGPQ-W crosslinked gels was less consistent. Unexpectedly, the KCGPQ-W crosslinked gels demonstrated a decrease in modulus after 2 hours of mPEG-Tz treatment before a rapid increase in modulus. The reason for this is unclear.

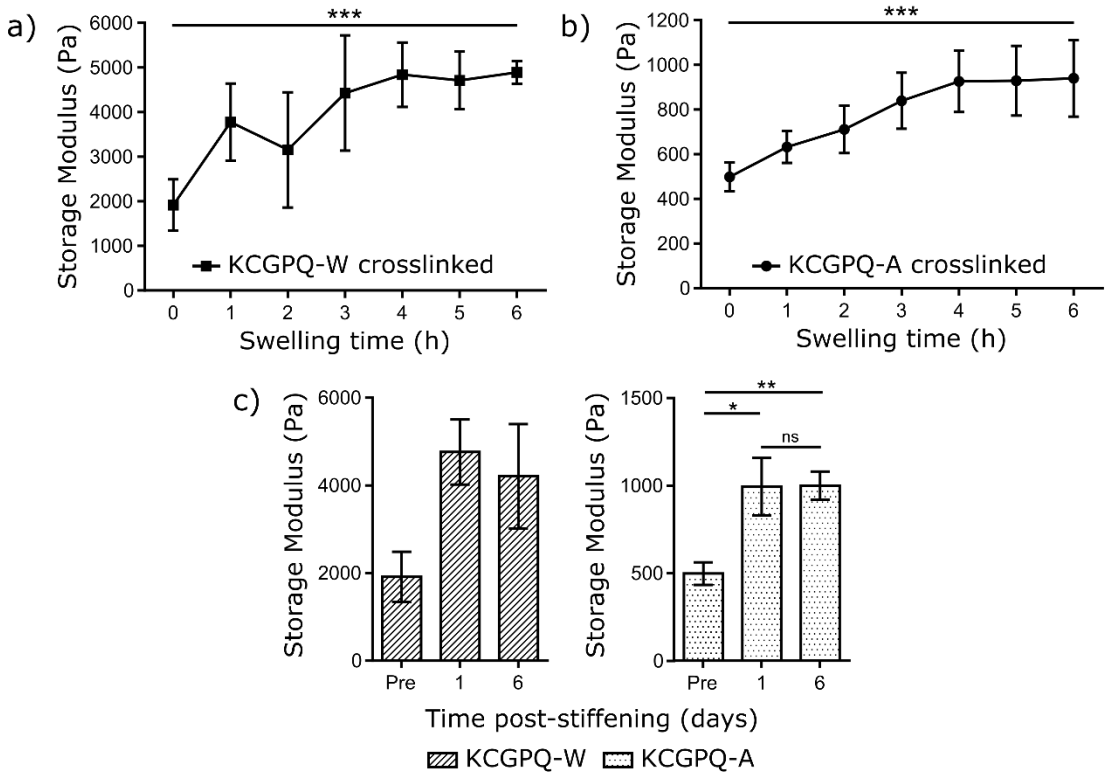

Figure III.6 (a) KCGPQ-W crosslinked gels exhibited an increase in shear storage modulus from 1918±573 to 4890±256 Pa over the course of 6 h of treatment with 5.32 mM 5 kDa mPEG-Tz. (b) KCGPQ-A crosslinked gels exhibited an increase in shear storage modulus from 499±65 to 940±172 Pa over the course of 6 h of treatment with 5.32 mM 5kDa mPEG-Tz. (c) The increase in modulus was found to persist 6 days after treatment and storage in PBS. Reprinted with permission from Holt et al.[196]

Notably, the starting modulus for both conditions was higher than that of the static control gels made with mPEG-SH occupying the free norbornene groups. We expect that this is due to the steric effects of the added pendant PEG-thiol-ene product groups, which would increase the space between polymer chains in the absence of the supramolecular interactions seen with the pTNCP, increasing the swelling and

decreasing the modulus of the gels. Additionally, the modulus of the KCGPQ-W crosslinked gels was higher than the KCGPQ-A crosslinked gels at every point, consistent with the static modulus data. This again suggests that the tryptophan residues contribute to gel stiffening through supramolecular interactions with either pTNCP or other tryptophan residues. Furthermore, it should be noted that the rheological methods used assessed the bulk modulus of the sample, though it is reasonable to expect heterogenous stiffening at a smaller scale throughout the gel over time as the mPEG-Tz diffuses into the network. The spatial heterogeneity of stiffening kinetics in three dimensions is an important topic for future study. Notably, the modulus effects of the added pTNCP were found to be long-lasting, with no significant difference in modulus between 1- and 6-days post-stiffening, **Figure III.6c**.

Notably, pTNCP-mediated stiffening yielded increases in modulus comparable to previously published covalent sequential and secondary crosslinking methods. Step growth, multi-arm PEG networks controllably stiffened via secondary crosslinking using beta cyclodextrin,[110] enzyme-mediated tyrosine ligation,[103, 199] and thiol-ene click chemistry[98] displayed between 1.25- and 2.5-fold increase in storage modulus. Dynamic stiffening through the addition of a secondary network of multi-arm PEG can produce significantly greater increases in modulus (up to 50-fold), however the dense final network restricts cell spreading and growth.[97] While other non-covalent stiffening methods may better accommodate cell spreading and migration, those employed in PEG-peptide hydrogels have demonstrated significantly smaller increases in modulus than pTNCP-stiffened networks. For instance, photomediated stiffening via azobenzene

configuration changes[194] and LOV2 protein domain configuration changes[190] demonstrated less than 1-fold change in modulus (60% and 15%, respectively). Additionally, the concentration-dependent effect of pTNCP on gel storage modulus suggests that greater net changes in gel modulus may be possible using polymer architectures which allow for a greater final concentration of pTNCP. Interestingly, recent work by Arkenberg et al. stiffened partially-crosslinked 8-arm PEG-norbornene networks by adding 4-arm PEG-tetrazine, tetrazine-modified heparin, or tetrazine-modified hyaluronic acid and observed 5- to 20-fold increases in gel storage modulus.[99] While the degree of stiffening observed using non-covalent pTNCP interactions is smaller, the mPEG-Tz added to the gel is significantly smaller than the tetrazine-functionalized macromers used by Arkenberg et al., which may result in faster and more uniform diffusion of the tetrazine throughout the gel. Furthermore, these results support that TNCP-mediated stiffening may also be applicable in gels containing heparin and hyaluronic acid. In addition, while the stiffnesses achieved by this system are within a physiologically relevant range,[200] the upper and lower limits of the achievable pre- and post-stiffening moduli remain to be determined. The pTNCP concentration, PEG macromer concentration and molecular weight, peptide structure and concentration, and inclusion of alternative aromatic moieties may all be adjusted to modify the achievable mechanical properties. Varying the structure of the monofunctional tetrazine species by changing the PEG molecular weight or by substituting an alternative hydrophilic moiety may also affect the kinetics and magnitude of gel stiffening.

III.2.15 Cytocompatibility of Dynamic Stiffening Platform

Finally, the cytocompatibility of the pTNCP dynamic stiffening method was assessed. First, the efficacy of the pTNCP dynamic stiffening method in cell culture media instead of PBS was investigated. A pre-gel solution using peptide crosslinker KCGPQ-W was prepared in complete culture media and UV polymerized as previously described. The installation of pTNCP was performed by swelling the gels in complete culture media supplemented with 5.32 mM mPEG-Tz under culture conditions (37°C and 5% CO_2) and the mechanical properties of the gels were assessed. The gels demonstrated a 664 Pa (67%) increase in modulus, from 990.5±67 Pa to 1654±108 Pa ($p = 0.0018$, $n = 3$), after 4 h of treatment with 5.32 mM mPEG-Tz in complete culture media, **Figure III.7a**. Additionally, the increased shear storage modulus persisted 1- and 3-days post-stiffening, though the modulus decreased slightly over time (1594±95 Pa and 1421±309 Pa, respectively, $p = 0.49$), **Figure III.7b**.

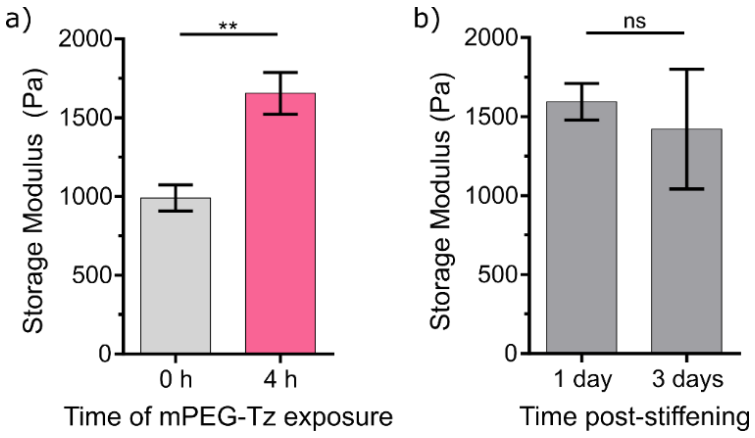

Figure III.7 (a) Gels UV polymerized and stiffened via pTNCP installation in complete culture media exhibited a 67% increase in shear storage modulus. (b) The increase in modulus persisted 1- and 3-days post-stiffening, though the average modulus decreased slightly but not significantly over time ($p = 0.49$). Reprinted with permission from Holt et al.[196]

Next, cell viability after stiffening was examined via live-dead assay. 3T3 murine fibroblasts were first encapsulated at a density of 20,000 cells/gel in a hydrogel made with 7.5% 40 kDa PEG-8-NB crosslinked with a bifunctional peptide at a 1:2 thiol-ene ratio with 1 mM CGRGDS and 2 mM LAP. Immediately after UV crosslinking, the pTNCP gels were submerged in a small amount of complete growth media supplemented with sterile 5.32 mM mPEG-Tz. Because modulus evolution experiments indicated the gel storage modulus plateaued around 4 hours, the media in both groups was supplemented with 1 mL complete growth media after 4 hours to prevent drying out of the sample. After 24 hours in culture, this media was removed and replaced with complete growth media for continued culture. The cell viability was assessed via Live/Dead assay at 1- and 3-days post-mPEG-Tz addition. After one day in culture, the

viability was 87±7% and remained high at 3 days (88±9%) as shown in **Figure III.8a-b**. There was no statistically significant difference in cell viability over the course of the experiment ($p = 0.82$). These data suggest that the installation of pTNCP has no effect on cell viability.

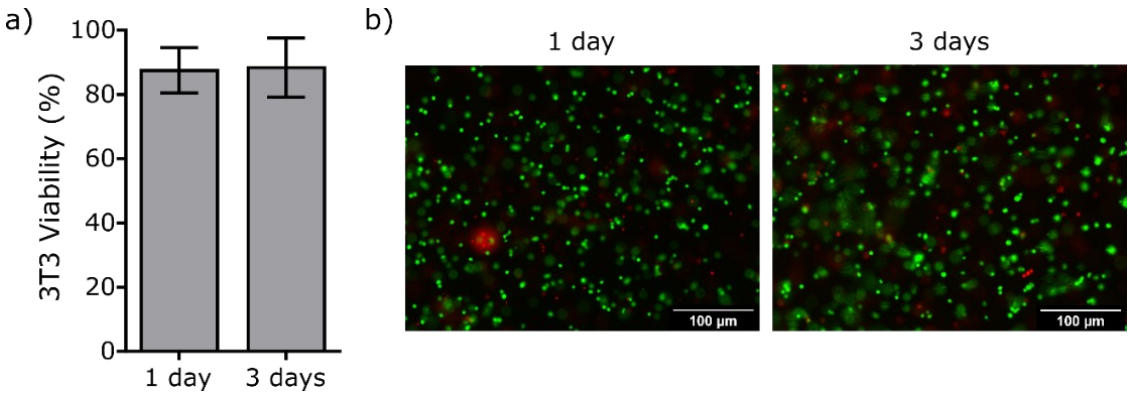

Figure III.8 (a) 3T3 fibroblasts demonstrated high viability 1 day after stiffening using mPEG-Tz (87±7%) and maintained high viability 3 days after stiffening (88±9%) with no significant statistical difference ($p = 0.82$, $n = 3$). (b) Representative images show high cell viability overall with some dead cells. Reprinted with permission from Holt et al.[196]

III.3 Conclusions

Overall, this work demonstrates a novel method with broad potential utility for controllably stiffening PEG-peptide hydrogels. Hydrogel stiffening is long-lasting and allows for but slows gel enzymatic degradability. The concentration-dependent effect of pTNCP on bulk hydrogel stiffness may allow for broad tunability of achievable properties. Also, the installation of pTNCP via IEDDA click chemistry is bio-orthogonal

and was shown to have no adverse effect on the viability of encapsulated 3T3 fibroblasts. However, future studies should investigate the effects of gel stiffening on cell morphology and migration within the gel. Future studies should also explore whether pTNCP-mediated stiffening can be applied in other polymer systems, including gelatin and hyaluronic acid, and to what degree the starting and final modulus as well as the stiffening kinetics can be controlled. Additionally, the photomediated thiol-ene reaction used to form the initial covalent gel network may allow for spatial control of the remaining free norbornene groups for the installation of pTNCP, enabling spatial control of gel stiffening. In the future, this platform has the potential to contribute to user-friendly and dynamic cell culture models of a broad spectrum of clinically important pathologies, including a variety of fibrotic diseases, cancers, and cardiovascular diseases.

CHAPTER IV

SELF-HEALING, INJECTABLE GELATIN-BASED HYDROGELS USING DYNAMIC SUPRAMOLECULAR CROSSLINKING

IV.1 Introduction

Extrudable and injectable hydrogels are of great interest for their potential use in extrusion bioprinting[122, 201, 202] as well as their myriad potential clinical applications, from the delivery of drugs and cell-based therapeutics to the facilitation of wound healing and tissue regeneration.[203-207] However, not all hydrogels are capable of being extruded. First, to be amenable to extrusion, the gel must exhibit a sufficiently low viscosity for flow under relevant shear rates and injection forces.[208] This is especially critical when the gel is used to deliver cells because high levels of shear stress during extrusion or injection can reduce cell viability.[209, 210] Second, the material must have a robust and stable polymer network after extrusion.[211] Unfortunately, these two requirements are often in direct contradiction, as mechanically robust networks have inherently high elasticity, and, if they can flow, high viscosity.[212] To address these needs, a wide variety of strategies have been explored to develop extrudable hydrogels which broadly fall into two categories: *in situ* crosslinking and shear-thinning dynamic crosslinking.

In situ crosslinking of the hydrogel polymer network allows injection of a low viscosity sol before the formation of the elastic gel at the site of installation. This has been achieved through stimulus-responsive controlled crosslinking, including a few

methods of stimulus-controlled physical crosslinking. Poly(N-isopropylacrylamide (PNIPAM) has been used repeatedly to introduce temperature-controlled physical gelation *in situ*, as it displays temperature-dependent phase transition behavior that yields a sol at low temperature and becomes a gel around physiologic temperature (37°C).[126] It can be grafted to natural polymers such as chitosan or hyaluronic acid[127] or synthetic polymers such as (R)-α-acryloyloxy-β,β-dimethyl-butyrolactone and Jeffamine acrylamide[128] to tune the swelling and degradability of the gel. Similarly, block-co-polymer systems can also exhibit a pH- or temperature-responsive phase transition. For example, Turabee et al. demonstrated the use of a block-co-polymer synthesized from PEG as well as peptides poly(γ-benzyl-L-glutamate) and oligo(sulfamethazine) for subcutaneous injection and delivery of cationic proteins.[125]

Alternatively, several stimuli-responsive covalent crosslinking methods have demonstrated application for *in situ* gelation. Many conventional covalent crosslinking reactions can also be controlled by exogenous stimuli or have a very slow reaction time which allows them to gel after extrusion. For instance, tuning the molecular weight, degree of substitution, and the concentration of thiol-functionalized hyaluronic acid (HA) and vinyl-sulfone-functionalized PEG or PEG functionalized with maleimide and thiol groups, can tune the time to gelation via Michael addition reaction to allow for injectability.[213, 214] Alternatively, UV-photocontrolled polymerization, including via radical-mediated thiol-ene chemistry[123] and radical polymerization of gelatin-methacrylate,[124] can also be used for *in situ* crosslinking post-injection. While *in situ* crosslinking methods have the potential to rapidly adopt the desired robust mechanical

properties at the delivery site, a slow-reacting gel may be deformed or the sol washed away before the polymerization reaction is complete. Furthermore, stimulus-controlled polymerization can be limited by the site of injection. For example, surgical applications of photo-controlled chemistries may be limited, as most tissues strongly attenuate light.

The second approach is to design shear-thinning hydrogels, which can display reduced flow under shear stress and then recover their properties after extrusion. These gels are typically physically crosslinked because the relatively weaker interactions can break and re-form, unlike irreversible covalent crosslinks. Firstly, several dynamic covalent crosslinking chemistries can be used to form shear-thinning hydrogels, including Schiff base linkages,[133] boronic ester bonds,[134] oxaborole-diol bonds,[135] and hydrazone bonds.[136] Of these shear-thinning gels, some rely on domain-specific supramolecular interactions. Various polymers can be functionalized with moieties that participate in supramolecular bonds while preserving other desired structural and functional characteristics of the gel. For instance, the Burdick group has developed shear-thinning hydrogels which utilize host-guest interactions between adamantane and β-cyclodextrin functional groups along an HA backbone. The mechanical profile of these gels can be tuned by changing the degree of functionalization of the HA, and by incorporating a secondary covalent Michael addition reaction,[131] the mechanical properties of the gel can be further stabilized after extrusion.[132] Several alternative strategies have taken advantage of domain-specific peptide self-assembly[215, 216] or protein-protein interactions.[66] While shear-thinning physical gels are generally weaker than those made from conventional covalent crosslinking methods, they are able to self-

heal and quickly recover their properties after extrusion. The domain-specific nature of these particular supramolecular gelling systems also allows a great deal of tunability and the integration of *in situ* covalent polymerization post-extrusion, which can offer the best features of both strategies.

Previously, we had observed similar domain-specific supramolecular interactions between the cycloaddition products of the tetrazine-norbornene inverse electron-demand Diels Alder click reaction, termed tetrazine-norbornene click products, or TNCP.[164] We were able to form supramolecular PEG hydrogels using these interactions,[164] and because the synthesis of the TNCP could be performed *in situ* in the presence of cells, we were able to install TNCP in a pre-existing covalent network that had been crosslinked via photo-controlled thiol-ene click chemistry.[196] Here, we hypothesized that TNCP functionalization could be leveraged to engineer a new class of extrudable hydrogels which combine the advantages of shear-thinning hydrogels and *in situ* gelation. We first demonstrated that TNCP supramolecular interactions could be utilized to modulate the mechanical properties of gels made from gelatin-norbornene (gelNB). Next, we synthesized a supramolecular gel by reacting gelNB with a monofunctional PEG-tetrazine to create TNCP-functionalized gelatin (gelTNCP). Finally, gelTNCP gels exhibited shear thinning and high cohesion during extrusion, and unreacted norbornene groups in the network could be leveraged for mechanical reinforcement through secondary covalent crosslinking. Taken together, these data support the broad applicability of TNCP supramolecular crosslinking in customizable injectable and extrudable hydrogels.

IV.2 Materials and Methods

IV.2.1 General Materials

4-arm, 20 kDa PEG-tetra-thiol (PEG-4-SH) and 3.4kDa PEG-di-thiol (PEG-2-SH) were purchased from Laysan Bio, Inc. and used without further modification. Lithium acylphosphinate (LAP) was purchased from Sigma-Aldrich and used without further modification.

IV.2.2 Gelatin-Norbornene Functionalization

Gelatin was functionalized with norbornene acid as previously described.[217] First, 0.684 M N-hydroxysuccinimide (NHS, Aldrich), 0.684 M 5-norbornene-2-carboxylic acid (Alfa Aesar), and 34.2 mM triethylamine (Alfa Aesar) were allowed to dissolve in anhydrous dichloromethane (DCM, Acros Organics) under nitrogen for 1 h. N,N'-diisopropylcarbodiimide (Alfa Aesar) was added dropwise to a final concentration of 0.684 M. The reaction was allowed to proceed while stirring under nitrogen for approximately 24 h, after which the reaction was filtered to remove precipitated urea by-product. The desired norbornene-NHS-ester product was collected via rotovap as a white, waxy product which was then utilized without further purification.

Type A gelatin from porcine skin (300 g bloom, Sigma) was dissolved at 10 w/v% in dimethyl sulfoxide (DMSO, VWR International) with 71 mM triethylamine at 50°C. The crude norbornene-NHS-ester from the previous step was added while stirring to a final concentration of 3.34 w/v%. The reaction was allowed to proceed at 50°C for 24 h and was then terminated by diluting the reaction in 2 volumes of distilled water. The product was dialyzed against ultrapure water at 45°C then frozen, lyophilized, and

stored at -20°C until further use. Functionalization was characterized via ^{1}H NMR as shown in **Figure IV.1** and the degree of functionalization of available amine groups on the gelNB was calculated using the method described by Tigner et al.[217] The concentration of norbornene groups was found to be 0.298 mmol per gram of gelNB.

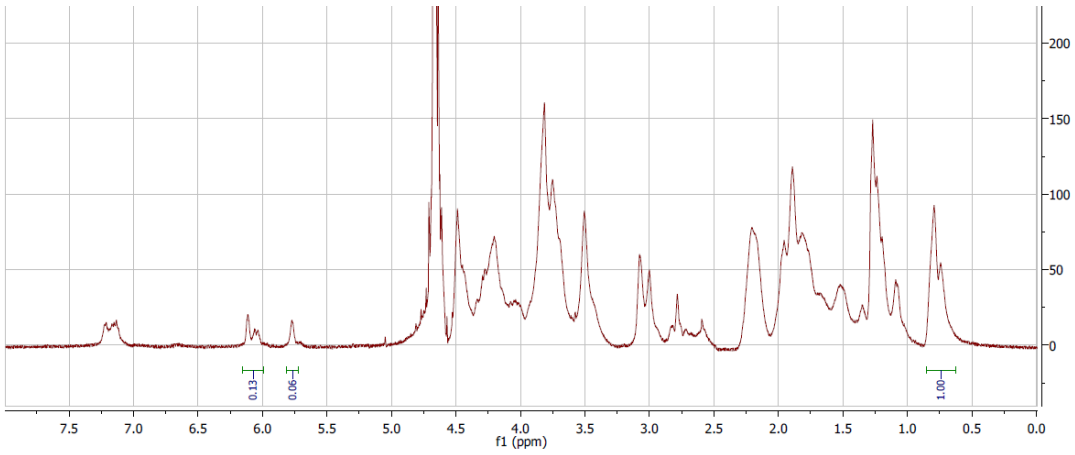

Figure IV.1 ^{1}H NMR Characterization of gelatin-norbornene functionalization (D_2O, 500 MHz). Peaks around δ 6.11 and δ 5.77 are associated with the alkene norbornene and were normalized to the methyl peak at δ 0.74.

IV.2.3 Methoxy-PEG-Tetrazine Functionalization

2 kDa methoxy-PEG-hydroxyl (mPEG-OH) was functionalized with tetrazine carboxylic acid (Tz-COOH) to yield monofunctional mPEG-tetrazine (mPEG-Tz). 1.0 g 2 kDa mPEG-NH_2 (0.50 mmol, 0.50 mmol -NH_2), 298 mg Tz-COOH (2X to NH_2, 1.00 mmol, BroadPharm), and 418 mg 1-Hydroxybenzotriazole monohydrate (HOBt, 5.5X to NH_2, Creosalus) were added to a dry, argon purged vessel. The dry components were

then dissolved in 10 mL anhydrous dimethylformamide (DMF, Acros Organics) and 0.28 mL triethylamine (4X to -NH_2, 2.00 mmol, Alfa Aesar) and 0.43 mL N,N'-diisopropylcarbodiimide (5.5X to -NH_2, 2.73 mmol, Sigma Aldrich) were added. The mixture was allowed to react for approximately 16 h under argon blanket. The reaction mixture was then precipitated in 150 mL cold diethyl ether (4°C) and centrifuged to remove the salt byproducts, then dried under vacuum and dialyzed against ultrapure water for 48 h and lyophilized. Tetrazine functionalization was verified via proton NMR and indicated 87% functionalization, **Figure IV.2**.

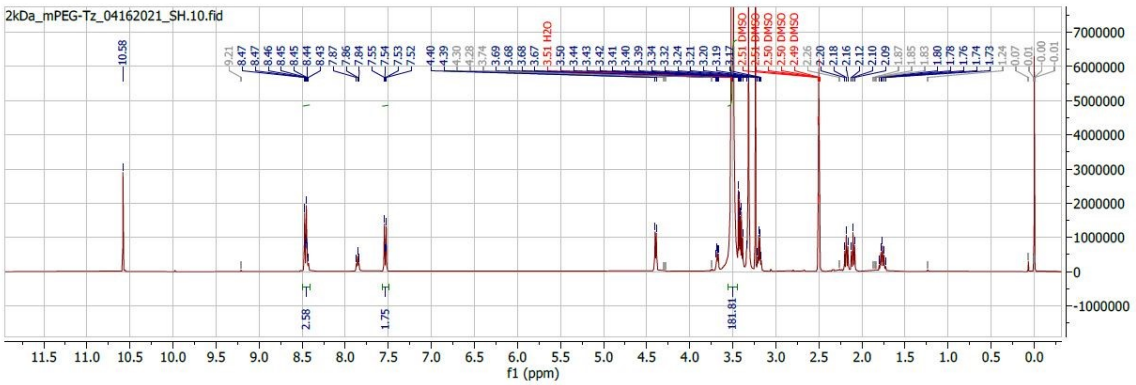

Figure IV.2 ^{1}H NMR Characterization of 2kDa mPEG-Tz in $CDCl_3$. 1H NMR (400 MHz, DMSO) δ 10.58 (s, 1H), 8.46 (dd, *J* = 7.0, 5.0 Hz, 3H), 7.86 (t, *J* = 5.7 Hz, 1H), 7.57 – 7.50 (m, 2H), 4.39 (d, *J* = 5.9 Hz, 2H), 3.68 (dd, *J* = 5.7, 4.0 Hz, 1H), 3.50 (s, 182H), 3.24 (s, 5H), 2.18 (t, *J* = 7.5 Hz, 2H), 2.10 (t, *J* = 7.4 Hz, 2H), 1.77 (h, *J* = 7.8 Hz, 2H).

IV.2.4 Gel Stiffening via In Situ TNCP Installation

GelNB at a concentration of 5 w/w% in phosphate-buffered saline (PBS) was combined with a thiol-functionalized PEG crosslinker, either 3.4 kDa PEG-2-SH or 20 kDa PEG-4-SH, at varying thiol–ene ratios as well as 2 mM of photoinitiator LAP. The solution was pipetted into 8 mm round silicone molds and UV exposed at 20 $mWcm^{-2}$ for 5 minutes, after which the gels were swelled overnight to equilibrium. The shear storage modulus for each sample (n=3) was measured via shear oscillatory rheology. An Anton Paar MCR Physica 301 rheometer was used to perform 60s time sweeps at 1% strain and 1 rad/s frequency. To test whether or not the installation of pendant TNCP would impact gel stiffness, the gel samples were then submerged in a 2kDa mPEG–Tz solution in PBS at a concentration of 5.32 mM. Each gel was incubated at room temperature on an orbital plate shaker in 400–500 μL of the corresponding mPEG–Tz solution for 6h, after which the gels were rinsed in PBS overnight and their storage modulus was assessed again. The gel samples were stored in PBS at 4°C when not in use to prevent degradation.

IV.2.5 In Situ Gelation and Modulus Evolution

Pre-gel solutions were prepared by first combining stock solutions of LAP and PEG-4-SH in sterile-filtered PBS at room temperature, then adding gel-NB warmed to 50°C for ease of pipetting and mixing briefly. This solution was kept on ice until warming for 3-5 minutes at 37°C immediately before use. Then, stock solution of 2kDa mPEG-Tz was added to the pre-gel solution and mixed via pipette. The final

concentrations of the components and ratios of reacting groups after the addition of mPEG-Tz are indicated in **Table IV.1** for the three formulations tested.

Table IV.1 Gel formulations for *in situ* gelation experiments

[mPEG-Tz] (mM); *(w/w%)*	**[GelNB] (w/w%)**	**[PEG-4-SH] (mM); *(w/w%)***	**Tz:NB Ratio**	**Thiol:NB Ratio**
4.47; *1.03*	5	0.37; *0.75*	0.30	0.10
7.45; *1.71*	5	0.37; *0.75*	0.50	0.10
7.45; *1.71*	5	0; *0*	0.50	0

The evolution of the shear storage and loss moduli of the sample was monitored via shear oscillatory rheology. Immediately following the addition of mPEG-Tz to the pre-gel solution, the sample was loaded onto the stage of an Anton Paar Physica MCR 301 rheometer, which was fitted with a transparent Peltier temperature control system. This allowed both consistent testing of the samples at 37°C and *in situ* UV polymerization of the samples. Gel samples were subject to an oscillatory time sweep for 15 min at 37°C, 1 rad/s, and 1% strain using an 8 mm diameter parallel plate geometry and a gap height of 0.5 mm. At 10 min after the beginning of the test, the samples were exposed to 365 nm UV light at an intensity of 10 $mWcm^{-2}$ for 3 min.

IV.2.6 Hydrogel Sample Preparation

GelNB at a concentration of 5 w/w% in PBS was combined with 20kDa PEG-4-SH at a concentration of 0.75 w/w % (0.37 mM, ratio of thiol:norbornene = 0.10), LAP

at a concentration of 2 mM, and 2kDa mPEG-Tz at a concentration of either 4.47 mM (tetrazine:norbornene ratio = 0.30) or 7.45 mM (tetrazine:norbornene ratio = 0.50). Samples were cast in 8 mm diameter and 1 mm thick molds made from silicone on glass slides treated with Sigmacote according to the manufacturer's protocol (Sigma-Aldrich). First, the samples were allowed to incubate in the molds at 37°C for 1 h to allow the IEDDA tetrazine reaction to proceed. Samples which also underwent UV-mediated thiol-ene polymerization were then exposed to 365 nm UV light for 3 min at an intensity of 10 $mWcm^{-2}$. Samples were then either tested immediately or stored at 4°C until use, tightly covered in the original mold to prevent evaporation.

IV.2.7 Rheological Characterization

Rheological testing was performed using a TA Instruments DHR2 Discovery hybrid stress-controlled rheometer with an 8 mm diameter parallel plate measurement geometry. All tests were performed at 37°C after a temperature equilibration period of 3 min with a 0.1 rad/s pre-shear applied for 10 s. Flow sweeps were performed using a logarithmic shear rate sweep from 0.1 to 100 s^{-1} with 5 points per decade with measurements taken at steady state flow. To characterize the recovery of the material after extrusion, peak hold tests were performed by subjecting the material to a period of low shear at a shear rate of 0.1 s^{-1} for 60 s, then a high shear period at a shear rate of 300 s^{-1} for 5 s, and then returning to low shear (0.1 s^{-1}) for 180 s.

IV.2.8 Extrusion Testing

The extrudability of the gels was assessed via filament testing. Briefly, pre-gel solutions prepared using the formulations specified in **Table IV.2** were loaded into 3 mL

syringes and allowed to polymerize for 1 hr. before extruding through the selected nozzles at 37°C. The hydrogel's capacity to form a continuous filament during extrusion was evaluated visually.

Table IV.2 GelTNCP formulations for extrusion filament testing

[mPEG-Tz] (mM); *(w/w%)*	**[GelNB] (w/w%)**	**[PEG-4-SH] (mM); *(w/w%)***	**Tz:NB Ratio**	**Thiol:NB Ratio**
4.47; *1.03*	5	0.37; *0.75*	0.30	0.10
7.45; *1.71*	5	0.37; *0.75*	0.50	0.10
4.47; *1.03*	4	0.30; *0.60*	0.375	0.10
7.45; *1.71*	4	0.30; *0.60*	0.63	0.10
4.47; *1.03*	3	0.22; *0.45*	0.5	0.10
7.45; *1.71*	3	0.22; *0.45*	0.83	0.10

IV.2.9 Statistical Analysis

Statistical analysis was performed using GraphPad Prism 6. For these data, significance was determined via ANOVA with post-hoc two-tailed Student's t-test. P values less than 0.05 were considered significant. Means are reported with standard deviations.

IV.3 Results and Discussion

IV.3.1 TNCP Supramolecular Interactions in Gelatin-Based Hydrogels

Previously, robust supramolecular gelation via TNCP interactions was demonstrated in PEG-based hydrogels.[164] Additionally, *in situ* functionalization of an

existing thiol-ene crosslinked PEG-peptide hydrogel network with pendant TNCP had yielded a controllable increase in bulk storage modulus of about 2-fold.[196] However, it remained unknown whether TNCP supramolecular interactions were unique to PEG-based hydrogels or would be present in gels made from alternative polymers. Furthermore, the impact of TNCP concentration on the mechanical properties of gelatin-based gels was unknown. To test whether TNCP interactions would be observed in gelatin-based hydrogels and, if so, what effect they would have on gel properties, we assessed the shear storage modulus of gelNB hydrogels before and after the installation of pendant TNCP. First, gelNB at a concentration of 5% w/w was combined with a thiol-functionalized PEG crosslinker, either PEG-2-SH or PEG-4-SH, at varying ratios of thiol to ene in PBS, as detailed in **Table IV.3**. Photoinitiator LAP was also added to this pre-gel mixture at a concentration of 2 mM.

Table IV.3 Gel formulations for comparing the effects of pendant TNCP installation on gelNB-based hydrogels.

Thiol-ene ratio	[Gel-NB] (w/w%)	[Norbornene] (mM)	PEG-SH functionality	[PEG-SH] (w/w%)	[SH] (mM)
0.50	5	14.9	2	1.27	7.45
0.40	5	14.9	2	1.01	5.96
0.30	5	14.9	2	0.76	4.47
0.20	5	14.9	2	0.51	2.98
0.20	5	14.9	4	1.49	2.98
0.10	5	14.9	4	0.75	1.49
0.05	5	14.9	4	0.38	0.75

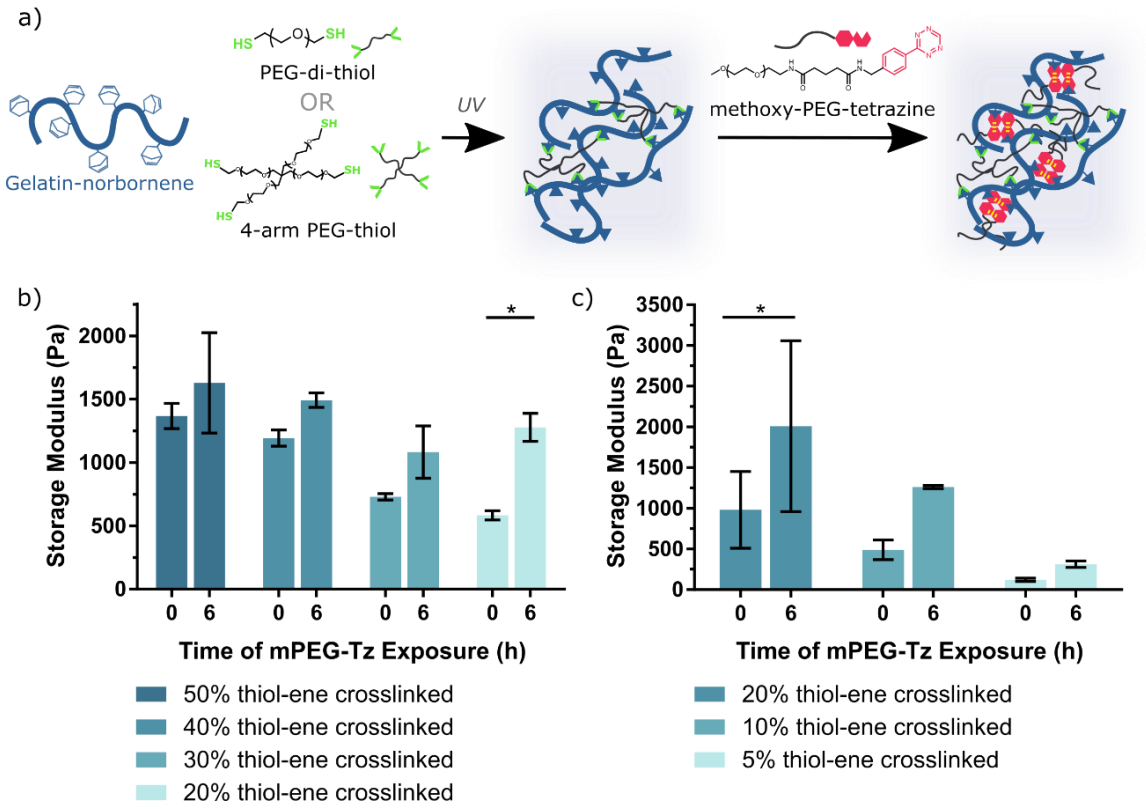

Figure IV.3 *In situ* installation of TNCP increased the shear storage moduli of partially-crosslinked covalent gelNB hydrogels. (a) Initial covalent networks were formed via radical-mediated thiol-ene click crosslinking, leaving free norbornene groups available for subsequent TNCP installation. (b) Comparison of shear storage moduli in gelNB gels crosslinked with 3.4 kDa PEG-2-SH before and after treatment with 2kDa mPEG-Tz. (c) Comparison of shear storage moduli of gelNB gels crosslinked with 20 kDa PEG-4-SH before and after treatment with 2 kDa mPEG-Tz. (n=3, * indicates $p < 0.05$)

Upon exposure to UV light, this mixture formed a covalent network via radical-mediated thiol-ene click chemistry while leaving free norbornene groups available for TNCP synthesis in the following step, **Figure IV.3a**. To facilitate *in situ* pendant TNCP functionalization, the gels were then submerged in a solution of 5.32 mM 2 kDa mPEG-Tz for 6 hours. The storage modulus of the gels was assessed via shear oscillatory

rheology after the initial covalent gels were swelled in PBS to equilibrium and again after treatment with mPEG-Tz. All experimental groups demonstrated an increase in the shear storage modulus (G') after treatment with mPEG-Tz, which indicated that the *in situ* formation of pendant TNCP yielded an increase in gel stiffness comparable to that observed in PEG-based gels, **Figure IV.3b-c**. Statistically significant differences ($p < 0.05$) were seen in both groups made with a 20% thiol-ene ratio, one crosslinked with PEG-2-SH (**Figure IV.3b**) and one crosslinked with PEG-4-SH (**Figure IV.3c**). Because of the higher functionality of the PEG-4-SH compared to PEG-2-SH, much lower thiol-ene ratios could be used and achieve gelation. These gels also had the greatest increase in G' following TNCP installation, approximately 2.6-fold in the 5% and 10% thiol-ene gels and 2.2-fold in the 20% thiol-ene gels. These data indicated that pendant TNCP did participate in supramolecular interactions which did indeed increase bulk stiffness in gelNB hydrogels.

Next, we hypothesized that TNCP supramolecular interactions alone would alone be sufficient to achieve gelation of gelatin-based hydrogels. To test this, gelNB at 5% w/w was mixed with 7.45 mM 2 kDa mPEG-Tz in PBS (tetrazine:ene ratio = 0.50) and were allowed to react *in situ* to yield TNCP-functionalized gelTNCP while storage and loss moduli were characterized via shear oscillatory rheology. As seen in PEG-based supramolecular gels, the gelTNCP gel exhibited storage modulus (G') crossover of the loss modulus (G"), indicating gelation, around 5 minutes after the beginning of the test, **Figure IV.4a**. Interestingly, these gels exhibited a G' around 100 Pa, which was significantly lower than that of those made from TNCP-functionalized 4-arm PEG

previously, which were around 8 kPa.[164] However, this lower modulus could potentially indicate the gels would be more amenable to extrusion. To test extrudability of the gelTNCP gels, samples were allowed to gel at 37°C and were then subjected to a peak hold rheological test. The gel viscosity was recorded as the gel was first subjected to a low rate of shear (0.01 s^{-1}) for 120 s, then a high rate of shear (200 s^{-1}) for 5 s, then a low rate of shear once more for an additional 120 s to monitor the gel's recovery of its initial viscosity. As shown in **Figure IV.4b**, these gels completely recovered their initial viscosity over the course of the test, with 80% recovery 50 s after the high shear. This strongly indicated the gels could withstand the shear forces of injection and extrusion.

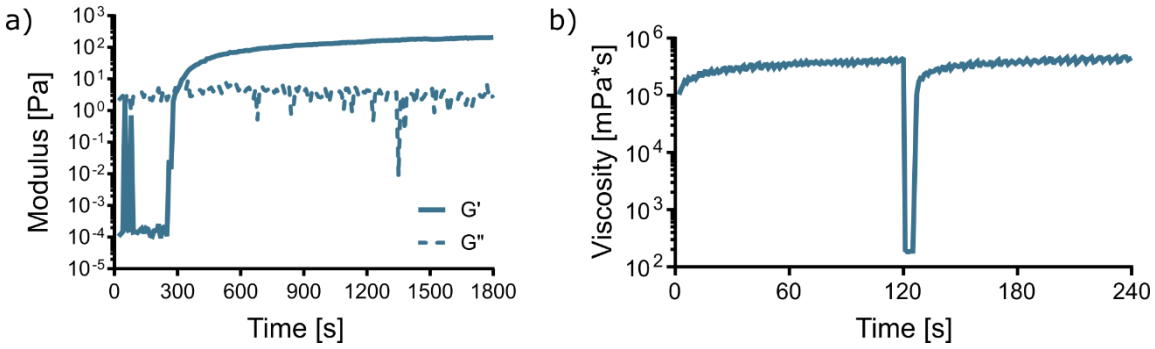

Figure IV.4 (a) TNCP-functionalized gelatin alone forms a gel within 5 minutes at 37°C and (b) is capable of viscosity recovery after shearing, with 80% recovery in approximately 50 s.

IV.3.2 Supramolecular GelTNCP Hydrogels with In-Situ Covalent Stabilization

While these results were promising, we speculated that the remaining free norbornene groups of the gelTNCP hydrogels might be leveraged for *in situ* stabilization post-injection using photocontrolled thiol-ene click chemistry, **Figure IV.5a**. The high functionality of the molecule relative to multi-arm PEG systems would in theory enable a high degree of tunability based on the concentration of TNCP functional moieties installed along the gelatin backbone. The sequential addition of covalent crosslinks could provide stabilization and mechanical reinforcement of the gels at the site of extrusion. Gels were made from 5% w/w gelNB in PBS, which is the lower concentration limit of gelatin-based extrudable gels, and at this concentration the gel must be cooled to be stiff or viscous enough to retain its shape post-extrusion.[218] To facilitate covalent crosslinking of the gels, 20 kDa PEG-4-SH was also added at a thiol:ene ratio of 0.10 (0.75% w/w; 0.375 mM) with 2 mM of photoinitiator LAP. Finally, 2 kDa mPEG-Tz was added to the mixture to initiate gelation via installation of pendant TNCP moieties. To determine whether differences in TNCP concentration would yield differences in gel properties, two concentrations of mPEG-Tz were compared: 4.47 mM (0.30 tetrazine:ene ratio) and 7.45 mM (0.50 tetrazine:ene ratio). Given these formulations, the maximum amount of available norbornene groups converted in the two formulations, accounting for the 10% of norbornene groups occupied by thiol-ene covalent crosslinks, would be 60% and 40%, respectively.

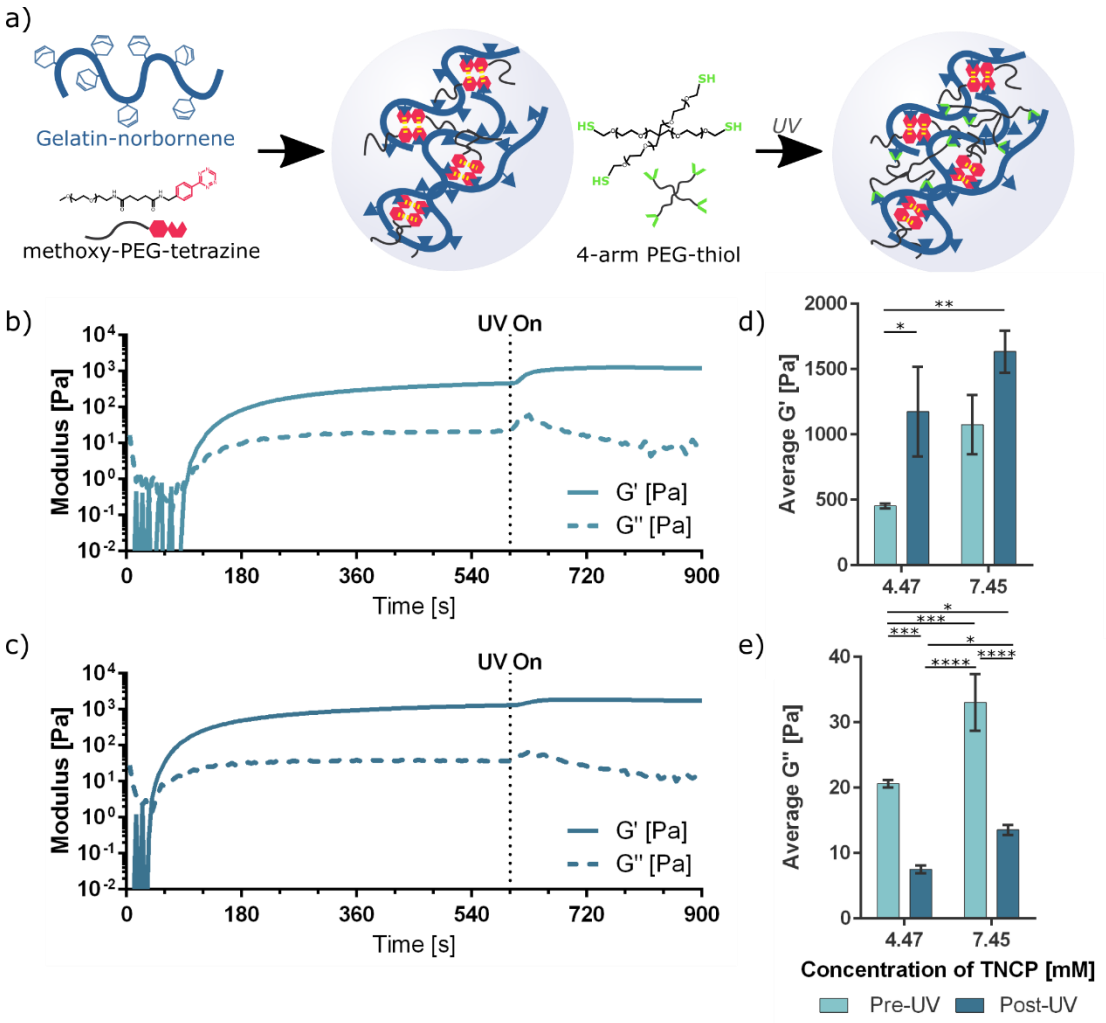

Figure IV.5 (a) *In situ* supramolecular gelation of gelTNCP with sequential thiol-ene covalent crosslinking for mechanical reinforcement. Shear storage modulus (G') crossover of shear loss modulus (G") indicates supramolecular gelation within the first two minutes of measurement for gels with both 4.47 mM (b) and 7.45 mM (c) TNCP. Average shear storage modulus, G' (d) and shear loss modulus, G" (e) of supramolecular hydrogels made with either 4.47 or 7.45 mM TNCP immediately following gelation and UV-mediated covalent stabilization. * $p < 0.05$, ** $p < 0.01$, *** $p < 0.005$, **** $p < 0.001$.

Gelation was monitored for both the 4.47 mM TNCP and 7.45 mM TNCP formulations using in situ rheology. As expected, both formulations demonstrated gelation from TNCP interactions, indicated by crossover of storage modulus G' over loss modulus G" at approximately 105 s for 4.47 mM TNCP and approximately 45 s for 7.45 mM TNCP as indicated in **Figure IV.5b-c**. Next, sequential covalent thiol-ene crosslinking was initiated via exposure to 365 nm UV light for 3 min at an intensity of 10 $mWcm^{-2}$. UV exposure was initiated 10 min after the start of the time sweep. Both gel formulations demonstrated a slight increase in G' as seen in **Figure IV.5b-c**. The initial modulus post-supramolecular and pre-covalent polymerization and the final modulus post-supramolecular and post-covalent polymerization were quantified. After supramolecular polymerization but before covalent polymerization, the 4.47 mM TNCP gels demonstrated a G' of 454 ± 19 Pa, lower than that of the 7.45 mM TNCP gels (1075 ± 227 Pa), **Figure IV.5d**. Additionally, the G' of both groups increased after UV exposure, however the 4.47 mM TNCP gels remained softer than the 7.45 mM TNCP gels (1174 ± 343 Pa and 1634 ± 161 Pa, respectively). This is consistent with previous observations of a concentration-dependent effect of pendant TNCP moieties on stiffness of PEG-based hydrogels.

Interestingly, while G' of both gel formulations increased following UV polymerization, there was a marked and highly consistent decrease in G" of both gel formulations, **Figure IV.5e**. In 4.47 mM TNCP gels, G" decreased from 33.0 ± 4.3 Pa to 13.5 ± 0.7 Pa. Loss modulus is less often reported than storage modulus for hydrogel biomaterials, as the elastic character of the gels represented by G' is more intuitively

connected to bulk gel stiffness. However, recent studies demonstrate that the viscoelastic behavior of hydrogel substrates, indicated in part by the loss modulus, has significant impact on cellular morphology and spreading.[91, 219] A decrease in viscous flow behavior of the gel material with the presence of covalent thiol-ene crosslinks makes intuitive sense, however, it remains to be seen whether that change in material would affect cell adhesion, spreading, and phenotype.

IV.3.3 Extrudability of GelTNCP Hydrogels

After demonstration of successful gelation and subsequent covalent stabilization of gelTNCP hydrogels, we explored the extrudability of these gels and their potential application for 3D bioprinting. To do so, we first investigated whether or not the supramolecular TNCP gelatin gels exhibited shear-thinning behavior. Gel samples were subject to a rheological shear rate sweep, essentially increasing the amount of shear experienced by the material, and the viscosity of the gel was measured. Furthermore, as before, gels made with 4.47 mM TNCP and 7.45 mM TNCP were compared. As expected, due to the supramolecular nature of the gel, both gels exhibited a decrease in viscosity with increasing shear, indicating shear-thinning behavior, **Figure IV.6a-b**. Furthermore, peak hold tests confirmed that the addition of PEG-4-SH and LAP did not affect the ability of the material to recover its viscosity after a short period of high shear, **Figure IV.6c**.

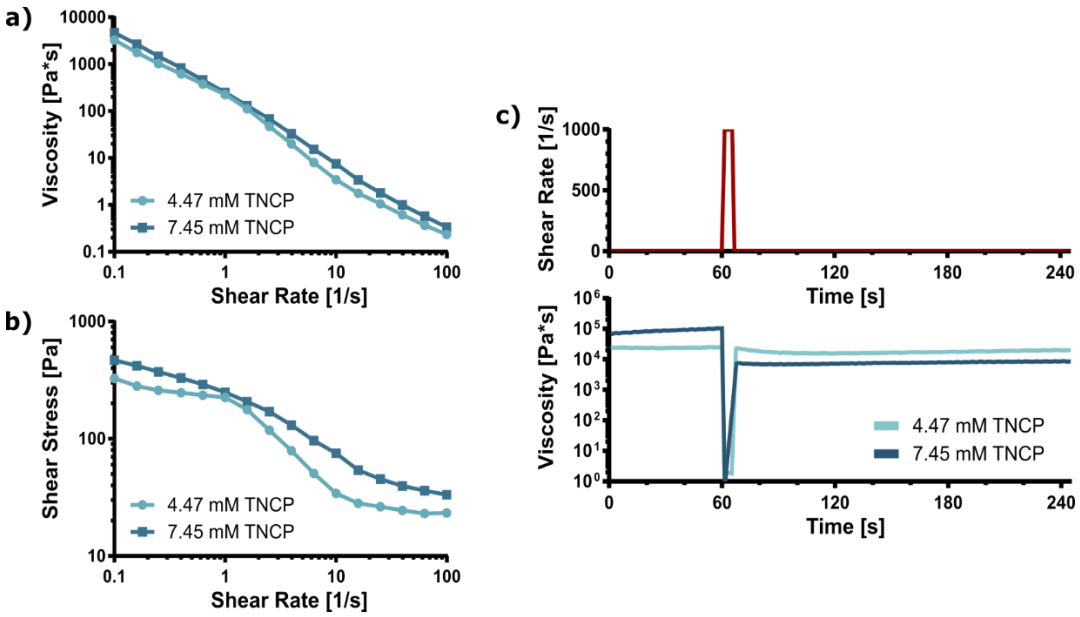

Figure IV.6 (a-b) Supramolecular gelTNCP hydrogels supplemented with uncrosslinked 20kDa PEG-4-SH at a thiol-ene ratio of 0.10 exhibit shear-thinning behavior at both a high (7.45 mM) and low (4.47 mM) concentration of TNCP. (c) Both gel formulations also display self-healing behavior as shown by viscosity recovery during a peak hold test.

Unexpectedly, the gels displayed very similar flow profiles as well. This may be due to similarities in the effects of shear forces on supramolecular TNCP interactions regardless of their concentration. Additionally, the gels were loaded into a syringe outfitted with a 22 ga. (0.41 mm inner diameter) extrusion nozzle and examined using a hanging filament test, **Figure IV.7**. To enable optimization, we attempted testing with formulations using varied gelNB concentration (3, 4, or 5 w/w%) as well as TNCP concentration (4.47 mM or 7.45 mM). The 5 w/w% gelatin formulations had the highest hanging filament length, with both approximately 5 cm before breaking. This indicates a

particularly high degree of cohesion within the gel, which is particularly promising for application in injectable gel delivery. The *in situ* covalent stabilization of the gel via thiol-ene crosslinking post-extrusion adds to this promise, as the mechanical stabilization of the gel would further improve potential for the retention of the gel at the site of delivery.

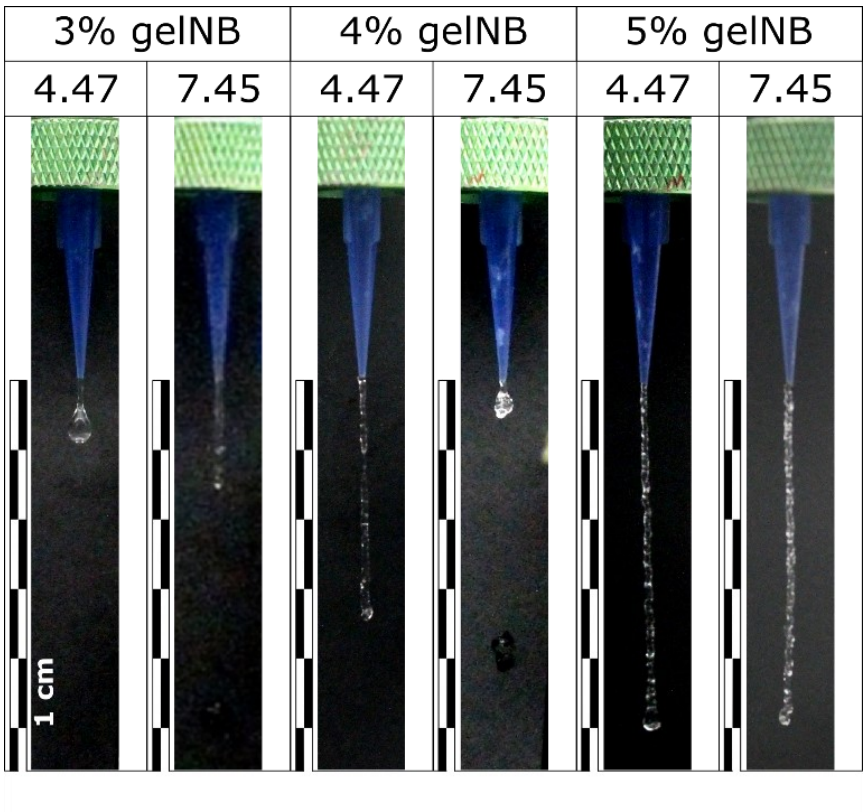

Figure IV.7 Hanging filament testing of varying gelTNCP formulations comparing gelatin concentration (3, 4, or 5 w/w% gelNB) and low (4.47 mM) or high (7.45 mM) concentration of TNCP.

IV.4 Conclusions

Overall, this work demonstrates that TNCP supramolecular interactions can be applied in gelatin-based hydrogels and can be used to create supramolecular, extrudable materials, broadening the range of their potential applicability. The *in situ* installation of pendant TNCP groups in a covalently crosslinked gelNB gel induced a clear stiffening effect on the gel network. Additionally, supramolecular gelTNCP gels were formed via *in situ* synthesis of TNCP via an IEDDA tetrazine click reaction between gelNB and mPEG-Tz. These supramolecular gels exhibited shear thinning behavior and recovery after shear, and also did so with the addition of PEG-4-SH and LAP in solution. These added components enabled the photocontrolled covalent stabilization of the gel, and in the future may be useful for 'setting' the gel after its injection or after extrusion bioprinting. Future studies will examine the cytocompatibility of this material and the viability of gel-encapsulated and extruded cells. Additionally, future investigations may further expound upon the broad applicability of TNCP supramolecular interactions in alternative biopolymer hydrogels, including protein-based materials such as collagen or even decellularized extracellular matrix along with polysaccharides like alginate and hyaluronic acid. This method of supramolecular crosslinking shows great promise as a potential bio-orthogonal mechanism for generating self-healing and extrudable gels for a wide variety of uses.

CHAPTER V

CONCLUSIONS

V.1 Summary

In summary, this work presents the discovery of supramolecular interactions between the cycloaddition products of the tetrazine-norbornene IEDDA click reaction, TNCP, and the application of these supramolecular interactions in hydrogel scaffolds for cell culture as well as an extrudable hydrogel platform. The discovery of TNCP supramolecular interactions challenges the assumption that click crosslinking reactions can be used interchangeably to synthesize hydrogels with identical properties, despite otherwise identical compositions. A head-to-head comparison of otherwise identical PEG hydrogels crosslinked with either radical-mediated thiol-ene click or tetrazine click showed significant differences in gel stiffness, swelling, and susceptibility to hydrolytic degradation (**Chapter II**). Thiol-ene- and tetrazine-crosslinked gels both exhibited high gel fractions, and NMR confirmed a high degree of norbornene conversion (~100%) in the thiol-ene gels, which meant the differences in gel properties could not be due to differences in crosslinking efficiency. Non-covalent gelation by TNCP end-functionalized 4-arm PEG confirmed the presence of supramolecular interactions between TNCP, which was also supported by molecular dynamics simulations.

Next, TNCP supramolecular interactions were applied to create PEG-peptide hydrogel scaffolds for cell culture which exhibit controllable dynamic stiffening via progressive, *in situ* installation of pendant TNCP groups in a pre-existing covalent

network (**Chapter III**). Partially covalently crosslinked networks were formed from 8-arm, norbornene-functionalized PEG and bis-cysteine enzymatically-labile peptides via radical-mediated thiol-ene click chemistry. A cell-adhesive cysteine-containing pendant peptide, CGRGDS, was also incorporated into the network at a concentration of 1 mM. This left about 50% of the norbornene groups present in the system available for the installation of pendant TNCP via reaction with a monofunctional methoxy-PEG-tetrazine. Pendant TNCP demonstrated a concentration-dependent effect on bulk gel stiffness and *in situ* installation of pendant TNCP resulted in an approximately 2 kPa increase in shear storage modulus over the course of 4-6 hours. Furthermore, this approach demonstrated no negative effect on the viability of encapsulated murine fibroblasts and the increase in gel stiffness was maintained in culture conditions over the course of several days.

Finally, supramolecular TNCP interactions were used to physically crosslink a gelatin-based shear-thinning and extrudable hydrogel (**Chapter IV**). The similar and robust effects of pendant TNCP functionalization on the properties of both PEG and gelatin hydrogels suggests potential for broad applicability in both synthetic and natural materials. Norbornene-functionalized gelatin was reacted with a monofunctional methoxy-PEG-tetrazine *in situ* to yield TNCP-functionalized gelatin, or gelTNCP. GelTNCP in aqueous solution formed shear-thinning and self-healing hydrogels via TNCP supramolecular interactions. These properties were conserved when 4-arm PEG-thiol and photoinitiator LAP were added to the gel to enable UV-mediated covalent crosslinking post-extrusion. Furthermore, gelTNCP gels exhibited high cohesion and

stability during extrusion. Taken together, these data indicate that gelTNCP hydrogels merit further investigation as an injectable carrier for cells and therapeutics.

V.2 Significance and Future Directions

The discovery and application of TNCP supramolecular crosslinking uniquely enables the *in situ,* bio-orthogonal synthesis of supramolecular interacting domains in the presence of cells and sensitive biomolecules, but further work is required to elucidate the biological impact of the presence of TNCPs and the materials which they create. First, further studies are needed to confirm whether or not TNCP supramolecular hydrogels maintain viability of extruded or injected cells. Additionally, the degree of cell spreading and migration supported by TNCP supramolecular hydrogels is also an important area of future study. Specifically, future work is required to address whether dynamic gel stiffening through the *in situ* installation of pendant TNCP restricts cell motility in a way comparable to secondary covalent crosslinking.

Because tetrazine and strained cyclic alkenes like norbornene are not found in nature, there is little concern of cross-reactivity with surrounding biomolecules. However, future work could investigate whether their presence impacts the retention and availability of bioactive signaling molecules. Particularly, hydrophobic small molecules with aromatic structures such as the neurotransmitter dopamine or steroid hormone estradiol may be preferentially retained in the gel due to pi-pi, electrostatic, or hydrogen bonding interactions or any combination of the three with the TNCP moiety. If these interactions exist, they could have interesting but certainly underexplored implications for gel applications in tissue engineering and regenerative medicine. For instance, there

is evidence that both dopamine and estradiol can regulate angiogenesis in wound healing.[220, 221] If such supramolecular interactions with biomolecules do exist, they could also have potential applications in drug delivery.

One of the important questions to be addressed in future studies is whether or not TNCP supramolecular crosslinking and orthogonal covalent click crosslinking can be used to create a hydrogel platform with the capacity to selectively tune viscoelasticity. Seminal work by Mooney et al. introduced an alginate-based ionotropically crosslinked hydrogel platform with independent tunability of the gel's elastic modulus and rate of stress relaxation, a measure of viscoelasticity.[91] However, the calcium-mediated crosslinking may present some confounding biological effects, particularly if one deigns to modify the level of crosslinking over time. In an investigation of the biomolecular regulation of cell spreading and morphology in this same alginate platform, the Chaudhuri group demonstrated that the tonicity of the surrounding environment could have an impact on cell volume and phenotype, and specifically implicated calcium ion channel TRPV4 in this process.[222] It follows that although it may be independent of the stress relaxation response of the material, an effort to tune the material elasticity by increasing or decreasing the concentration of calcium will have a confounding biological impact. In contrast, the bioorthogonality of the tetrazine click reaction and the thiol-ene click reaction, as applied in the dynamic stiffening 3D culture matrix in **Chapter III**, would avoid these concerns and could allow for modification of the viscoelastic profile of the hydrogel *in situ* in the presence of cells.

Additionally, photomediated thiol-ene click chemistry could not only be used to spatially pattern matrix elasticity via covalent crosslinking, but could also selectively react available pendant norbornene groups to spatially control where TNCP supramolecular interactions will be localized upon addition of monofunctional tetrazine species. As non-destructive longitudinal mechanical and biological characterization methods such as Brillouin and Raman spectroscopy and fluorescence lifetime imaging microscopy (FLIM) improve and become more widely adopted, a bio-orthogonal and controllable method for spatial and temporal modification of hydrogel viscoelasticity could be used to recreate complex processes driven by spatial and temporal changes in matrix viscoelasticity, such as embryonic development.[223]

Overall, this work introduces new complexities to the understanding of hydrogel click crosslinking, and leverages that understanding to create novel materials with exciting potential applications. The future of TNCP supramolecular chemistry offers fascinating potential roads for investigation by integrating a new level of spatial and temporal control of hydrogel viscoelasticity. While the biological impacts of this innovation remain to be discovered, the growing body of work on dynamic hydrogel crosslinking suggests exciting and impactful things to come.

REFERENCES

1. Peppas, N. A.; Hilt, J. Z.; Khademhosseini, A.; Langer, R., Hydrogels in biology and medicine: From molecular principles to bionanotechnology. *Adv. Mater.* **2006,** *18* (11), 1345-1360.

2. Rizzo, F.; Kehr, N. S., Recent Advances in Injectable Hydrogels for Controlled and Local Drug Delivery. *Adv. Healthcare Mater.* **2021**, *10*, Article 2001341. DOI: 10.1002/adhm.202001341.

3. Caliari, S. R.; Burdick, J. A., A practical guide to hydrogels for cell culture. *Nat. Methods* **2016,** *13* (5), 405-414.

4. Li, Y.; Wang, X. N.; Han, Y. Y.; Sun, H. Y.; Hilborn, J.; Shi, L. Y., Click chemistry-based biopolymeric hydrogels for regenerative medicine. *Biomed. Mater.* **2021**, *16*, Article 022003. DOI: 10.1088/1748-605X/abc0b3.

5. Madl, C. M.; Heilshorn, S. C.; Blau, H. M., Bioengineering strategies to accelerate stem cell therapeutics. *Nature* **2018,** *557* (7705), 335-342.

6. Slaughter, B. V.; Khurshid, S. S.; Fisher, O. Z.; Khademhosseini, A.; Peppas, N. A., Hydrogels in Regenerative Medicine. *Adv. Mater.* **2009,** *21* (32-33), 3307-3329.

7. Braun, D.; Cherdron, H.; Rehahn, M.; Ritter, H.; Voit, B., *Polymer Synthesis : Theory and Practice : Fundamentals, Methods, Experiments*. 4th ed. ed.; Springer: 2005.

8. Sawhney, A. S.; Pathak, C. P.; Hubbell, J. A., Bioerodible hydrogels based on photopolymerized poly(ethylene glycol)-co-poly(.alpha.-hydroxy acid) diacrylate macromers. *Macromolecules* **1993,** *26* (4), 581-587.

9. Hern, D. L.; Hubbell, J. A., Incorporation of adhesion peptides into nonadhesive hydrogels useful for tissue resurfacing. *Journal of Biomedical Materials Research* **1998,** *39* (2), 266-276.

10. Mann, B. K.; Gobin, A. S.; Tsai, A. T.; Schmedlen, R. H.; West, J. L., Smooth muscle cell growth in photopolymerized hydrogels with cell adhesive and proteolytically degradable domains: Synthetic ECM analogs for tissue engineering. *Biomaterials* **2001,** *22* (22), 3045-3051.

11. Omidian, H.; Park, K.; Kandalam, U.; Rocca, J. G., Swelling and Mechanical Properties of Modified HEMA-based Superporous Hydrogels. *Journal of Bioactive and Compatible Polymers* **2010,** *25* (5), 483-497.

12. Kulik, E.; Ikada, Y., In vitro platelet adhesion to nonionic and ionic hydrogels with different water contents. *Journal of Biomedical Materials Research* **1996,** *30* (3), 295-304.

13. Jeon, O.; Bouhadir, K. H.; Mansour, J. M.; Alsberg, E., Photocrosslinked alginate hydrogels with tunable biodegradation rates and mechanical properties. *Biomaterials* **2009,** *30* (14), 2724-2734.

14. Nichol, J. W.; Koshy, S. T.; Bae, H.; Hwang, C. M.; Yamanlar, S.; Khademhosseini, A., Cell-laden microengineered gelatin methacrylate hydrogels. *Biomaterials* **2010,** *31* (21), 5536-5544.

15. Kolesky, D. B.; Truby, R. L.; Gladman, A. S.; Busbee, T. A.; Homan, K. A.; Lewis, J. A., 3D Bioprinting of Vascularized, Heterogeneous Cell-Laden Tissue Constructs. *Adv. Mater.* **2014,** *26* (19), 3124-3130.

16. Billiet, T.; Gevaert, E.; De Schryver, T.; Cornelissen, M.; Dubruel, P., The 3D printing of gelatin methacrylamide cell-laden tissue-engineered constructs with high cell viability. *Biomaterials* **2014,** *35* (1), 49-62.

17. Eke, G.; Mangir, N.; Hasirci, N.; MacNeil, S.; Hasirci, V., Development of a UV crosslinked biodegradable hydrogel containing adipose derived stem cells to promote vascularization for skin wounds and tissue engineering. *Biomaterials* **2017,** *129*, 188-198.

18. Pedron, S.; Harley, B. A. C., Impact of the biophysical features of a 3D gelatin microenvironment on glioblastoma malignancy. *Journal of Biomaterials Research A* **2013,** *101A* (12), 3404-3415.

19. Kaemmerer, E.; Melchels, F. P. W.; Holzapfel, B. M.; Meckel, T.; Hutmacher, D. W.; Loessner, D., Gelatine methacrylamide-based hydrogels: An alternative three-dimensional cancer cell culture system. *Acta Biomater.* **2014,** *10* (6), 2551-2562.

20. Loessner, D.; Meinert, C.; Kaemmerer, E.; Martine, L. C.; Yue, K.; Levett, P. A.; Klein, T. J.; Melchels, F. P. W.; Khademhosseini, A.; Hutmacher, D. W., Functionalization, preparation and use of cell-laden gelatin methacryloyl-based hydrogels as modular tissue culture platforms. *Nature Protocols* **2016,** *11* (4), 727-746.

21. Roberts, J. J.; Bryant, S. J., Comparison of photopolymerizable thiol-ene PEG and acrylate-based PEG hydrogels for cartilage development. *Biomaterials* **2013,** *34* (38), 9969-9979.

22. Vats, K.; Marsh, G.; Harding, K.; Zampetakis, I.; Waugh, R. E.; Benoit, D. S. W., Nanoscale physicochemical properties of chain- and step-growth polymerized PEG

hydrogels affect cell-material interactions. *J. Biomed. Mater. Res. Part A* **2017,** *105* (4), 1112-1122.

23. Kolb, H. C.; Finn, M. G.; Sharpless, K. B., Click Chemistry: Diverse Chemical Function from a Few Good Reactions. *Angew. Chem. Int. Ed.* **2001,** *40* (11), 2004-2021.

24. Nwe, K.; Brechbiel, M. W., Growing Applications of "Click Chemistry" for Bioconjugation in Contemporary Biomedical Research. *Cancer Biotherapy and Radiopharmaceuticals* **2009,** *24* (3), 289-302.

25. Meghani, N. M.; Amin, H. H.; Lee, B.-J., Mechanistic applications of click chemistry for pharmaceutical drug discovery and drug delivery. *Drug Discovery Today* **2017,** *22* (11), 1604-1619.

26. Kumar, S.; Sharma, B.; Mehra, V.; Kumar, V., Recent accomplishments on the synthetic/biological facets of pharmacologically active 1H-1,2,3-triazoles. *European Journal of Medicinal Chemistry* **2021,** *212*, 113069.

27. Parker, C. G.; Pratt, M. R., Click Chemistry in Proteomic Investigations. *Cell* **2020,** *180* (4), 605-632.

28. DeForest, C. A.; Anseth, K. S., Advances in Bioactive Hydrogels to Probe and Direct Cell Fate. *Annu. Rev. Chem. Biomol. Eng.* **2012,** *3* (1), 421-444.

29. Lutolf, M. P.; Hubbell, J. A., Synthesis and Physicochemical Characterization of End-Linked Poly(ethylene glycol)-co-peptide Hydrogels Formed by Michael-Type Addition. *Biomacromolecules* **2003,** *4* (3), 713-722.

30. Lutolf, M. P.; Raeber, G. P.; Zisch, A. H.; Tirelli, N.; Hubbell, J. A., Cell-Responsive Synthetic Hydrogels. *Adv. Mater.* **2003,** *15* (11), 888-892.

31. Fairbanks, B. D.; Schwartz, M. P.; Halevi, A. E.; Nuttelman, C. R.; Bowman, C. N.; Anseth, K. S., A Versatile Synthetic Extracellular Matrix Mimic via Thiol-Norbornene Photopolymerization. *Adv. Mater.* **2009,** *21* (48), 5005-5010.

32. Ossipov, D. A.; Hilborn, J., Poly(vinyl alcohol)-based hydrogels formed by "click chemistry". *Macromolecules* **2006,** *39* (5), 1709-1718.

33. Liu, S. Q.; Ee, P. L. R.; Ke, C. Y.; Hedrick, J. L.; Yang, Y. Y., Biodegradable poly(ethylene glycol)-peptide hydrogels with well-defined structure and properties for cell delivery. *Biomaterials* **2009,** *30* (8), 1453-1461.

34. Deforest, C. A.; Sims, E. A.; Anseth, K. S., Peptide-Functionalized Click Hydrogels with Independently Tunable Mechanics and Chemical Functionality for 3D Cell Culture. *Chem. Mater.* **2010,** *22* (16), 4783-4790.

35. Alge, D. L.; Azagarsamy, M. A.; Donohue, D. F.; Anseth, K. S., Synthetically Tractable Click Hydrogels for Three-Dimensional Cell Culture Formed Using Tetrazine-Norbornene Chemistry. *Biomacromolecules* **2013,** *14* (4), 949-953.

36. Wang, H. Y.; Heilshorn, S. C., Adaptable Hydrogel Networks with Reversible Linkages for Tissue Engineering. *Adv. Mater.* **2015,** *27* (25), 3717-3736.

37. Perera, M. M.; Ayres, N., Dynamic covalent bonds in self-healing, shape memory, and controllable stiffness hydrogels. *Polym. Chem.* **2020,** *11* (8), 1410-1423.

38. McKinnon, D. D.; Domaille, D. W.; Cha, J. N.; Anseth, K. S., Bis-Aliphatic Hydrazone-Linked Hydrogels Form Most Rapidly at Physiological pH: Identifying the Origin of Hydrogel Properties with Small Molecule Kinetic Studies. *Chem. Mater.* **2014,** *26* (7), 2382-2387.

39. Richardson, B. M.; Wilcox, D. G.; Randolph, M. A.; Anseth, K. S., Hydrazone covalent adaptable networks modulate extracellular matrix deposition for cartilage tissue engineering. *Acta Biomater.* **2019,** *83*, 71-82.

40. Grover, G. N.; Lam, J.; Nguyen, T. H.; Segura, T.; Maynard, H. D., Biocompatible Hydrogels by Oxime Click Chemistry. *Biomacromolecules* **2012,** *13* (10), 3013-3017.

41. Smith, L. J.; Taimoory, S. M.; Tam, R. Y.; Baker, R. E. G.; Mohammad, N. B.; Trant, J. F.; Shoichet, M. S., Diels Alder Click-Cross-Linked Hydrogels with Increased Reactivity Enable 3D Cell Encapsulation. *Biomacromolecules* **2018,** *19* (3), 926-935.

42. Zhang, Y. L.; Yang, B.; Xu, L. X.; Zhang, X. Y.; Tao, L.; Wei, Y., Self-healing Hydrogels Based on Dynamic Chemistry and Their Biomedical Applications. *Acta Chim. Sinica* **2013,** *71* (4), 485-492.

43. Kuo, C. K.; Ma, P. X., Maintaining dimensions and mechanical properties of ionically crosslinked alginate hydrogel scaffolds in vitro. *J. Biomed. Mater. Res. Part A* **2008,** *84A* (4), 899-907.

44. Mangione, M. R.; Giacomazza, D.; Bulone, D.; Martorana, V.; Cavallaro, G.; San Biagio, P. L., K+ and Na+ effects on the gelation properties of κ-Carrageenan. *Biophys. Chem.* **2005,** *113* (2), 129-135.

45. Bakarich, S. E.; Panhuis, M. I. H.; Beirne, S.; Wallace, G. G.; Spinks, G. M., Extrusion printing of ionic-covalent entanglement hydrogels with high toughness. *J. Mat. Chem. B* **2013,** *1* (38), 4939-4946.

46. Mihaila, S. M.; Gaharwar, A. K.; Reis, R. L.; Marques, A. P.; Gomes, M. E.; Khademhosseini, A., Photocrosslinkable Kappa-Carrageenan Hydrogels for Tissue Engineering Applications. *Adv. Healthcare Mater.* **2013,** *2* (6), 895-907.

47. Puppi, D.; Migone, C.; Morelli, A.; Bartoli, C.; Gazzarri, M.; Pasini, D.; Chiellini, F., Microstructured chitosan/poly(γ-glutamic acid) polyelectrolyte complex hydrogels by computer-aided wet-spinning for biomedical three-dimensional scaffolds. *Journal of Bioactive and Compatible Polymers* **2016,** *31* (5), 531-549.

48. Murakawa, K.; King, D. R.; Sun, T.; Guo, H.; Kurokawa, T.; Gong, J. P., Polyelectrolyte complexation via viscoelastic phase separation results in tough and self-recovering porous hydrogels. *J. Mat. Chem. B* **2019,** *7* (35), 5296-5305.

49. Suneetha, M.; Rao, K. M.; Han, S. S., Mechanically improved porous hydrogels with polysaccharides via polyelectrolyte complexation for bone tissue engineering. *Int. J. Biol. Macromol.* **2020,** *144*, 160-169.

50. Vegners, R.; Shestakova, I.; Kalvinsh, I.; Ezzell, R. M.; Janmey, P. A., Use of a gel-forming dipeptide derivative as a carrier for antigen presentation. *J. Pept. Sci.* **1995,** *1* (6), 371-378.

51. Williams, R. J.; Hall, T. E.; Glattauer, V.; White, J.; Pasic, P. J.; Sorensen, A. B.; Waddington, L.; McLean, K. M.; Currie, P. D.; Hartley, P. G., The in vivo performance of an enzyme-assisted self-assembled peptide/protein hydrogel. *Biomaterials* **2011,** *32* (22), 5304-5310.

52. Liang, L.; Xu, X. D.; Chen, C. S.; Fang, J. H.; Jiang, F. G.; Zhang, X. Z.; Zhuo, R. X., Evaluation of the Biocompatibility of Novel Peptide Hydrogel in Rabbit Eye. *J. Biomed. Mater. Res. Part B* **2010,** *93B* (2), 324-332.

53. Baek, K.; Noblett, A. D.; Ren, P. Y.; Suggs, L. J., Design and Characterization of Nucleopeptides for Hydrogel Self-Assembly. *ACS Appl. Bio Mater.* **2019,** *2* (7), 2812-2821.

54. Arokianathan, J. F.; Ramya, K. A.; Janeena, A.; Deshpande, A. P.; Ayyadurai, N.; Leemarose, A.; Shanmugam, G., Non-proteinogenic amino acid based supramolecular hydrogel material for enhanced cell proliferation. *Colloid Surf. B-Biointerfaces* **2020**, *185*, Article 110581. DOI: 10.1016/j.colsurfb.2019.110581.

55. Vilaca, H.; Castro, T.; Costa, F. M. G.; Melle-Franco, M.; Hilliou, L.; Hamley, I. W.; Castanheira, E. M. S.; Martins, J. A.; Ferreira, P. M. T., Self-assembled RGD dehydropeptide hydrogels for drug delivery applications. *J. Mat. Chem. B* **2017,** *5* (43), 8607-8617.

56. Panda, J. J.; Mishra, A.; Basu, A.; Chauhan, V. S., Stimuli Responsive Self-Assembled Hydrogel of a Low Molecular Weight Free Dipeptide with Potential for Tunable Drug Delivery. *Biomacromolecules* **2008,** *9* (8), 2244-2250.

57. Wu, C. G.; Wang, X.; Shi, Y. F.; Wang, B. C.; Xue, W.; Zhang, Y., Transforming sustained release into on-demand release: self-healing guanosine-borate supramolecular hydrogels with multiple responsiveness for Acyclovir delivery. *Biomater. Sci.* **2020,** *8* (22), 6190-6203.

58. Lalitha, K.; Prasad, Y. S.; Maheswari, C. U.; Sridharan, V.; John, G.; Nagarajan, S., Stimuli responsive hydrogels derived from a renewable resource: synthesis, self-assembly in water and application in drug delivery. *J. Mat. Chem. B* **2015,** *3* (27), 5560-5568.

59. Dankers, P. Y. W.; Harmsen, M. C.; Brouwer, L. A.; Van Luyn, M. J. A.; Meijer, E. W., A modular and supramolecular approach to bioactive scaffolds for tissue engineering. *Nat. Mater.* **2005,** *4* (7), 568-574.

60. Wang, Q.; Shi, Z.; Shou, Y. F.; Zhang, K. X.; Li, G. F.; Xia, P. F.; Yan, S. F.; Yin, J. B., Stack-Based Hydrogels with Mechanical Enhancement, High Stability, Self-Healing Property, and Thermoplasticity from Poly(L-glutamic acid) and Ureido-Pyrimidinone. *ACS Biomater. Sci. Eng.* **2020,** *6* (3), 1715-1726.

61. Wietor, J.-L.; van Beek, D. J. M.; Peters, G. W.; Mendes, E.; Sijbesma, R. P., Effects of Branching and Crystallization on Rheology of Polycaprolactone Supramolecular Polymers with Ureidopyrimidinone End Groups. *Macromolecules* **2011,** *44* (5), 1211-1219.

62. Lewis, C. L.; Anthamatten, M., Synthesis, swelling behavior, and viscoelastic properties of functional poly(hydroxyethyl methacrylate) with ureidopyrimidinone side-groups. *Soft Matter* **2013,** *9* (15), 4058-4066.

63. Maleki, S. E.; Shokrollahi, P.; Barzin, J., Impact of supramolecular interactions on swelling and release behavior of UPy functionalized HEMA-based hydrogels. *Polym. Adv. Technol.* **2018,** *29* (6), 1670-1683.

64. Balavigneswaran, C. K.; Muthuvijayan, V., Nanohybrid-Reinforced Gelatin-Ureidopyrimidinone-Based Self-healing Injectable Hydrogels for Tissue Engineering Applications. *ACS Appl. Bio Mater.* **2021,** *4* (6), 5362-5377.

65. Guo, M.; Pitet, L. M.; Wyss, H. M.; Vos, M.; Dankers, P. Y. W.; Meijer, E. W., Tough Stimuli-Responsive Supramolecular Hydrogels with Hydrogen-Bonding Network Junctions. *J. Am. Chem. Soc.* **2014,** *136* (19), 6969-6977.

66. Wong Po Foo, C. T. S.; Lee, J. S.; Mulyasasmita, W.; Parisi-Amon, A.; Heilshorn, S. C., Two-component protein-engineered physical hydrogels for cell encapsulation. *Proceedings of the National Academy of Sciences* **2009,** *106* (52), 22067-22072.

67. Mulyasasmita, W.; Lee, J. S.; Heilshorn, S. C., Molecular-Level Engineering of Protein Physical Hydrogels for Predictive Sol–Gel Phase Behavior. *Biomacromolecules* **2011,** *12* (10), 3406-3411.

68. Chu, T.-W.; Feng, J.; Yang, J.; Kopeček, J., Hybrid polymeric hydrogels via peptide nucleic acid (PNA)/DNA complexation. *J. Controlled Release* **2015,** *220*, 608-616.

69. Chen, G.; Jiang, M., Cyclodextrin-based inclusion complexation bridging supramolecular chemistry and macromolecular self-assembly. *Chem. Soc. Rev.* **2011,** *40* (5), 2254-2266.

70. Li, J.; Harada, A.; Kamachi, M., Sol–Gel Transition during Inclusion Complex Formation between α-Cyclodextrin and High Molecular Weight Poly(ethylene glycol)s in Aqueous Solution. *Polym. J.* **1994,** *26* (9), 1019-1026.

71. Wang, J.; Williamson, G. S.; Yang, H., Branched polyrotaxane hydrogels consisting of alpha-cyclodextrin and low-molecular-weight four-arm polyethylene glycol and the utility of their thixotropic property for controlled drug release. *Colloids and Surfaces B: Biointerfaces* **2018,** *165*, 144-149.

72. Huh, K. M.; Cho, Y. W.; Chung, H.; Kwon, I. C.; Jeong, S. Y.; Ooya, T.; Lee, W. K.; Sasaki, S.; Yui, N., Supramolecular hydrogel formation based on inclusion complexation between poly(ethylene glycol)-modified chitosan and alpha-cyclodextrin. *Macromol. Biosci.* **2004,** *4* (2), 92-99.

73. Huh, K. M.; Ooya, T.; Lee, W. K.; Sasaki, S.; Kwon, I. C.; Jeong, S. Y.; Yui, N., Supramolecular-Structured Hydrogels Showing a Reversible Phase Transition by Inclusion Complexation between Poly(ethylene glycol) Grafted Dextran and α-Cyclodextrin. *Macromolecules* **2001,** *34* (25), 8657-8662.

74. Li, J.; Li, X.; Zhou, Z.; Ni, X.; Leong, K. W., Formation of Supramolecular Hydrogels Induced by Inclusion Complexation between Pluronics and α-Cyclodextrin. *Macromolecules* **2001,** *34* (21), 7236-7237.

75. Feng, Q.; Wei, K. C.; Lin, S. E.; Xu, Z.; Sun, Y. X.; Shi, P.; Li, G.; Bian, L. M., Mechanically resilient, injectable, and bioadhesive supramolecular gelatin hydrogels crosslinked by weak host-guest interactions assist cell infiltration and in situ tissue regeneration. *Biomaterials* **2016,** *101*, 217-228.

76. Yang, B.; Wei, Z.; Chen, X.; Wei, K.; Bian, L., Manipulating the mechanical properties of biomimetic hydrogels with multivalent host–guest interactions. *J. Mat. Chem. B* **2019,** *7* (10), 1726-1733.

77. Lee, S. Y.; Jeon, S. I.; Sim, S. B.; Byun, Y.; Ahn, C.-H., A supramolecular host-guest interaction-mediated injectable hydrogel system with enhanced stability and sustained protein release. *Acta Biomater.* **2021,** *131*, 286-301.

78. Appel, E. A.; Biedermann, F.; Rauwald, U.; Jones, S. T.; Zayed, J. M.; Scherman, O. A., Supramolecular Cross-Linked Networks via Host−Guest Complexation with Cucurbit[8]uril. *J. Am. Chem. Soc.* **2010,** *132* (40), 14251-14260.

79. Appel, E. A.; Loh, X. J.; Jones, S. T.; Dreiss, C. A.; Scherman, O. A., Sustained release of proteins from high water content supramolecular polymer hydrogels. *Biomaterials* **2012,** *33* (18), 4646-4652.

80. Hong, K. H.; Song, S.-C., 3D hydrogel stem cell niche controlled by host-guest interaction affects stem cell fate and survival rate. *Biomaterials* **2019**, *218*, Article 119338. DOI: https://doi.org/10.1016/j.biomaterials.2019.119338.

81. Ren, P.; Wang, F.; Bernaerts, K. V.; Fu, Y.; Hu, W.; Zhou, N.; Dai, J.; Liang, M.; Zhang, T., Self-Assembled Supramolecular Hybrid Hydrogels Based on Host–Guest Interaction: Formation and Application in 3D Cell Culture. *ACS Appl. Bio Mater.* **2020,** *3* (10), 6768-6778.

82. Hoyle, C. E.; Bowman, C. N., Thiol–Ene Click Chemistry. *Angew. Chem. Int. Ed.* **2010,** *49* (9), 1540-1573.

83. Mũnoz, Z.; Shih, H.; Lin, C.-C., Gelatin hydrogels formed by orthogonal thiol–norbornene photochemistry for cell encapsulation. *Biomater. Sci.* **2014,** *2* (8), 1063-1072.

84. Gramlich, W. M.; Kim, I. L.; Burdick, J. A., Synthesis and orthogonal photopatterning of hyaluronic acid hydrogels with thiol-norbornene chemistry. *Biomaterials* **2013,** *34* (38), 9803-9811.

85. Lee, S. H.; Moon, J. J.; West, J. L., Three-dimensional micropatterning of bioactive hydrogels via two-photon laser scanning photolithography for guided 3D cell migration. *Biomaterials* **2008,** *29* (20), 2962-2968.

86. Azagarsamy, M. A.; Alge, D. L.; Radhakrishnan, S. J.; Tibbitt, M. W.; Anseth, K. S., Photocontrolled nanoparticles for on-demand release of proteins. *Biomacromolecules* **2012,** *13* (8), 2219-2224.

87. Kloxin, A. M.; Kasko, A. M.; Salinas, C. N.; Anseth, K. S., Photodegradable Hydrogels for Dynamic Tuning of Physical and Chemical Properties. *Science* **2009,** *324* (April), 59-64.

88. Paszek, M. J.; Zahir, N.; Johnson, K. R.; Lakins, J. N.; Rozenberg, G. I.; Gefen, A.; Reinhart-King, C. A.; Margulies, S. S.; Dembo, M.; Boettiger, D.; Hammer, D. A.; Weaver, V. M., Tensional homeostasis and the malignant phenotype. *Cancer Cell* **2005,** *8* (3), 241-254.

89. Engler, A. J.; Sen, S.; Sweeney, H. L.; Discher, D. E., Matrix Elasticity Directs Stem Cell Lineage Specification. *Cell* **2006,** *126* (4), 677-689.

90. Ulrich, T. A.; de Juan Pardo, E. M.; Kumar, S., The Mechanical Rigidity of the Extracellular Matrix Regulates the Structure , Motility , and Proliferation of Glioma Cells. *Cancer Research* **2009,** *69* (10), 4167-4175.

91. Chaudhuri, O.; Gu, L.; Klumpers, D.; Darnell, M.; Bencherif, S. A.; Weaver, J. C.; Huebsch, N.; Lee, H.-p.; Lippens, E.; Duda, G. N.; Mooney, D. J., Hydrogels with tunable stress relaxation regulate stem cell fate and activity. *Nat. Mater.* **2016,** *15* (3), 326-334.

92. Wei, Z.; Schnellmann, R.; Pruitt, H. C.; Gerecht, S., Hydrogel Network Dynamics Regulate Vascular Morphogenesis. *Cell Stem Cell* **2020,** *27* (5), 798-812.

93. Young, J. L.; Engler, A. J., Hydrogels with time-dependent material properties enhance cardiomyocyte differentiation in vitro. *Biomaterials* **2011,** *32* (4), 1002-1009.

94. Young, J. L.; Tuler, J.; Braden, R.; Schup-Magoffin, P.; Schaefer, J.; Kretchmer, K.; Christman, K. L.; Engler, A. J., In vivo response to dynamic hyaluronic acid hydrogels. *Acta Biomater.* **2013,** *9* (7), 7151-7157.

95. Ondeck, M. G.; Engler, A. J., Mechanical Characterization of a Dynamic and Tunable Methacrylated Hyaluronic Acid Hydrogel. *J. Biomech. Eng.* **2016**, *138*, Article 021003. DOI: 10.1115/1.4032429.

96. Duan, B.; Yin, Z. Y.; Kang, L. H.; Magin, R. L.; Butcher, J. T., Active tissue stiffness modulation controls valve interstitial cell phenotype and osteogenic potential in 3D culture. *Acta Biomater.* **2016,** *36*, 42-54.

97. Mabry, K. M.; Lawrence, R. L.; Anseth, K. S., Dynamic stiffening of poly(ethylene glycol)-based hydrogels to direct valvular interstitial cell phenotype in a three-dimensional environment. *Biomaterials* **2015,** *49*, 47-56.

98. Wiley, K. L.; Ovadia, E. M.; Calo, C. J.; Huber, R. E.; Kloxin, A. M., Rate-based approach for controlling the mechanical properties of 'thiol–ene' hydrogels formed with visible light. *Polym. Chem.* **2019,** *10* (32), 4428-4440.

99. Arkenberg, M. R.; Dimmitt, N. H.; Johnson, H. C.; Koehler, K. R.; Lin, C. C., Dynamic Click Hydrogels for Xeno-Free Culture of Induced Pluripotent Stem Cells. *Adv. Biosyst.* **2020**, *4*, Article 2000129. DOI: 10.1002/adbi.202000129.

100. Liu, H. Y.; Greene, T.; Lin, T. Y.; Dawes, C. S.; Korc, M.; Lin, C. C., Enzyme-mediated stiffening hydrogels for probing activation of pancreatic stellate cells. *Acta Biomater.* **2017,** *48*, 258-269.

101. Liu, H.-Y.; Korc, M.; Lin, C.-C., Biomimetic and enzyme-responsive dynamic hydrogels for studying cell-matrix interactions in pancreatic ductal adenocarcinoma. *Biomaterials* **2018,** *160*, 24-36.

102. Nguyen, H. D.; Liu, H. Y.; Hudson, B. N.; Lin, C. C., Enzymatic Cross-Linking of Dynamic Thiol-Norbornene Click Hydrogels. *ACS Biomater. Sci. Eng.* **2019,** *5* (3), 1247-1256.

103. Liu, H. Y.; Nguyen, H. D.; Lin, C. C., Dynamic PEG-Peptide Hydrogels via Visible Light and FMN-Induced Tyrosine Dimerization. *Adv. Healthcare Mater.* **2018**, *7*, Article 1800954. DOI: 10.1002/adhm.201800954.

104. McBeath, R.; Pirone, D. M.; Nelson, C. M.; Bhadriraju, K.; Chen, C. S., Cell shape, cytoskeletal tension, and RhoA regulate stem cell lineage commitment. *Dev. Cell* **2004,** *6* (4), 483-495.

105. Kilian, K. A.; Bugarija, B.; Lahn, B. T.; Mrksich, M., Geometric cues for directing the differentiation of mesenchymal stem cells. *Proc. Natl. Acad. Sci. U. S. A.* **2010,** *107* (11), 4872-4877.

106. Lee, J.; Abdeen, A. A.; Wycislo, K. L.; Fan, T. M.; Kilian, K. A., Interfacial geometry dictates cancer cell tumorigenicity. *Nat. Mater.* **2016,** *15* (8), 856-862.

107. Vasilevich, A. S.; Vermeulen, S.; Kamphuis, M.; Roumans, N.; Eroume, S.; Hebels, D.; van de Peppel, J.; Reihs, R.; Beijer, N. R. M.; Carlier, A.; Carpenter, A. E.; Singh, S.; de Boer, J., On the correlation between material-induced cell shape and phenotypical response of human mesenchymal stem cells. *Sci. Rep.* **2020**, *10*, Article 18988. DOI: 10.1038/s41598-020-76019-z.

108. Stowers, R. S.; Allen, S. C.; Suggs, L. J., Dynamic phototuning of 3D hydrogel stiffness. *Proc. Natl. Acad. Sci. U. S. A.* **2015,** *112* (7), 1953-1958.

109. Previtera, M. L.; Trout, K. L.; Verma, D.; Chippada, U.; Schloss, R. S.; Langrana, N. A., Fibroblast Morphology on Dynamic Softening of Hydrogels. *Ann. Biomed. Eng.* **2012,** *40* (5), 1061-1072.

110. Shih, H.; Lin, C. C., Tuning stiffness of cell-laden hydrogel via host-guest interactions. *J. Mater. Chem. B* **2016,** *4* (29), 4969-4974.

111. Freeberg, M. A. T.; Perelas, A.; Rebman, J. K.; Phipps, R. P.; Thatcher, T. H.; Sime, P. J., Mechanical Feed-Forward Loops Contribute to Idiopathic Pulmonary Fibrosis. *Am. J. Pathol.* **2021,** *191* (1), 18-25.

112. Chen, G. B.; Xia, B.; Fu, Q.; Huang, X.; Wang, F. P.; Chen, Z. M.; Lv, Y. G., Matrix Mechanics as Regulatory Factors and Therapeutic Targets in Hepatic Fibrosis. *Int. J. Biol. Sci.* **2019,** *15* (12), 2509-2521.

113. Gaetani, R.; Zizzi, E. A.; Deriu, M. A.; Morbiducci, U.; Pesce, M.; Messina, E., When Stiffness Matters: Mechanosensing in Heart Development and Disease. *Frontiers in Cell and Developmental Biology* **2020**, *8*, Article 334. DOI: 10.3389/fcell.2020.00334.

114. Zieman, S. J.; Melenovsky, V.; Kass, D. A., Mechanisms, pathophysiology, and therapy of arterial stiffness. *Arterioscler. Thromb. Vasc. Biol.* **2005,** *25* (5), 932-943.

115. Piersma, B.; Hayward, M. K.; Weaver, V. M., Fibrosis and cancer: A strained relationship. *Biochim. Biophys. Acta, Rev. Cancer* **2020**, *1873*, Article 188356. DOI: 10.1016/j.bbcan.2020.188356.

116. Chevalier, N. R.; Gazguez, E.; Bidault, L.; Guilbert, T.; Vias, C.; Vian, E.; Watanabe, Y.; Muller, L.; Germain, S.; Bondurand, N.; Dufour, S.; Fleury, V., How Tissue Mechanical Properties Affect Enteric Neural Crest Cell Migration. *Sci. Rep.* **2016**, *6*, Article 20927. DOI: 10.1038/srep20927.

117. Barriga, E. H.; Franze, K.; Charras, G.; Mayor, R., Tissue stiffening coordinates morphogenesis by triggering collective cell migration in vivo. *Nature* **2018,** *554*, 523-527.

118. Majkut, S.; Idema, T.; Swift, J.; Krieger, C.; Liu, A.; Discher, D. E., Heart-Specific Stiffening in Early Embryos Parallels Matrix and Myosin Expression to Optimize Beating. *Curr. Biol.* **2013,** *23* (23), 2434-2439.

119. Klein, E. A.; Yin, L. Q.; Kothapalli, D.; Castagnino, P.; Byfield, F. J.; Xu, T. N.; Levental, I.; Hawthorne, E.; Janmey, P. A.; Assoian, R. K., Cell-Cycle Control by Physiological Matrix Elasticity and In Vivo Tissue Stiffening. *Curr. Biol.* **2009,** *19* (18), 1511-1518.

120. Aguado, B. A.; Mulyasasmita, W.; Su, J.; Lampe, K. J.; Heilshorn, S. C., Improving Viability of Stem Cells During Syringe Needle Flow Through the Design of Hydrogel Cell Carriers. *Tissue Eng. Part A* **2012,** *18* (7-8), 806-815.

121. Bajaj, P.; Schweller, R. M.; Khademhosseini, A.; West, J. L.; Bashir, R., 3D Biofabrication Strategies for Tissue Engineering and Regenerative Medicine. In *Annual Review of Biomedical Engineering, Vol 16*, Yarmush, M. L., Ed. Annual Reviews: Palo Alto, 2014; Vol. 16, pp 247-276.

122. Li, J. H.; Wu, C. T.; Chu, P. K.; Gelinsky, M., 3D printing of hydrogels: Rational design strategies and emerging biomedical applications. *Mater. Sci. Eng. R-Rep.* **2020**, *140*, Article 100543. DOI: 10.1016/j.mser.2020.100543.

123. Zheng Shu, X.; Liu, Y.; Palumbo, F. S.; Luo, Y.; Prestwich, G. D., In situ crosslinkable hyaluronan hydrogels for tissue engineering. *Biomaterials* **2004,** *25* (7), 1339-1348.

124. Lin, R.-Z.; Chen, Y.-C.; Moreno-Luna, R.; Khademhosseini, A.; Melero-Martin, J. M., Transdermal regulation of vascular network bioengineering using a photopolymerizable methacrylated gelatin hydrogel. *Biomaterials* **2013,** *34* (28), 6785-6796.

125. Turabee, M. H.; Thambi, T.; Duong, H. T. T.; Jeong, J. H.; Lee, D. S., A pH- and temperature-responsive bioresorbable injectable hydrogel based on polypeptide block copolymers for the sustained delivery of proteins in vivo. *Biomater. Sci.* **2018,** *6* (3), 661-671.

126. Chen, S. B.; Zhong, H.; Gu, B.; Wang, Y. Z.; Li, X. M.; Cheng, Z. P.; Zhang, L. L.; Yao, C., Thermosensitive phase behavior and drug release of in situ N-isopropylacrylamide copolymer. *Mater. Sci. Eng. C-Mater. Biol. Appl.* **2012,** *32* (8), 2199-2204.

127. Chou, P. Y.; Chen, S. H.; Chen, C. H.; Chen, S. H.; Fong, Y. T.; Chen, J. P., Thermo-responsive in-situ forming hydrogels as barriers to prevent post-operative peritendinous adhesion. *Acta Biomater.* **2017,** *63*, 85-95.

128. Overstreet, D. J.; Huynh, R.; Jarbo, K.; McLemore, R. Y.; Vernon, B. L., In situ forming, resorbable graft copolymer hydrogels providing controlled drug release. *J. Biomed. Mater. Res. Part A* **2013,** *101* (5), 1437-1446.

129. Saim, A. B.; Cao, Y.; Weng, Y.; Chang, C.-N.; Vacanti, M. A.; Vacanti, C. A.; Eavey, R. D., Engineering Autogenous Cartilage in the Shape of a Helix Using an Injectable Hydrogel Scaffold. *The Laryngoscope* **2000,** *110* (10), 1694-1697.

130. DesNoyer, J. R.; McHugh, A. J., The effect of Pluronic on the protein release kinetics of an injectable drug delivery system. *J. Controlled Release* **2003,** *86* (1), 15-24.

131. Rodell, C. B.; Kaminski, A. L.; Burdick, J. A., Rational Design of Network Properties in Guest–Host Assembled and Shear-Thinning Hyaluronic Acid Hydrogels. *Biomacromolecules* **2013,** *14* (11), 4125-4134.

132. Rodell, C. B.; MacArthur Jr., J. W.; Dorsey, S. M.; Wade, R. J.; Wang, L. L.; Woo, Y. J.; Burdick, J. A., Shear-Thinning Supramolecular Hydrogels with Secondary Autonomous Covalent Crosslinking to Modulate Viscoelastic Properties In Vivo. *Adv. Funct. Mater.* **2015,** *25* (4), 636-644.

133. Qu, J.; Zhao, X.; Ma, P. X.; Guo, B., pH-responsive self-healing injectable hydrogel based on N-carboxyethyl chitosan for hepatocellular carcinoma therapy. *Acta Biomater.* **2017,** *58*, 168-180.

134. Huang, Z.; Delparastan, P.; Burch, P.; Cheng, J.; Cao, Y.; Messersmith, P. B., Injectable dynamic covalent hydrogels of boronic acid polymers cross-linked by bioactive plant-derived polyphenols. *Biomater. Sci.* **2018,** *6* (9), 2487-2495.

135. Wang, Y. N.; Li, L.; Kotsuchibashi, Y.; Vshyvenko, S.; Liu, Y.; Hall, D.; Zeng, H. B.; Narain, R., Self-Healing and Injectable Shear Thinning Hydrogels Based on Dynamic Oxaborole-Diol Covalent Cross-Linking. *ACS Biomater. Sci. Eng.* **2016,** *2* (12), 2315-2323.

136. Chen, J.; Li, X.; Gao, L.; Hu, Y.; Zhong, W.; Xing, M. M., A Facile Strategy for In Situ Controlled Delivery of Doxorubicin with a pH-Sensitive Injectable Hydrogel. *Nano LIFE* **2014**, *04*, Article 1441001. DOI: 10.1142/s1793984414410013.

137. Lin, C. C.; Raza, A.; Shih, H., PEG hydrogels formed by thiol-ene photo-click chemistry and their effect on the formation and recovery of insulin-secreting cell spheroids. *Biomaterials* **2011,** *32* (36), 9685-9695.

138. Blackman, M. L.; Royzen, M.; Fox, J. M., Tetrazine ligation: Fast bioconjugation based on inverse-electron-demand Diels-Alder reactivity. *J. Am. Chem. Soc.* **2008,** *130* (41), 13518-13519.

139. Barker, I. A.; Hall, D. J.; Hansell, C. F.; Du Prez, F. E.; O'Reilly, R. K.; Dove, A. P., Tetrazine-Norbornene Click Reactions to Functionalize Degradable Polymers Derived from Lactide. *Macromol. Rapid Commun.* **2011,** *32* (17), 1362-1366.

140. Hansell, C. F.; Espeel, P.; Stamenovic, M. M.; Barker, I. A.; Dove, A. P.; Du Prez, F. E.; O'Reilly, R. K., Additive-Free Clicking for Polymer Functionalization and Coupling by Tetrazine-Norbornene Chemistry. *J. Am. Chem. Soc.* **2011,** *133* (35), 13828-13831.

141. Hansell, C. F.; O'Reilly, R. K., A "Mix-and-Click" Approach to Double Core-Shell Micelle Functionalization. *ACS Macro Lett.* **2012,** *1* (7), 896-901.

142. Li, Z. B.; Cai, H. C.; Hassink, M.; Blackman, M. L.; Brown, R. C. D.; Conti, P. S.; Fox, J. M., Tetrazine-trans-cyclooctene ligation for the rapid construction of F-18 labeled probes. *Chem. Commun.* **2010,** *46* (42), 8043-8045.

143. Selvaraj, R.; Liu, S. L.; Hassink, M.; Huang, C. W.; Yap, L. P.; Park, R.; Fox, J. M.; Li, Z. B.; Conti, P. S., Tetrazine-trans-cyclooctene ligation for the rapid construction of integrin alpha(v)beta(3) targeted PET tracer based on a cyclic RGD peptide. *Bioorg. Med. Chem. Lett.* **2011,** *21* (17), 5011-5014.

144. Liu, D. S.; Tangpeerachaikul, A.; Selvaraj, R.; Taylor, M. T.; Fox, J. M.; Ting, A. Y., Diels-Alder Cycloaddition for Fluorophore Targeting to Specific Proteins inside Living Cells. *J. Am. Chem. Soc.* **2012,** *134* (2), 792-795.

145. Lang, K.; Davis, L.; Wallace, S.; Mahesh, M.; Cox, D. J.; Blackman, M. L.; Fox, J. M.; Chin, J. W., Genetic Encoding of Bicyclononynes and trans-Cyclooctenes for Site-Specific Protein Labeling in Vitro and in Live Mammalian Cells via Rapid Fluorogenic Diels-Alder Reactions. *J. Am. Chem. Soc.* **2012,** *134* (25), 10317-10320.

146. Hansell, C. F.; Lu, A.; Patterson, J. P.; O'Reilly, R. K., Exploiting the tetrazine-norbornene reaction for single polymer chain collapse. *Nanoscale* **2014,** *6* (8), 4102-4107.

147. Wilks, T. R.; O'Reilly, R. K., Efficient DNA-Polymer Coupling in Organic Solvents: A Survey of Amide Coupling, Thiol-Ene and Tetrazine-Norbornene Chemistries Applied to Conjugation of Poly(N-Isopropylacrylamide). *Sci. Rep.* **2016**, *6*, Article 39192. DOI: 10.1038/srep39192.

148. Desai, R. M.; Koshy, S. T.; Hilderbrand, S. A.; Mooney, D. J.; Joshi, N. S., Versatile click alginate hydrogels crosslinked via tetrazine-norbornene chemistry. *Biomaterials* **2015,** *50*, 30-37.

149. Lueckgen, A.; Garske, D. S.; Ellinghaus, A.; Desai, R. M.; Stafford, A. G.; Mooney, D. J.; Duda, G. N.; Cipitria, A., Hydrolytically-degradable click-crosslinked alginate hydrogels. *Biomaterials* **2018,** *181*, 189-198.

150. Koshy, S. T.; Desai, R. M.; Joly, P.; Li, J. Y.; Bagrodia, R. K.; Lewin, S. A.; Joshi, N. S.; Mooney, D. J., Click-Crosslinked Injectable Gelatin Hydrogels. *Adv. Healthcare Mater.* **2016,** *5* (5), 541-547.

151. Koshy, S. T.; Zhang, D. K. Y.; Grolman, J. M.; Stafford, A. G.; Mooney, D. J., Injectable nanocomposite cryogels for versatile protein drug delivery. *Acta Biomater.* **2018,** *65*, 36-43.

152. Jivan, F.; Yegappan, R.; Pearce, H.; Carrow, J. K.; McShane, M.; Gaharwar, A. K.; Alge, D. L., Sequential Thiol-Ene and Tetrazine Click Reactions for the Polymerization and Functionalization of Hydrogel Microparticles. *Biomacromolecules* **2016,** *17* (11), 3516-3523.

153. Zhang, H.; Dicker, K. T.; Xu, X.; Jia, X.; Fox, J. M., Interfacial bioorthogonal cross-linking. *ACS Macro Lett.* **2014,** *3* (8), 727-731.

154. Zhang, H.; Trout, W. S.; Liu, S.; Andrade, G. A.; Hudson, D. A.; Scinto, S. L.; Dicker, K. T.; Li, Y.; Lazouski, N.; Rosenthal, J.; Thorpe, C.; Jia, X. Q.; Fox, J. M., Rapid Bioorthogonal Chemistry Turn-on through Enzymatic or Long Wavelength Photocatalytic Activation of Tetrazine Ligation. *J. Am. Chem. Soc.* **2016,** *138* (18), 5978-5983.

155. Dicker, K. T.; Song, J.; Moore, A. C.; Zhang, H.; Li, Y.; Burris, D. L.; Jia, X.; Fox, J. M., Core-shell patterning of synthetic hydrogels via interfacial bioorthogonal chemistry for spatial control of stem cell behavior. *Chemical Science* **2018,** *9* (24), 5394-5404.

156. Hao, Y.; Song, J.; Ravikrishnan, A.; Dicker, K. T.; Fowler, E. W.; Zerdoum, A. B.; Li, Y.; Zhang, H.; Rajasekaran, A. K.; Fox, J. M.; Jia, X. Q., Rapid Bioorthogonal Chemistry Enables in Situ Modulation of the Stem Cell Behavior in 3D without External Triggers. *Acs Applied Materials & Interfaces* **2018,** *10* (31), 26016-26027.

157. Liu, S.; Moore, A. C.; Zerdoum, A. B.; Zhang, H.; Scinto, S. L.; Zhang, H.; Gong, L.; Burris, D. L.; Rajasekaran, A. K.; Fox, J. M.; Jia, X. Q., Cellular interactions with hydrogel microfibers synthesized via interfacial tetrazine ligation. *Biomaterials* **2018,** *180*, 24-35.

158. Truong, V. X.; Ablett, M. P.; Richardson, S. M.; Hoyland, J. A.; Dove, A. P., Simultaneous Orthogonal Dual-Click Approach to Tough, in-Situ-Forming Hydrogels for Cell Encapsulation. *J. Am. Chem. Soc.* **2015,** *137* (4), 1618-1622.

159. Zustiak, S. P.; Leach, J. B., Hydrolytically degradable poly(ethylene glycol) hydrogel scaffolds with tunable degradation and mechanical properties. *Biomacromolecules* **2010,** *11* (5), 1348-1357.

160. Phelps, E. A.; Enemchukwu, N. O.; Fiore, V. F.; Sy, J. C.; Murthy, N.; Sulchek, T. A.; Barker, T. H.; García, A. J., Maleimide Cross-Linked Bioactive PEG Hydrogel Exhibits Improved Reaction Kinetics and Cross-Linking for Cell Encapsulation and In Situ Delivery. *Adv. Mater.* **2012,** *24* (1), 64-70.

161. Xu, J.; Filion, T. M.; Prifti, F.; Song, J., Cytocompatible Poly(ethylene glycol)-co-polycarbonate Hydrogels Cross-Linked by Copper-Free, Strain-Promoted Click Chemistry. *Chemistry – An Asian Journal* **2011,** *6* (10), 2730-2737.

162. Shih, H.; Lin, C.-C., Cross-Linking and Degradation of Step-Growth Hydrogels Formed by Thiol–Ene Photoclick Chemistry. *Biomacromolecules* **2012,** *13* (7), 2003-2012.

163. Fairbanks, B. D.; Schwartz, M. P.; Bowman, C. N.; Anseth, K. S., Photoinitiated polymerization of PEG-diacrylate with lithium phenyl-2,4,6-

trimethylbenzoylphosphinate: polymerization rate and cytocompatibility. *Biomaterials* **2009,** *30* (35), 6702-6707.

164. Holt, S. E.; Rakoski, A.; Jivan, F.; Pérez, L. M.; Alge, D. L., Hydrogel Synthesis and Stabilization via Tetrazine Click-Induced Secondary Interactions. *Macromol. Rapid Commun.* **2020**, *41*, Article 2000287. DOI: 10.1002/marc.202000287.

165. Alge, D. L.; Donohue, D. F.; Anseth, K. S., Facile and efficient Lewis acid catalyzed synthesis of an asymmetric tetrazine useful for bio-orthogonal click chemistry applications. *Tetrahedron Lett.* **2013,** *54* (41), 5639-5641.

166. Devaraj, N. K.; Weissleder, R.; Hilderbrand, S. A., Tetrazine-Based Cycloadditions: Application to Pretargeted Live Cell Imaging. *Bioconjugate Chem.* **2008,** *19* (12), 2297-2299.

167. Bowers, K. J.; Chow, E.; Xu, H.; Dror, R. O.; Eastwood, M. P.; Gregersen, B. A.; Klepeis, J. L.; Kolossvary, I.; Moraes, M. A.; Sacerdoti, F. D.; Salmon, J. K.; Shan, Y.; Shaw, D. E., Scalable algorithms for molecular dynamics simulations on commodity clusters. In *Proceedings of the 2006 ACM/IEEE conference on Supercomputing*, Association for Computing Machinery: Tampa, Florida, 2006; p 84.

168. *Schrödinger Release 2018-4: Maestro-Desmond Interoperability Tools*, Schrödinger: New York, NY, 2018.

169. *Schrödinger Release 2018-4: Desmond Molecular Dynamics System*, D.E. Shaw Research: New York, NY, 2019.

170. Lin, C.-C.; Raza, A.; Shih, H., PEG hydrogels formed by thiol-ene photo-click chemistry and their effect on the formation and recovery of insulin-secreting cell spheroids. *Biomaterials* **2011,** *32* (36), 9685-9695.

171. Stockmayer, W. H., Theory of Molecular Size Distribution and Gel Formation in Branched-Chain Polymers. *J. Chem. Phys.* **1943,** *11* (2), 45-55.

172. Flory, P. J., Molecular Size Distribution in Three Dimensional Polymers. I. Gelation. *J. Am. Chem. Soc.* **1941,** *63* (11), 3083-3090.

173. Sperinde, J. J.; Griffith, L. G., Control and Prediction of Gelation Kinetics in Enzymatically Cross-Linked Poly(ethylene glycol) Hydrogels. *Macromolecules* **2000,** *33* (15), 5476-5480.

174. Lin, F.; Yu, J.; Tang, W.; Zheng, J.; Defante, A.; Guo, K.; Wesdemiotis, C.; Becker, M. L., Peptide-Functionalized Oxime Hydrogels with Tunable Mechanical Properties and Gelation Behavior. *Biomacromolecules* **2013,** *14* (10), 3749-3758.

175. Lu, H. D.; Charati, M. B.; Kim, I. L.; Burdick, J. A., Injectable shear-thinning hydrogels engineered with a self-assembling Dock-and-Lock mechanism. *Biomaterials* **2012,** *33* (7), 2145-2153.

176. Mulyasasmita, W.; Cai, L.; Dewi, R. E.; Jha, A.; Ullmann, S. D.; Luong, R. H.; Huang, N. F.; Heilshorn, S. C., Avidity-controlled hydrogels for injectable co-delivery of induced pluripotent stem cell-derived endothelial cells and growth factors. *J. Controlled Release* **2014,** *191*, 71-81.

177. Du, X.; Zhou, J.; Shi, J.; Xu, B., Supramolecular Hydrogelators and Hydrogels: From Soft Matter to Molecular Biomaterials. *Chem. Rev.* **2015,** *115* (24), 13165-13307.

178. Tzokova, N.; Fernyhough, C. M.; Topham, P. D.; Sandon, N.; Adams, D. J.; Butler, M. F.; Armes, S. P.; Ryan, A. J., Soft Hydrogels from Nanotubes of Poly(ethylene oxide)−Tetraphenylalanine Conjugates Prepared by Click Chemistry. *Langmuir* **2009,** *25* (4), 2479-2485.

179. Díaz, D. D.; Morin, E.; Schön, E. M.; Budin, G.; Wagner, A.; Remy, J.-S., Tailoring drug release profile of low-molecular-weight hydrogels by supramolecular co-assembly and thiol–ene orthogonal coupling. *J. Mater. Chem.* **2011,** *21* (3), 641-644.

180. Ramírez-López, P.; Torre, M. C. d. l.; Asenjo, M.; Ramírez-Castellanos, J.; González-Calbet, J. M.; Rodríguez-Gimeno, A.; Arellano, C. R. d.; Sierra, M. A., A new family of "clicked" estradiol-based low-molecular-weight gelators having highly symmetry-dependent gelation ability. *Chem. Commun.* **2011,** *47* (37), 10281-10283.

181. Umesh, V.; Rape, A. D.; Ulrich, T. A.; Kumar, S., Microenvironmental Stiffness Enhances Glioma Cell Proliferation by Stimulating Epidermal Growth Factor Receptor Signaling. *PLoS One* **2014**, *9*, Article e101771. DOI: 10.1371/journal.pone.0101771.

182. Wang, C.; Sinha, S.; Jiang, X.; Murphy, L.; Fitch, S.; Wilson, C.; Grant, G.; Yang, F., Matrix Stiffness Modulates Patient-Derived Glioblastoma Cell Fates in Three-Dimensional Hydrogels. *Tissue Eng., Part A* **2021,** *27* (5-6), 390-401.

183. Guan, X. F.; Avci-Adali, M.; Alarcin, E.; Cheng, H.; Kashaf, S. S.; Li, Y. X.; Chawla, A.; Jang, H. L.; Khademhosseini, A., Development of hydrogels for regenerative engineering. *Biotechnol. J.* **2017**, *12*, Article 1600394. DOI: 10.1002/biot.201600394.

184. Kolb, H. C.; Sharpless, K. B., The growing impact of click chemistry on drug discovery. *Drug Discovery Today* **2003,** *8* (24), 1128-1137.

185. Nimmo, C. M.; Shoichet, M. S., Regenerative Biomaterials that "Click": Simple, Aqueous-Based Protocols for Hydrogel Synthesis, Surface Immobilization, and 3D Patterning. *Bioconjugate Chem.* **2011,** *22*, 2199-2209.

186. Azagarsamy, M. A.; Anseth, K. S., Bioorthogonal Click Chemistry: An Indispensable Tool to Create Multifaceted Cell Culture Scaffolds. *ACS Macro Lett.* **2013,** *2* (1), 5-9.

187. Zou, Y.; Zhang, L.; Yang, L.; Zhu, F.; Ding, M. M.; Lin, F.; Wang, Z.; Li, Y. W., "Click" chemistry in polymeric scaffolds: Bioactive materials for tissue engineering. *J. Controlled Release* **2018,** *273*, 160-179.

188. LeValley, P. J.; Kloxin, A. M., Chemical Approaches to Dynamically Modulate the Properties of Synthetic Matrices. *ACS Macro Lett.* **2019,** *8* (1), 7-16.

189. Arkenberg, M. R.; Nguyen, H. D.; Lin, C. C., Recent advances in bio-orthogonal and dynamic crosslinking of biomimetic hydrogels. *J. Mater. Chem. B* **2020,** *8* (35), 7835-7855.

190. Liu, L. M.; Shadish, J. A.; Arakawa, C. K.; Shi, K.; Davis, J.; DeForest, C. A., Cyclic Stiffness Modulation of Cell-Laden Protein-Polymer Hydrogels in Response to User-Specified Stimuli Including Light. *Adv. Biosyst.* **2018**, *2*, Article 1800240. DOI: 10.1002/adbi.201800240.

191. Fu, L. L.; Haage, A.; Kong, N.; Tanentzapf, G.; Li, H. B., Dynamic protein hydrogels with reversibly tunable stiffness regulate human lung fibroblast spreading reversibly. *Chem. Commun.* **2019,** *55* (36), 5235-5238.

192. Arkenberg, M. R.; Moore, D. M.; Lin, C. C., Dynamic control of hydrogel crosslinking via sortase-mediated reversible transpeptidation. *Acta Biomater.* **2019,** *83*, 83-95.

193. Rosales, A. M.; Mabry, K. M.; Nehls, E. M.; Anseth, K. S., Photoresponsive Elastic Properties of Azobenzene-Containing Poly(ethylene-glycol)-Based Hydrogels. *Biomacromolecules* **2015,** *16*, 798-806.

194. Rosales, A. M.; Rodell, C. B.; Chen, M. H.; Morrow, M. G.; Anseth, K. S.; Burdick, J. A., Reversible Control of Network Properties in Azobenzene-Containing Hyaluronic Acid-Based Hydrogels. *Bioconjugate Chem.* **2018,** *29* (4), 905-913.

195. Abdeen, A. A.; Lee, J.; Bharadwaj, N. A.; Ewoldt, R. H.; Kilian, K. A., Temporal Modulation of Stem Cell Activity Using Magnetoactive Hydrogels. *Adv. Healthcare Mater.* **2016,** *5* (19), 2536-2544.

196. Holt, S. E.; Arroyo, J.; Poux, E.; Fricks, A.; Agurcia, I.; Heintschel, M.; Rakoski, A.; Alge, D. L., Supramolecular Click Product Interactions Induce Dynamic Stiffening of Extracellular Matrix-Mimetic Hydrogels. *Biomacromolecules* **2021,** *22* (7), 3040-3048.

197. Samanta, U.; Pal, D.; Chakrabarti, P., Packing of aromatic rings against tryptophan residues in proteins. *Acta Crystallogr. Sect. D. Biol. Crystallogr.* **1999,** *55* (8), 1421-1427.

198. Rahman, M. M.; Muhseen, Z. T.; Junaid, M.; Zhang, H. J., The Aromatic Stacking Interactions Between Proteins and their Macromolecular Ligands. *Curr. Protein Pept. Sci.* **2015,** *16* (6), 502-512.

199. Arkenberg, M. R.; Lin, C. C., Orthogonal enzymatic reactions for rapid crosslinking and dynamic tuning of PEG-peptide hydrogels. *Biomater. Sci.* **2017,** *5* (11), 2231-2240.

200. Cox, T. R.; Erler, J. T., Remodeling and homeostasis of the extracellular matrix: implications for fibrotic diseases and cancer. *Disease Models & Mechanisms* **2011,** *4* (2), 165-178.

201. Panwar, A.; Tan, L. P., Current Status of Bioinks for Micro-Extrusion-Based 3D Bioprinting. *Molecules* **2016**, *21*, Article 685. DOI: 10.3390/molecules21060685.

202. Kyle, S.; Jessop, Z. M.; Al-Sabah, A.; Whitaker, I. S., 'Printability' of Candidate Biomaterials for Extrusion Based 3D Printing: State-of-the-Art. *Adv. Healthcare Mater.* **2017,** *6* (16), 1700264.

203. Ercan, H.; Durkut, S.; Koc-Demir, A.; Elçin, A. E.; Elçin, Y. M., Clinical Applications of Injectable Biomaterials. In *Novel Biomaterials for Regenerative Medicine*, Chun, H. J.; Park, K.; Kim, C.-H.; Khang, G., Eds. Springer Singapore: Singapore, 2018; pp 163-182.

204. Zhou, H.; Liang, C.; Wei, Z.; Bai, Y.; Bhaduri, S. B.; Webster, T. J.; Bian, L.; Yang, L., Injectable biomaterials for translational medicine. *Mater. Today* **2019,** *28*, 81-97.

205. Spector, M.; Lim, T. C., Injectable biomaterials: a perspective on the next wave of injectable therapeutics. *Biomed. Mater.* **2016**, *11*, Article 014110. DOI: 10.1088/1748-6041/11/1/014110.

206. Birman, T.; Seliktar, D., Injectability of Biosynthetic Hydrogels: Consideration for Minimally Invasive Surgical Procedures and 3D Bioprinting. *Adv. Funct. Mater.* **2021**, *31*, Article 2100628. DOI: 10.1002/adfm.202100628.

207. Gao, F. Y.; Jiao, C. C.; Yu, B.; Cong, H. L.; Shen, Y. Q., Preparation and biomedical application of injectable hydrogels. *Mat. Chem. Front.* **2021,** *5* (13), 4912-4936.

208. Chen, M. H.; Wang, L. L.; Chung, J. J.; Kim, Y.-H.; Atluri, P.; Burdick, J. A., Methods To Assess Shear-Thinning Hydrogels for Application As Injectable Biomaterials. *ACS Biomater. Sci. Eng.* **2017,** *3* (12), 3146-3160.

209. Klak, M.; Kowalska, P.; Dobrzański, T.; Tymicki, G.; Cywoniuk, P.; Gomółka, M.; Kosowska, K.; Bryniarski, T.; Berman, A.; Dobrzyń, A.; Sadowski, W.; Górecki, B.; Wszoła, M., Bionic Organs: Shear Forces Reduce Pancreatic Islet and Mammalian Cell Viability during the Process of 3D Bioprinting. *Micromachines* **2021**, *12*, Article 304. DOI: 10.3390/mi12030304.

210. Reina-Romo, E.; Mandal, S.; Amorim, P.; Bloemen, V.; Ferraris, E.; Geris, L., Towards the Experimentally-Informed In Silico Nozzle Design Optimization for Extrusion-Based Bioprinting of Shear-Thinning Hydrogels. *Front. Bioeng. Biotechnol.* **2021**, *9*, Article 701778. DOI: 10.3389/fbioe.2021.701778.

211. Tu, Y. J.; Chen, N. A.; Li, C. P.; Liu, H. Q.; Zhu, R.; Chen, S. F.; Xiao, Q.; Liu, J. H.; Ramakrishna, S.; He, L. M., Advances in injectable self-healing biomedical hydrogels. *Acta Biomater.* **2019,** *90*, 1-20.

212. De France, K. J.; Cranston, E. D.; Hoare, T., Mechanically Reinforced Injectable Hydrogels. *ACS Applied Polymer Materials* **2020,** *2* (3), 1016-1030.

213. Jin, R.; Moreira Teixeira, L. S.; Krouwels, A.; Dijkstra, P. J.; van Blitterswijk, C. A.; Karperien, M.; Feijen, J., Synthesis and characterization of hyaluronic acid–poly(ethylene glycol) hydrogels via Michael addition: An injectable biomaterial for cartilage repair. *Acta Biomater.* **2010,** *6* (6), 1968-1977.

214. Fu, Y.; Kao, W. Y. J., In situ forming poly(ethylene glycol)-based hydrogels via thiol-maleimide Michael-type addition. *J. Biomed. Mater. Res. Part A* **2011,** *98A* (2), 201-211.

215. Haines-Butterick, L.; Rajagopal, K.; Branco, M.; Salick, D.; Rughani, R.; Pilarz, M.; Lamm, M. S.; Pochan, D. J.; Schneider, J. P., Controlling hydrogelation kinetics by peptide design for three-dimensional encapsulation and injectable delivery of cells. *Proceedings of the National Academy of Sciences* **2007,** *104* (19), 7791-7796.

216. Dong, H.; Paramonov, S. E.; Aulisa, L.; Bakota, E. L.; Hartgerink, J. D., Self-Assembly of Multidomain Peptides: Balancing Molecular Frustration Controls Conformation and Nanostructure. *J. Am. Chem. Soc.* **2007,** *129* (41), 12468-12472.

217. Tigner, T. J.; Rajput, S.; Gaharwar, A. K.; Alge, D. L., Comparison of Photo Cross Linkable Gelatin Derivatives and Initiators for Three-Dimensional Extrusion Bioprinting. *Biomacromolecules* **2020,** *21* (2), 454-463.

218. Shie, M. Y.; Lee, J.; Ho, C. C.; Yen, S. Y.; Ng, H. Y.; Chen, Y. W., Effects of Gelatin Methacrylate Bio-ink Concentration on Mechano-Physical Properties and Human Dermal Fibroblast Behavior. *Polymers* **2020**, *12*, Article 1930. DOI: 10.3390/polym12091930.

219. Yang, B.; Wei, K.; Loebel, C.; Zhang, K.; Feng, Q.; Li, R.; Wong, S. H. D.; Xu, X.; Lau, C.; Chen, X.; Zhao, P.; Yin, C.; Burdick, J. A.; Wang, Y.; Bian, L., Enhanced mechanosensing of cells in synthetic 3D matrix with controlled biophysical dynamics. *Nat. Commun.* **2021**, *12*, Article 3514. DOI: 10.1038/s41467-021-23120-0.

220. Shome, S.; Dasgupta, P. S.; Basu, S., Dopamine regulates mobilization of mesenchymal stem cells during wound angiogenesis. *PLoS One* **2012**, *7*, Article e31682. DOI: 10.1371/journal.pone.0031682.

221. Troncoso, F.; Herlitz, K.; Acurio, J.; Aguayo, C.; Guevara, K.; Castro, F. O.; Godoy, A. S.; San Martin, S.; Escudero, C., Advantages in Wound Healing Process in Female Mice Require Upregulation A(2A)-Mediated Angiogenesis under the Stimulation of 17β-Estradiol. *Int. J. Mol. Sci.* **2020,** *21* (19).

222. Lee, H.-p.; Stowers, R.; Chaudhuri, O., Volume expansion and TRPV4 activation regulate stem cell fate in three-dimensional microenvironments. *Nat. Commun.* **2019**, *10*, Article 529. DOI: 10.1038/s41467-019-08465-x.

223. Meng, Z.; Hanson, J.; Yakovlev, V. In *Watching embryonic development in a new light: elasticity specific imaging with dual Brillouin/Raman microspectroscopy*, SPIE BiOS, San Francisco, CA, USA, 2016; SPIE: San Francisco, CA, USA, 2016.